TICRA

In-flight Retrieval of Geometrical information on the Planck Telescope

RFM2

RF performance of HFI beams

Author: Per Heighwood Nielsen

December, 2015 S-1563-15

TICRA
LÆDERSTRÆDE 34 · DK-1201 COPENHAGEN K DENMARK
TELEPHONE +45 33 12 45 72 TELEFAX +45 33 12 08 80
E-MAIL ticra@ticra.com http://www.ticra.com

VAT REGISTRATION NO. DK-1055 8697
TICRA FOND, CVR REG. NO. 1055 8697

TABLE OF CONTENTS

1. Introduction.

The present study is prepared for ESTEC under contract no. 18395/04/NL/NB, CCN no. 8.

The title of the work is

"In-flight Retrieval of Geometrical information on the Planck Telescope"

This Report presents a computation of all the HFI beam patterns using the retrieved telescope geometry RFM2 developed in Report S-1563-13. The patterns are compared with the fitted deconvoluted and combined measured patterns from three scans of the planets Saturn and Jupiter, see Report S-1563-05 and Report S-1563-07, to visualize the remaining differences.

All calculated patterns are analysed at the centre frequency using Physical Optics on both mirrors and calculated in uv directions defined in the Field-of-View, FOV, coordinate system as

$$u = \sin(\theta)\cos(\varphi)$$
$$v = \sin(\theta)\sin(\varphi)$$

The radiation from the planets is unpolarized so both co- and cross-components of the calculated radiated field are measured. Therefore, all field data from the planet scan is given as power only.

2. RF performance of LFI beams.

The final RF performance of the retrieved telescope geometry model, RFM2, and for all LFI detector positions are given in the following Figure 2-1 to Figure 2-43. The calculated performances are compared with the fitted deconvoluted measured beams down to their respective noise levels in contour plots, where the full lines are for the measured field.

The azimuthally integrated power within the main beam and down to the noise level is calculated for all beams and the retrieved and measured results are compared. The differences of these two integrated powers are shown also. Both the measured and the retrieved pattern are integrated down to the noise level for the individual beams and the powers in this total region are equalized. This gives a normalization of the measured beam and the zero shown near the end of the plot.

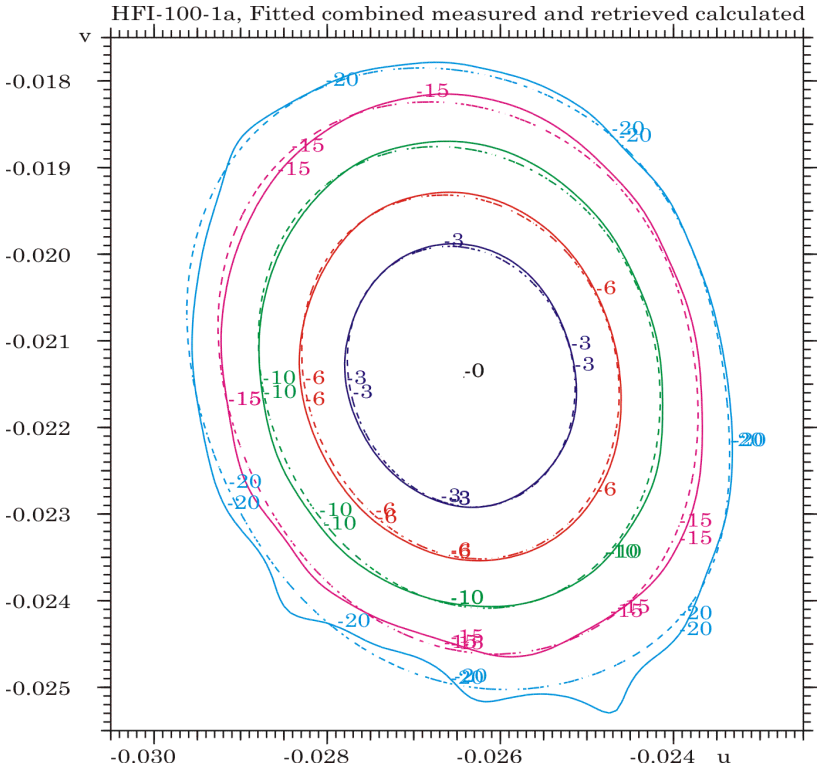

a) Measured (full line) and retrieved (dashed) power pattern

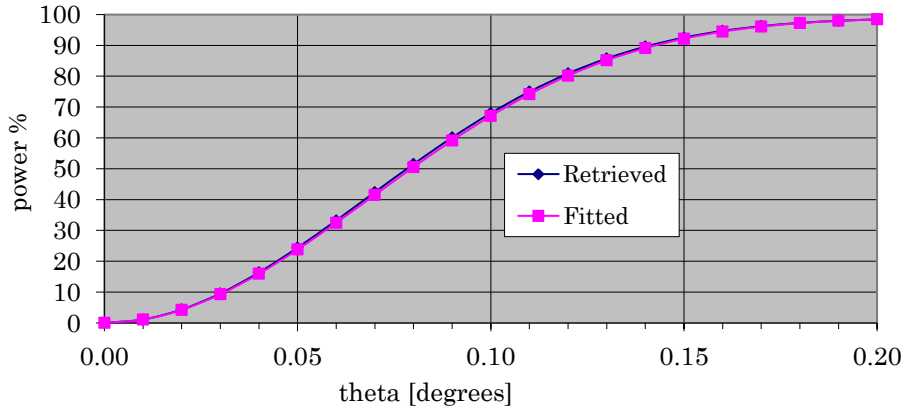

b) Azimuthally integrated power

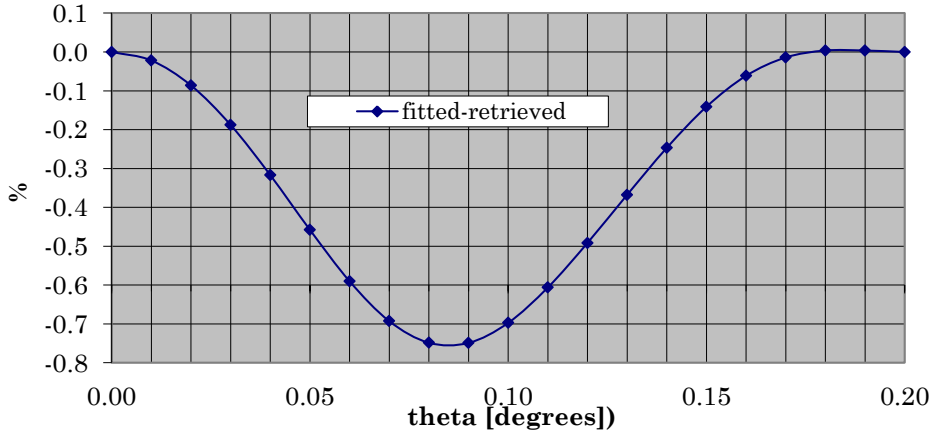

c) Difference

Figure 2-1 Kriging fitted measured and retrieved power pattern for 100 GHz detector, HFI-100-1a.

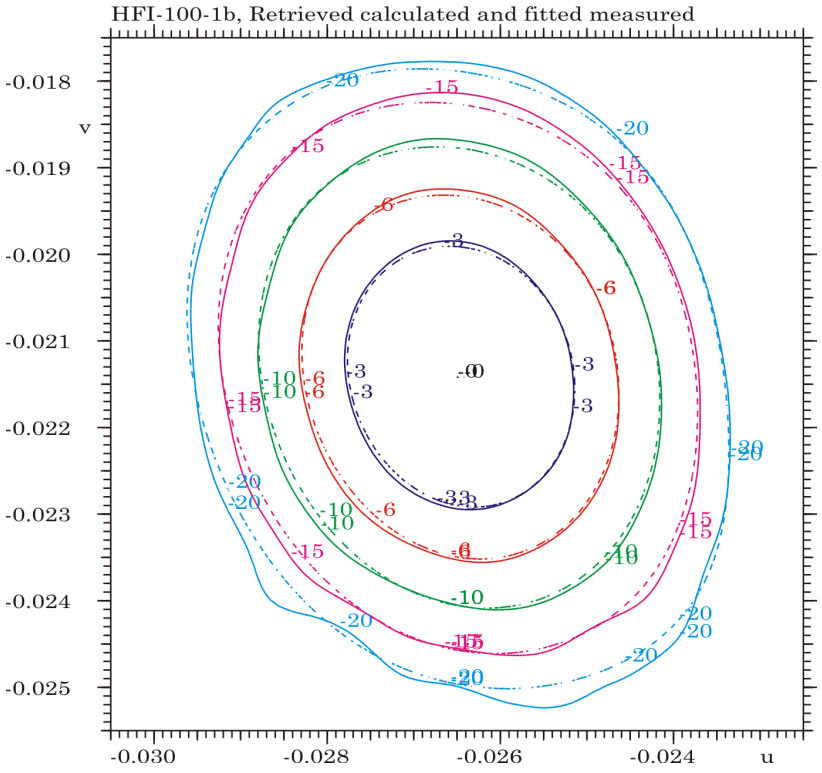

a) Measured (full line) and retrieved (dashed) power pattern

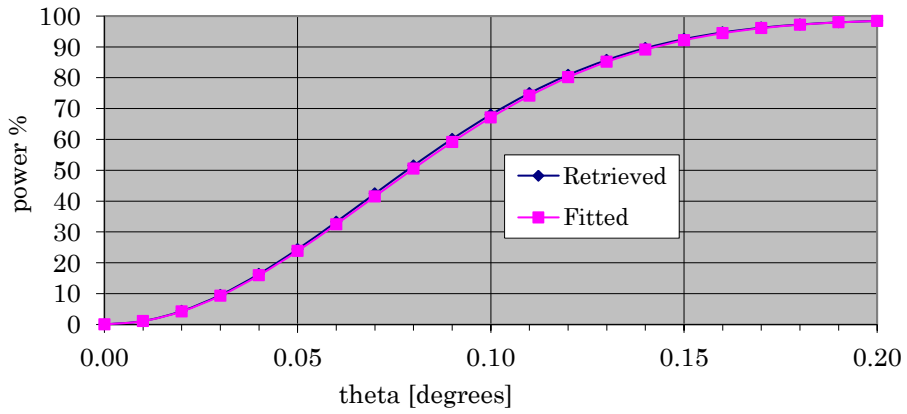

b) Azimuthally integrated power

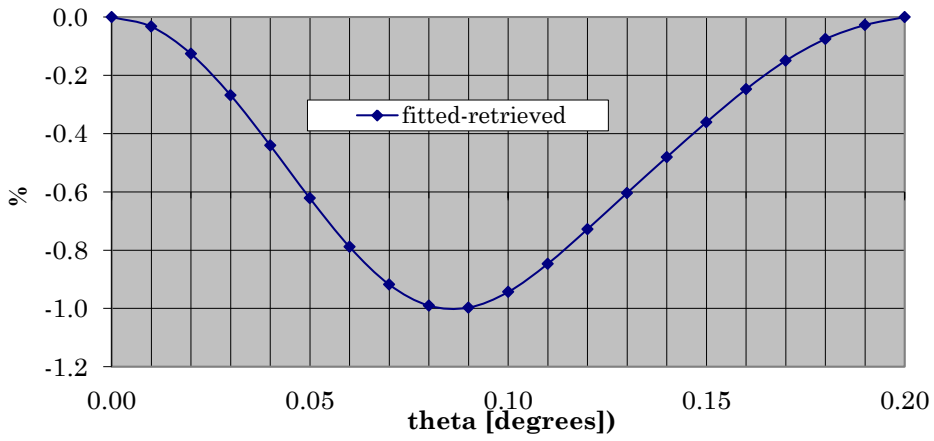

c) Difference

Figure 2-2 Kriging fitted measured and retrieved power pattern for 100 GHz detector, HFI-100-1b.

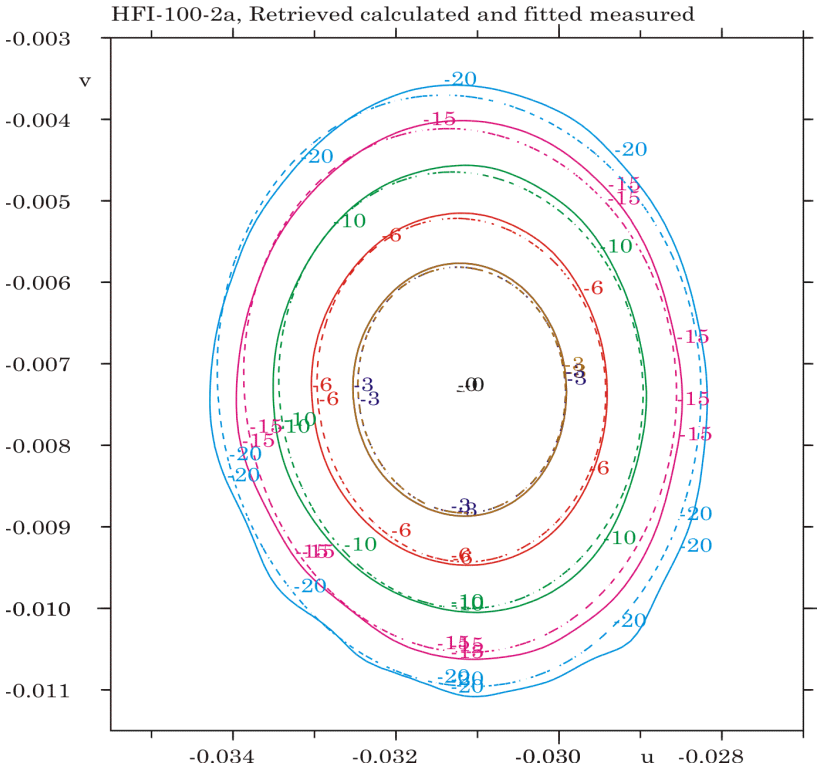

a) Measured (full line) and retrieved (dashed) power pattern

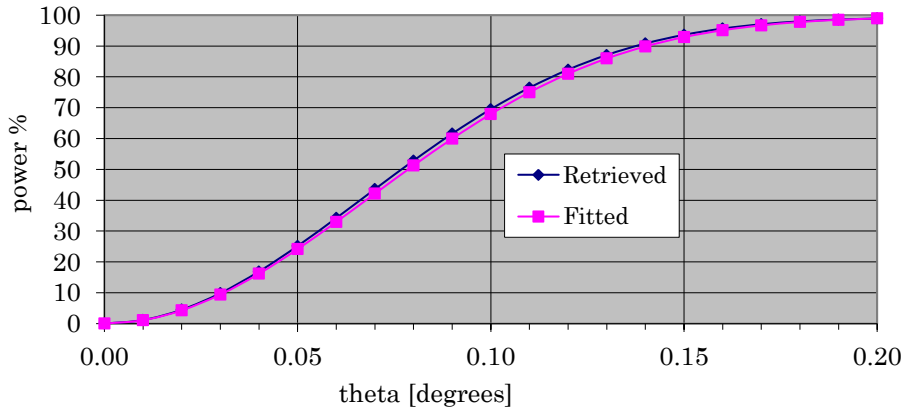

b) Azimuthally integrated power

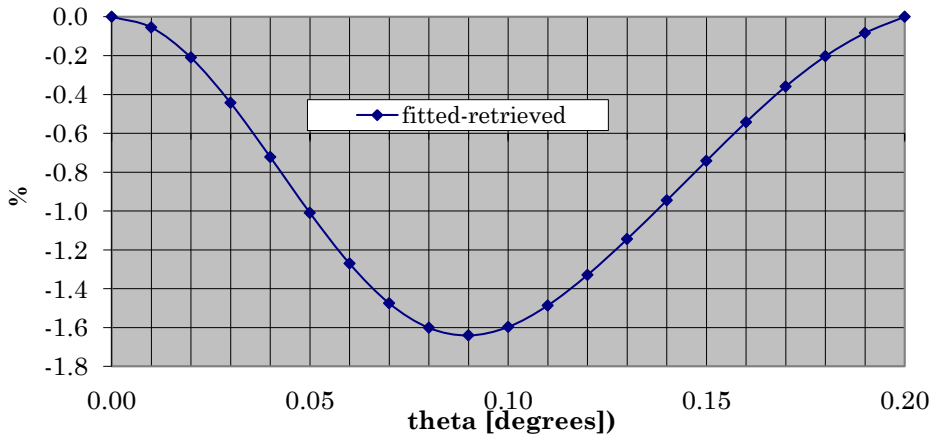

c) Difference

Figure 2-3 Kriging fitted measured and retrieved power pattern for 100 GHz detector, HFI-100-2a.

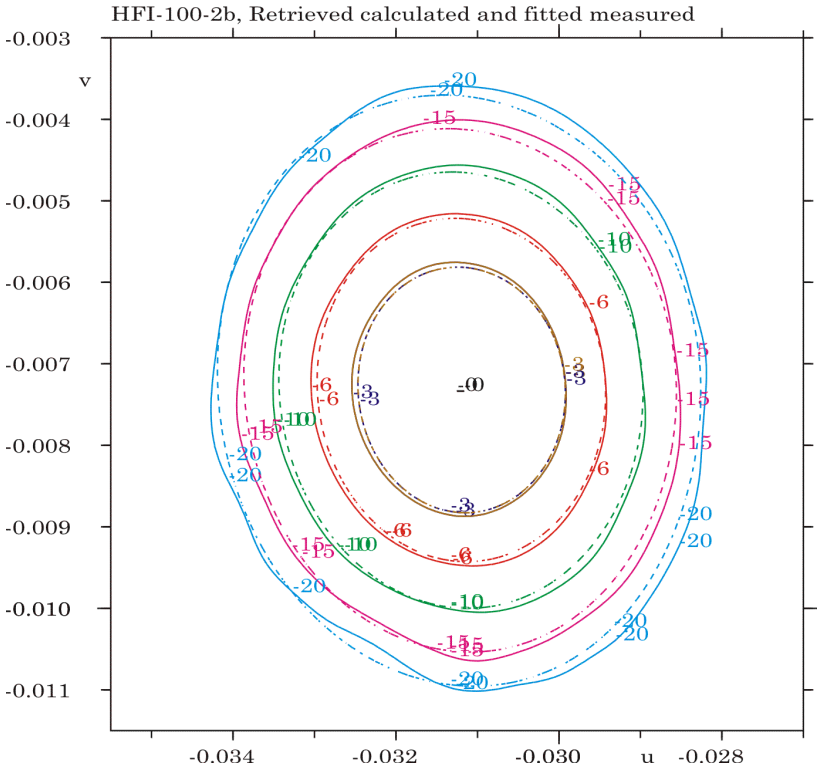

a) Measured (full line) and retrieved (dashed) power pattern

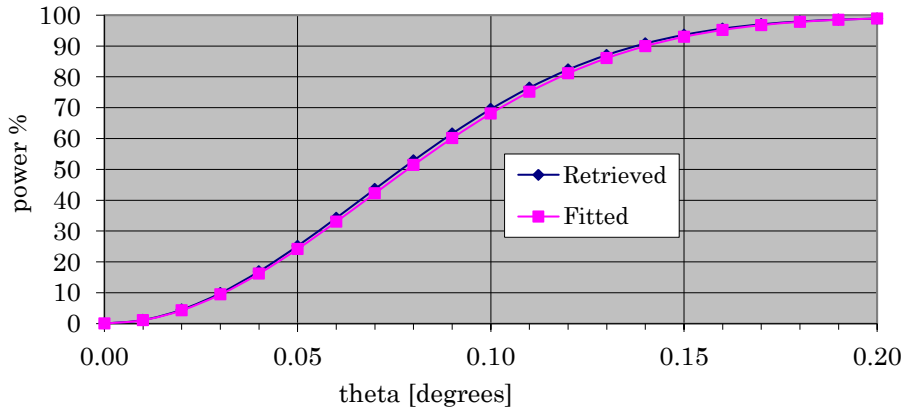

b) Azimuthally integrated power

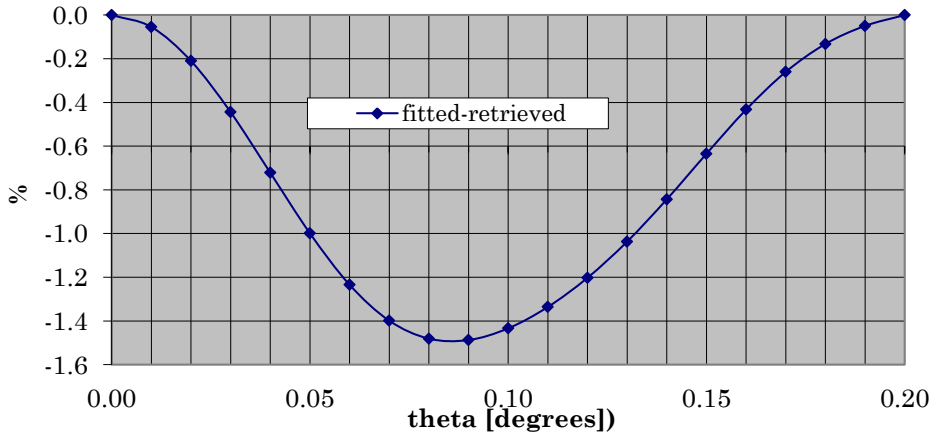

c) Difference

Figure 2-4 Kriging fitted measured and retrieved power pattern for 100 GHz detector, HFI-100-2b.

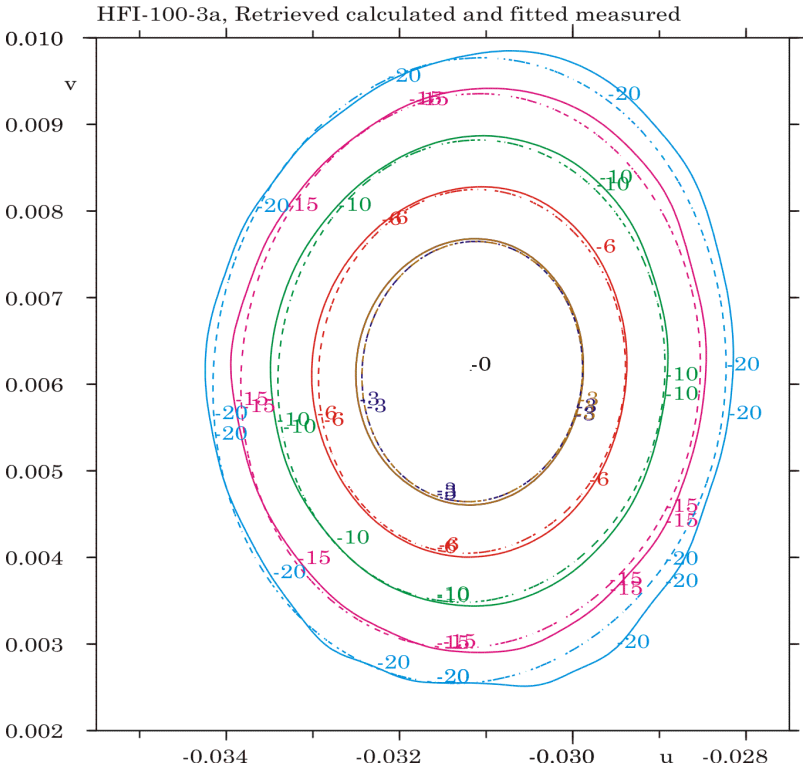

a) Measured (full line) and retrieved (dashed) power pattern

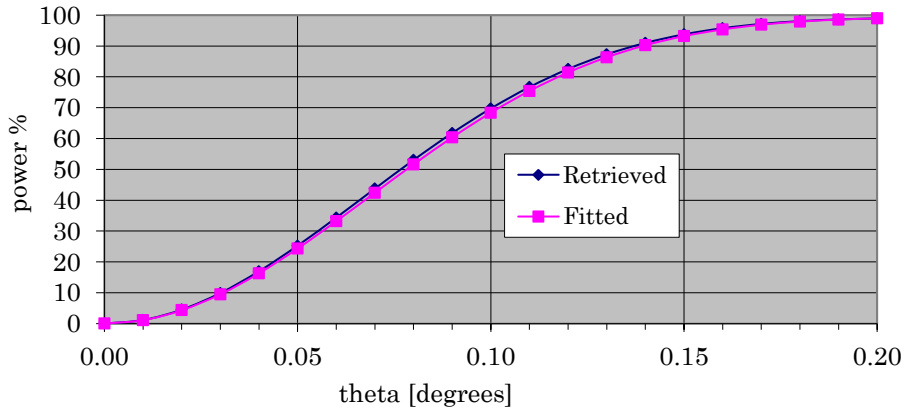

b) Azimuthally integrated power

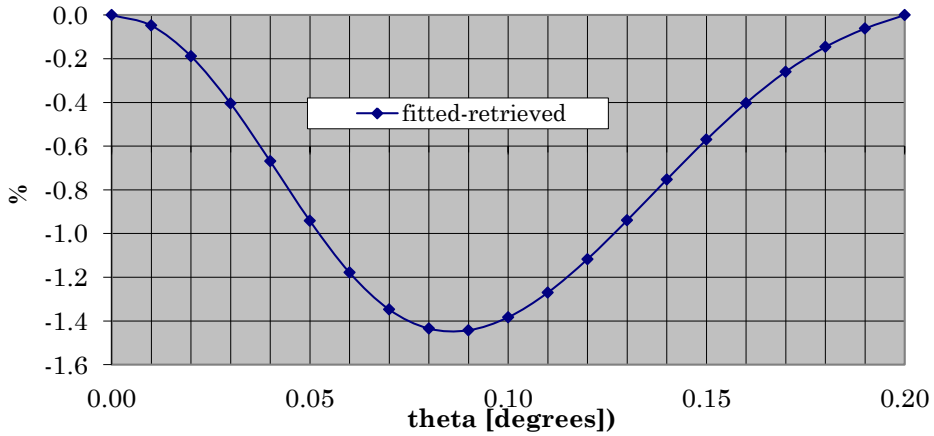

c) Difference

Figure 2-5 Kriging fitted measured and retrieved power pattern for 100 GHz detector, HFI-100-3a.

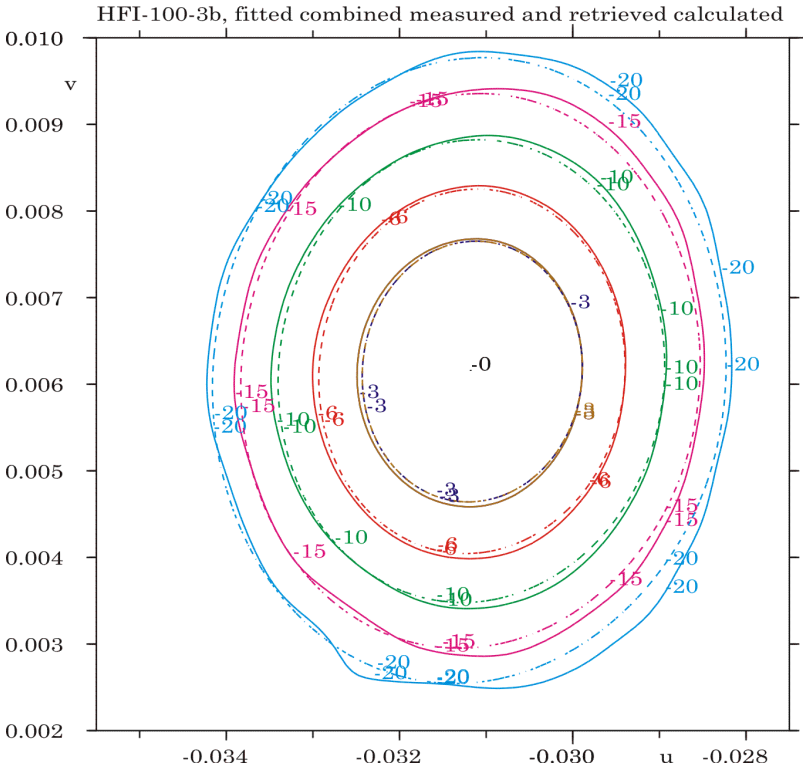

a) Measured (full line) and retrieved (dashed) power pattern

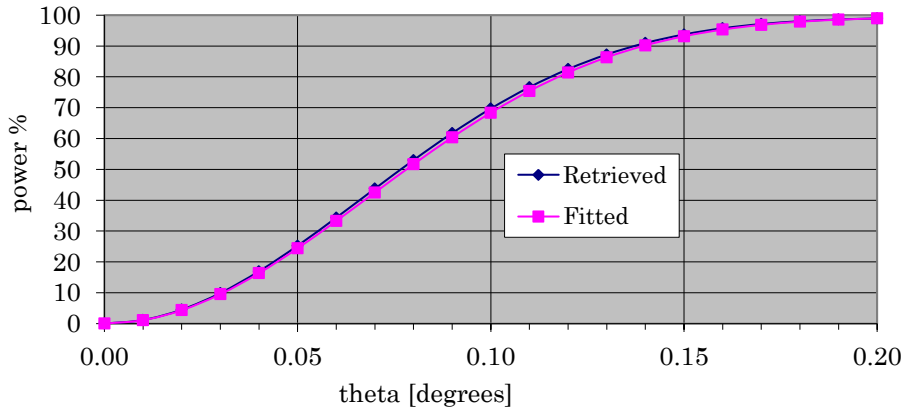

b) Azimuthally integrated power

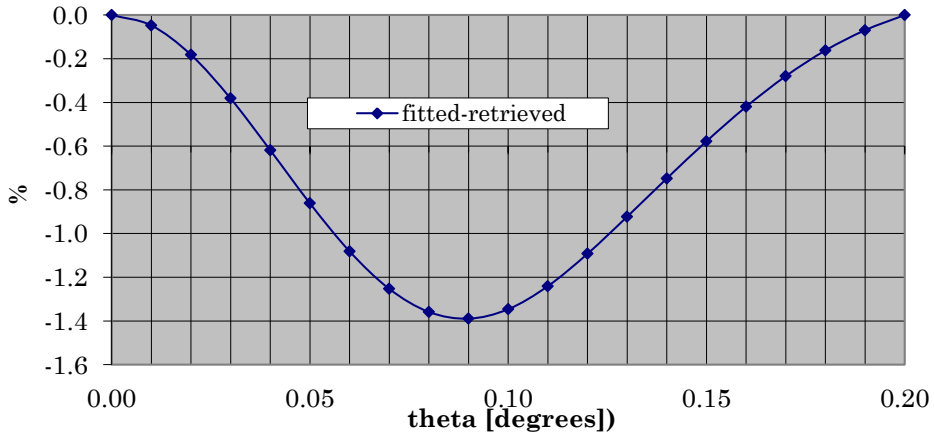

c) Difference

Figure 2-6 Kriging fitted measured and retrieved power pattern for 100 GHz detector, HFI-100-3b.

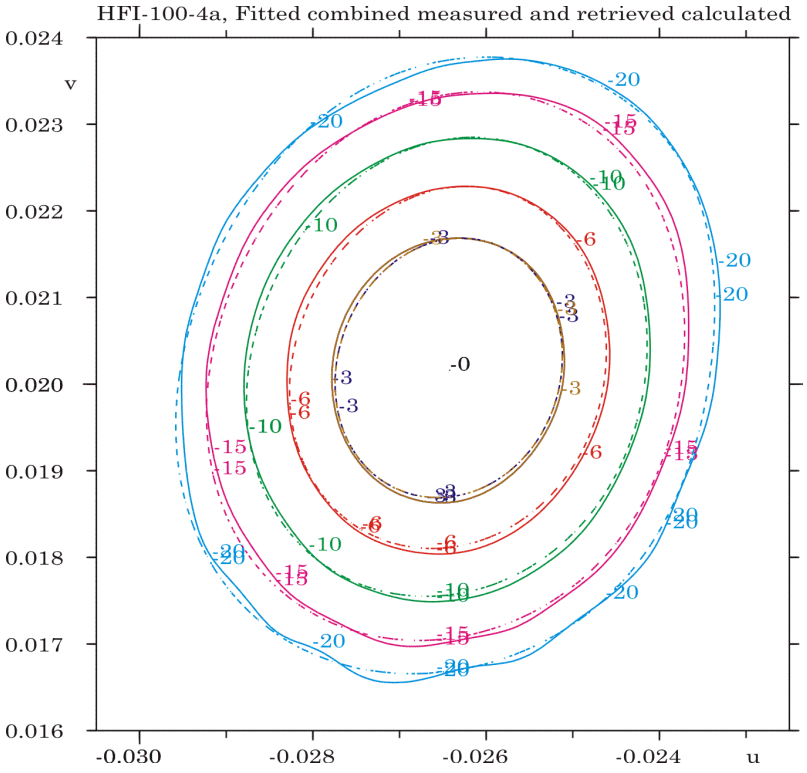

a) Measured (full line) and retrieved (dashed) power pattern

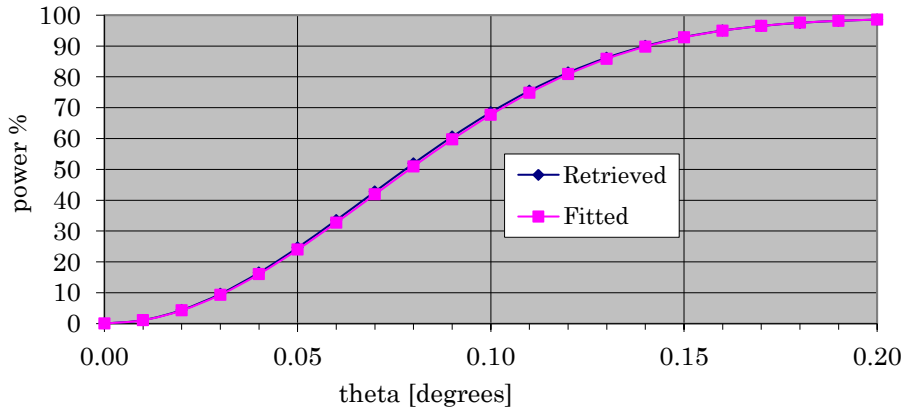

b) Azimuthally integrated power

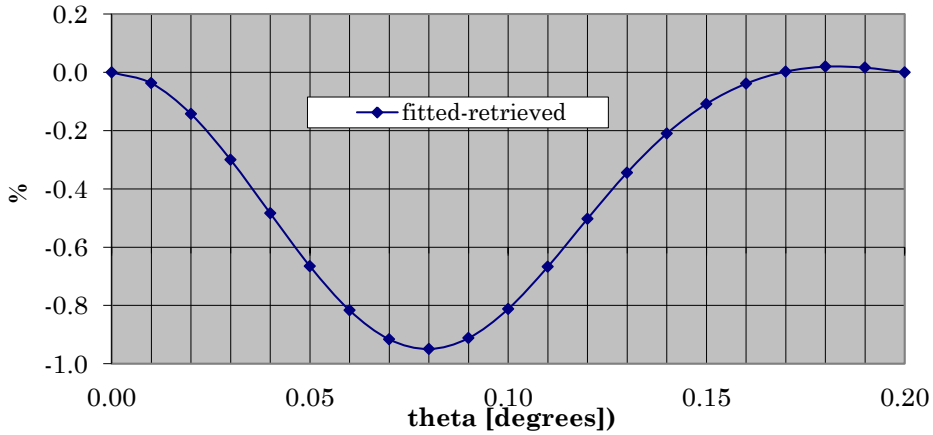

c) Difference

Figure 2-7 Kriging fitted measured and retrieved power pattern for 100 GHz detector, HFI-100-4a.

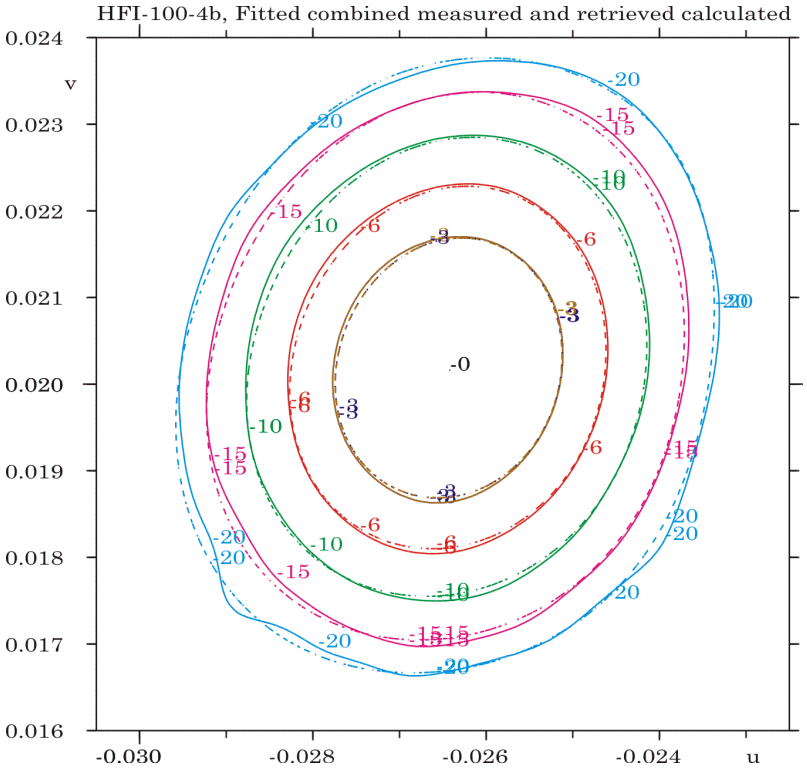

a) Measured (full line) and retrieved (dashed) power pattern

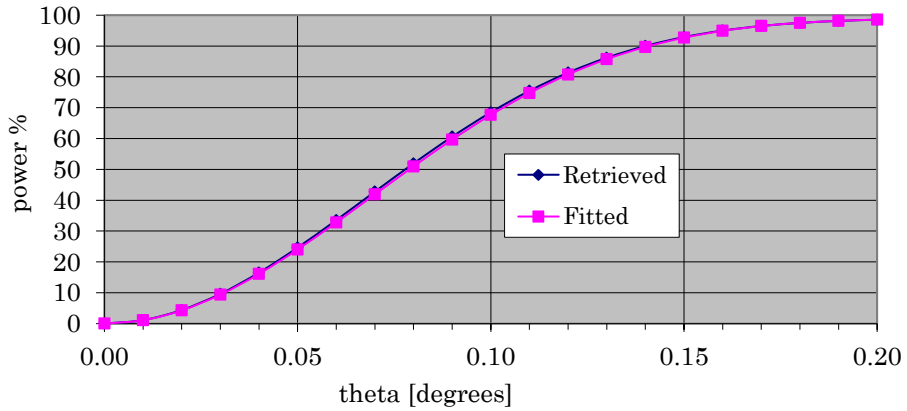

b) Azimuthally integrated power

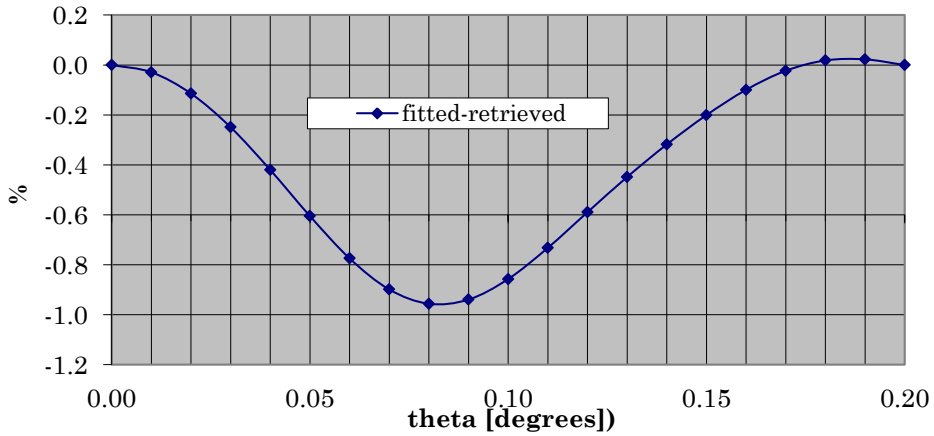

c) Difference

Figure 2-8 Kriging fitted measured and retrieved power pattern for 100 GHz detector, HFI-100-4b.

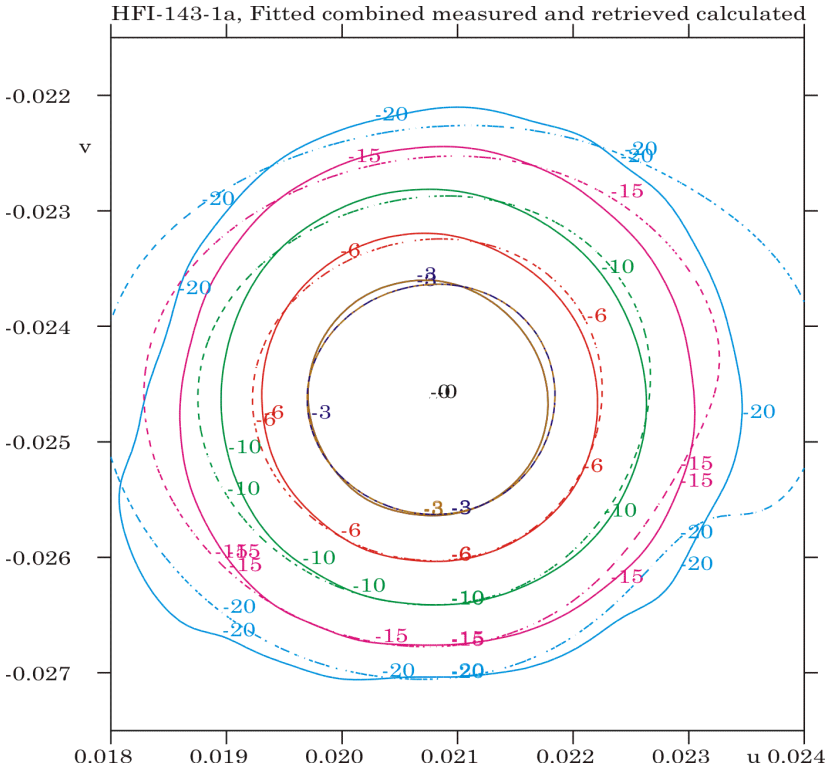

a) Measured (full line) and retrieved (dashed) power pattern

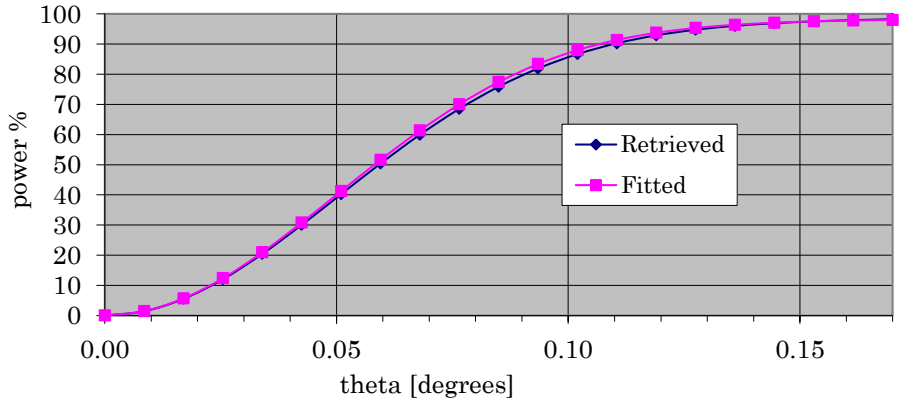

b) Azimuthally integrated power

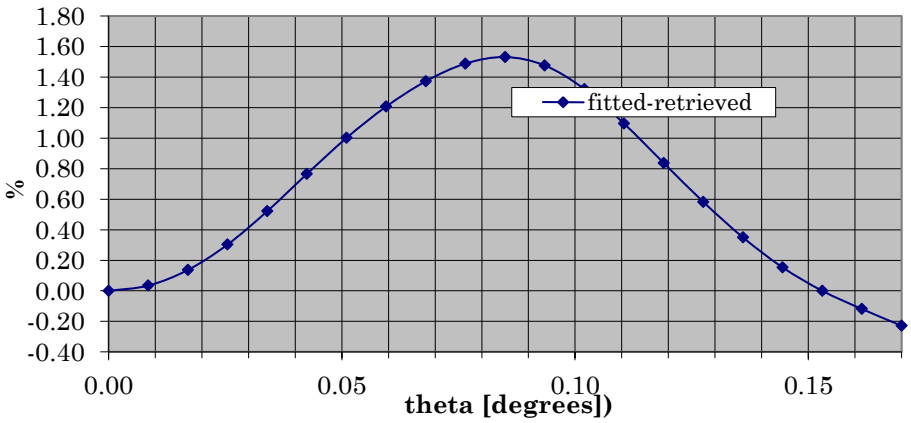

c) Difference

Figure 2-9 Kriging fitted measured and retrieved power pattern for 143 GHz detector, HFI-143-1a.

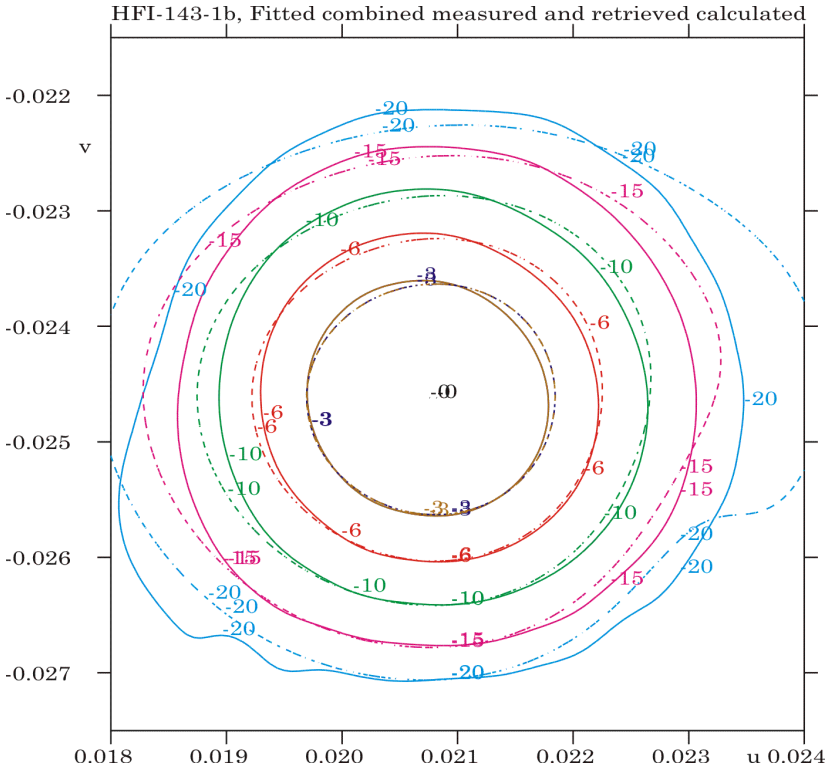

a) Measured (full line) and retrieved (dashed) power pattern

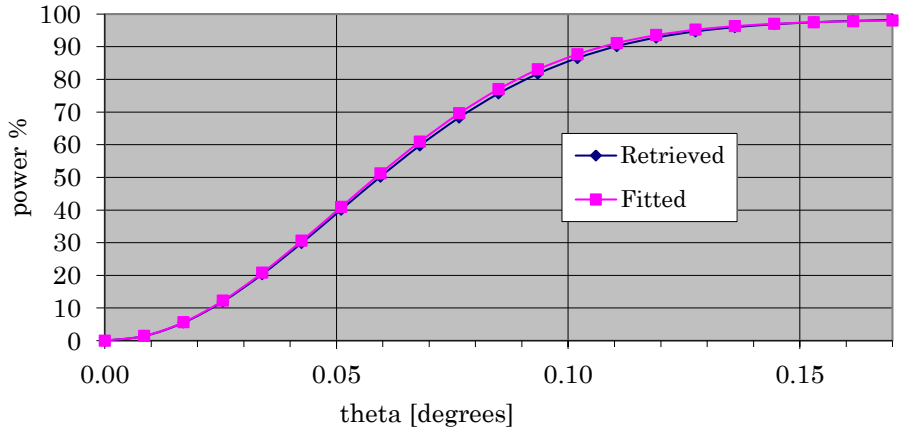

b) Azimuthally integrated power

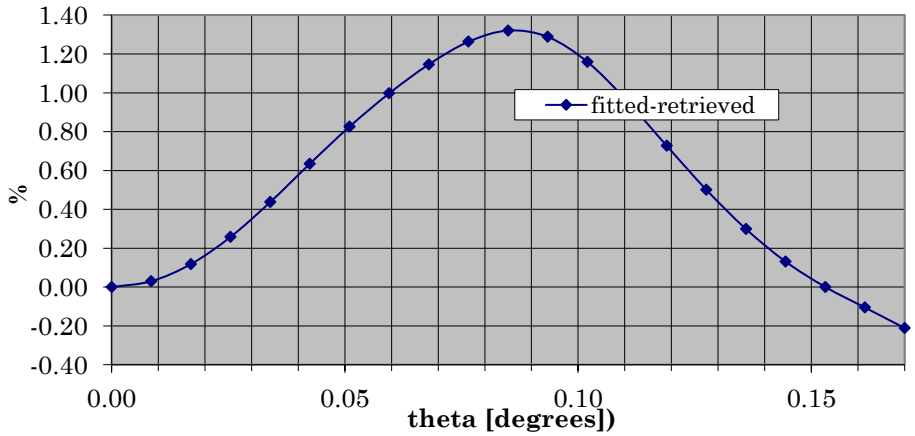

c) Difference

Figure 2-10 Kriging fitted measured and retrieved power pattern for 143 GHz detector, HFI-143-1b.

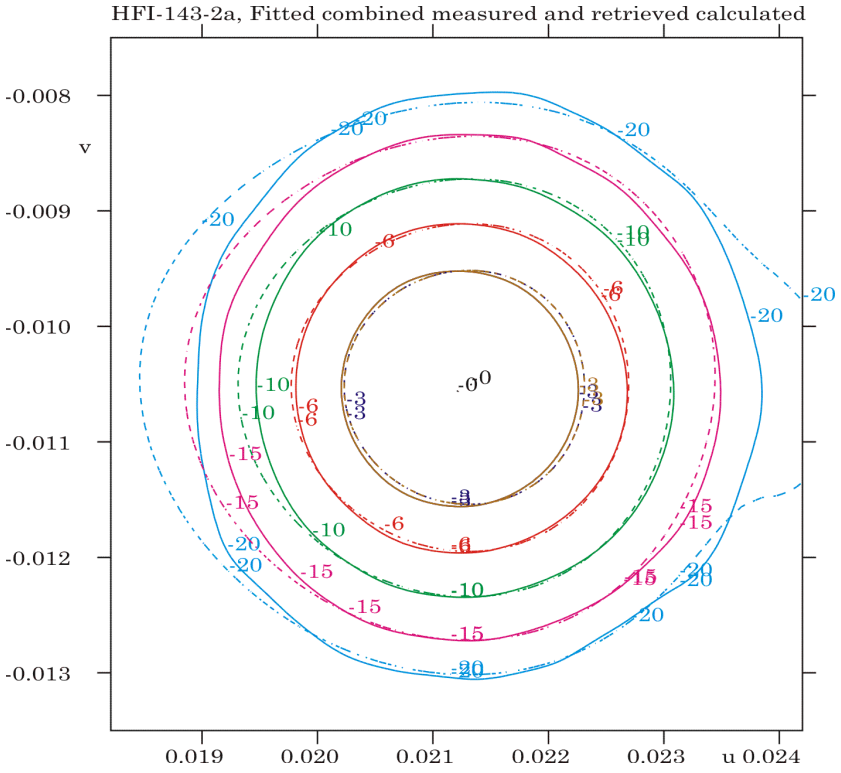

a) Measured (full line) and retrieved (dashed) power pattern

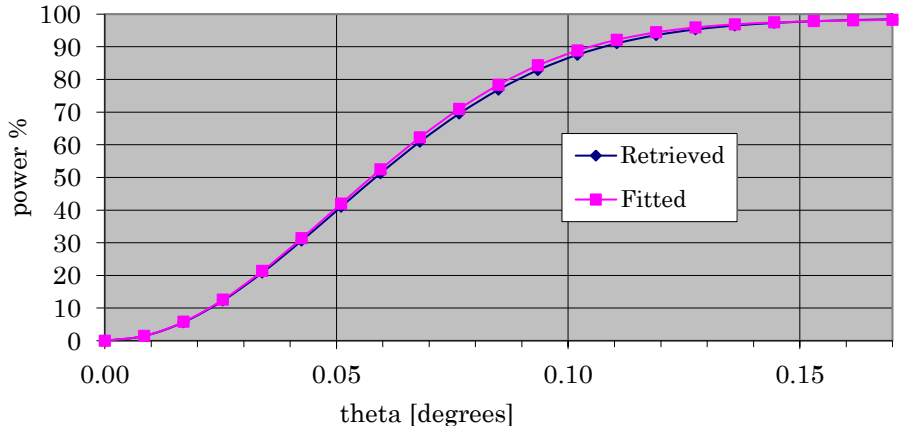

b) Azimuthally integrated power

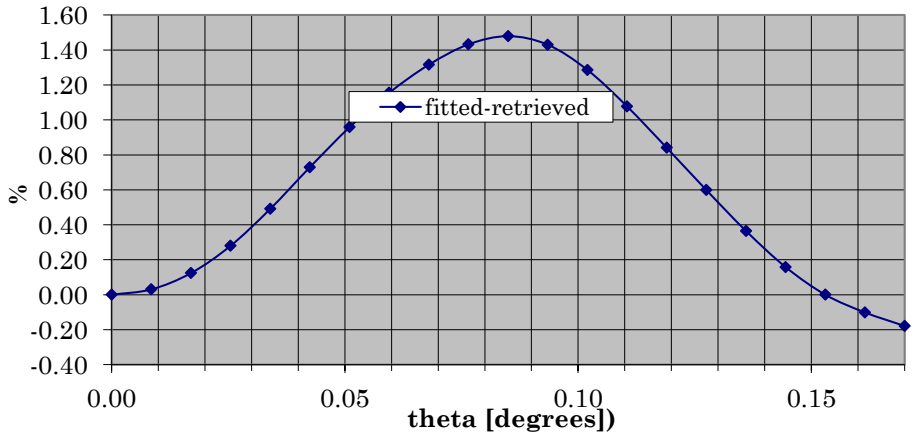

c) Difference

Figure 2-11 Kriging fitted measured and retrieved power pattern for 143 GHz detector, HFI-143-2a.

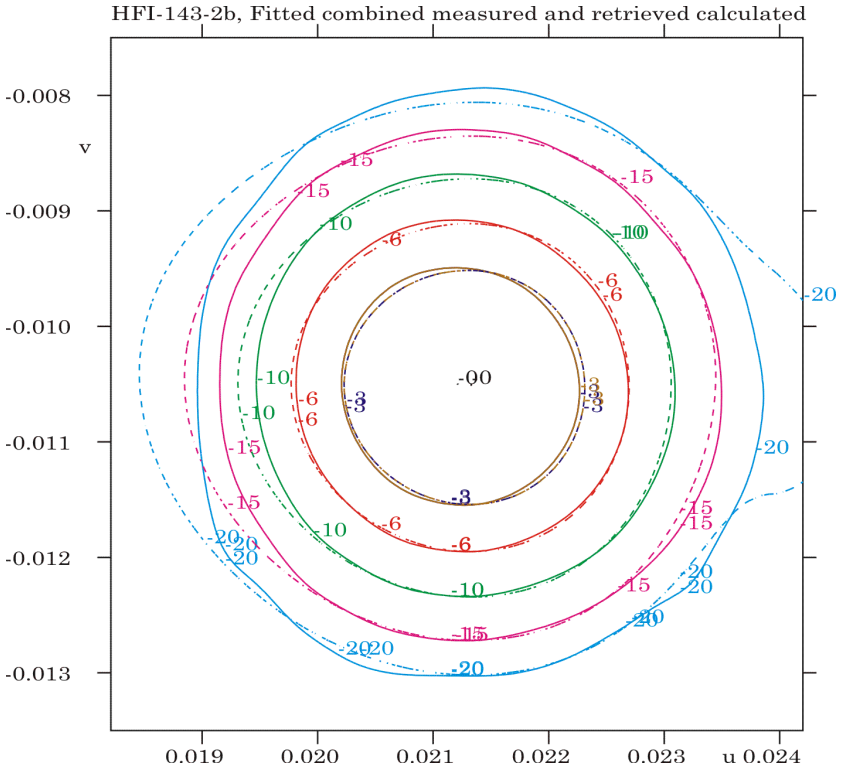

a) Measured (full line) and retrieved (dashed) power pattern

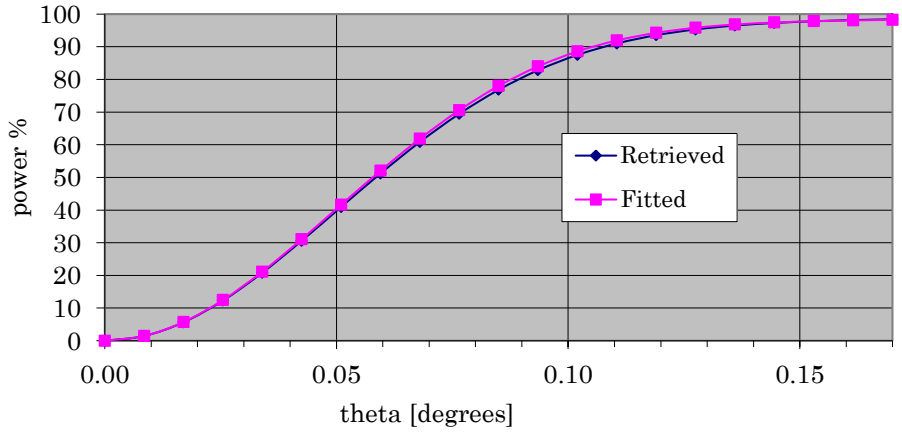

b) Azimuthally integrated power

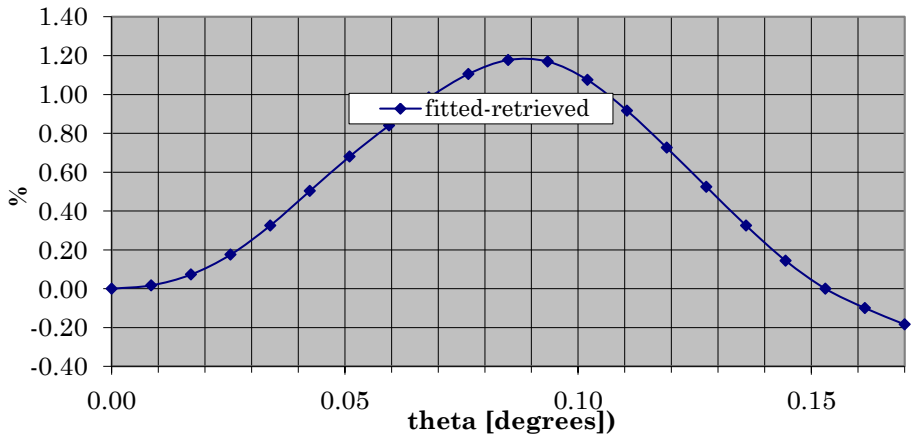

c) Difference

Figure 2-12 Kriging fitted measured and retrieved power pattern for 143 GHz detector, HFI-143-2b.

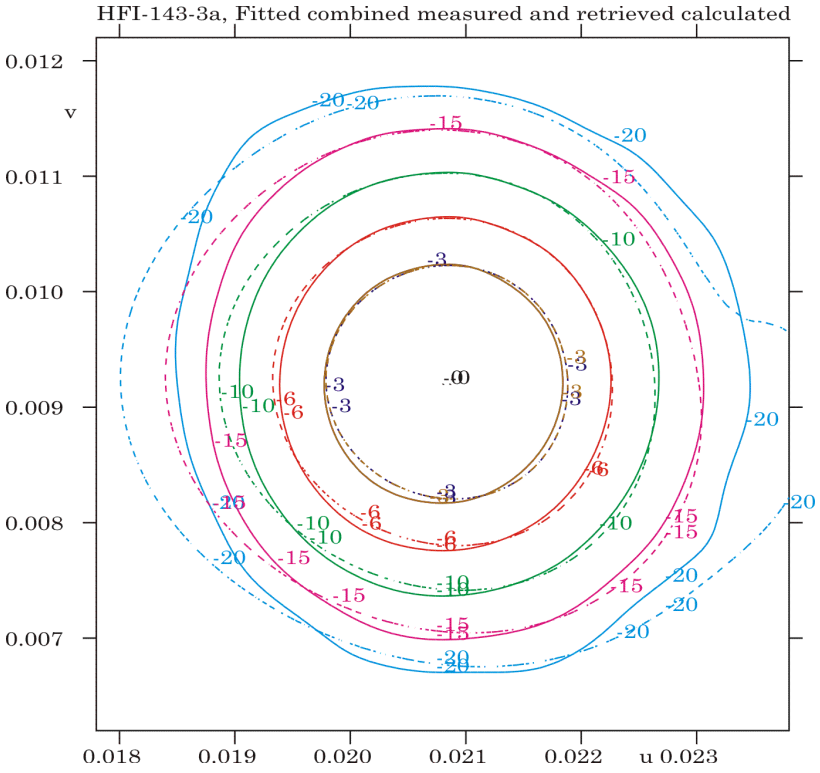

a) Measured (full line) and retrieved (dashed) power pattern

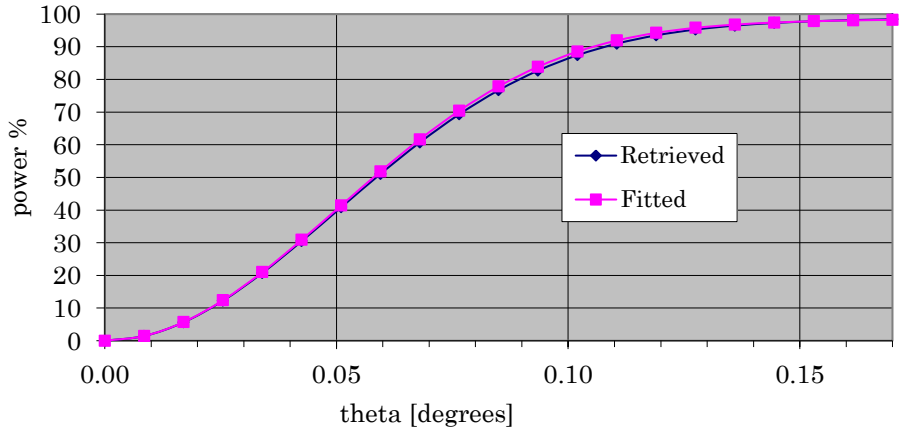

b) Azimuthally integrated power

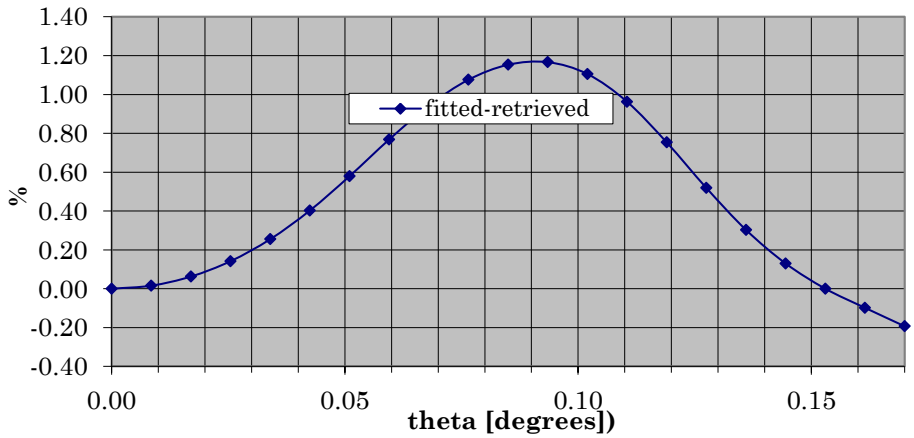

c) Difference

Figure 2-13 Kriging fitted measured and retrieved power pattern for 143 GHz detector, HFI-143-3a.

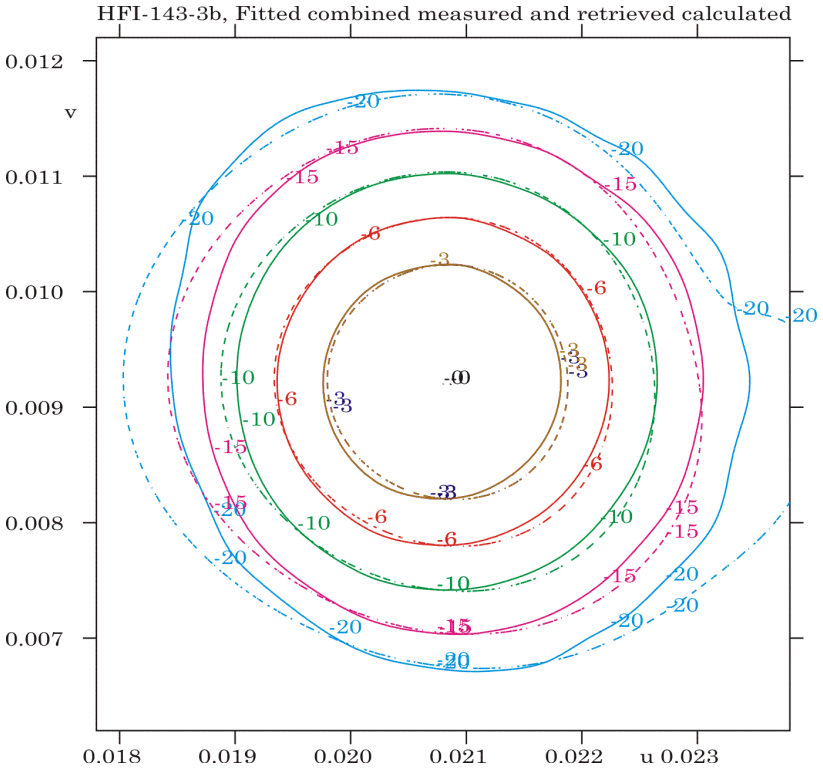

a) Measured (full line) and retrieved (dashed) power pattern

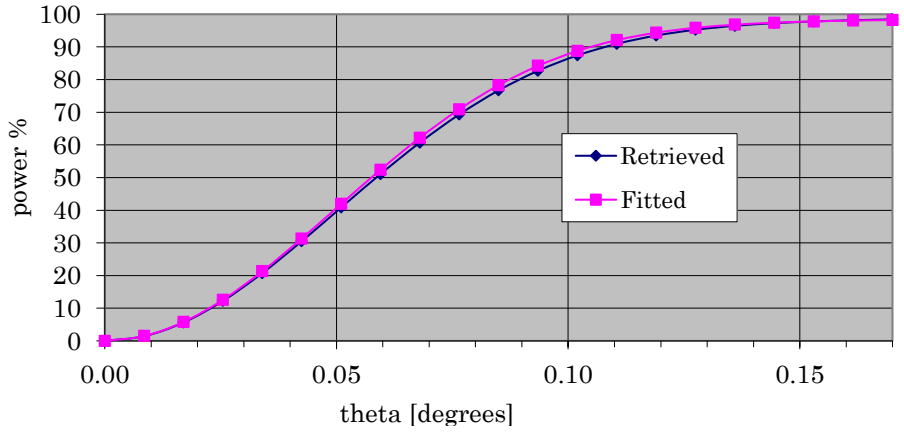

b) Azimuthally integrated power

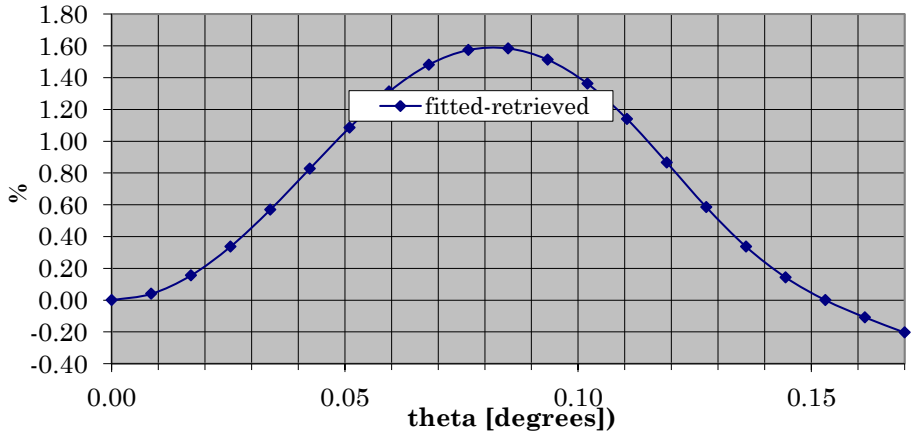

c) Difference

Figure 2-14 Kriging fitted measured and retrieved power pattern for 143 GHz detector, HFI-143-3b.

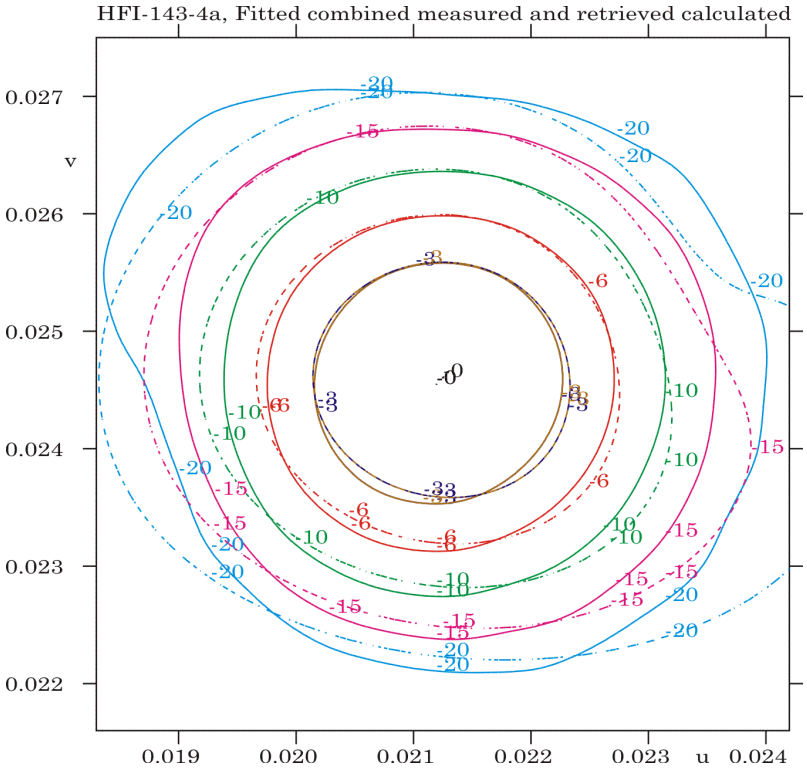

a) Measured (full line) and retrieved (dashed) power pattern

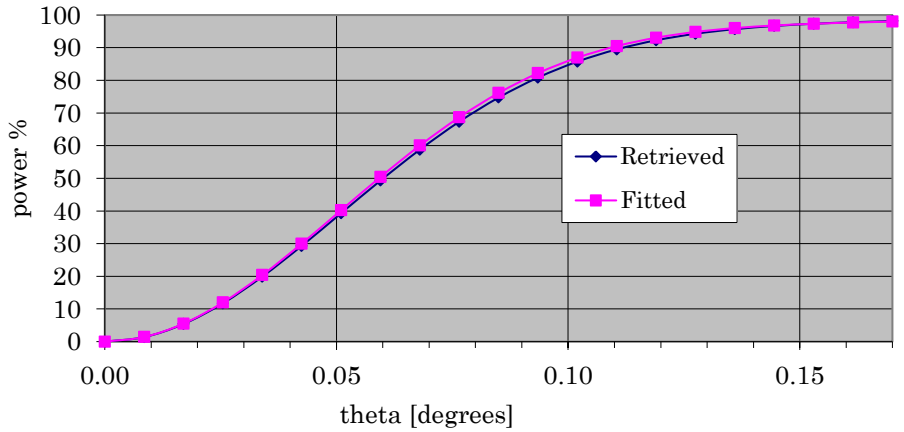

b) Azimuthally integrated power

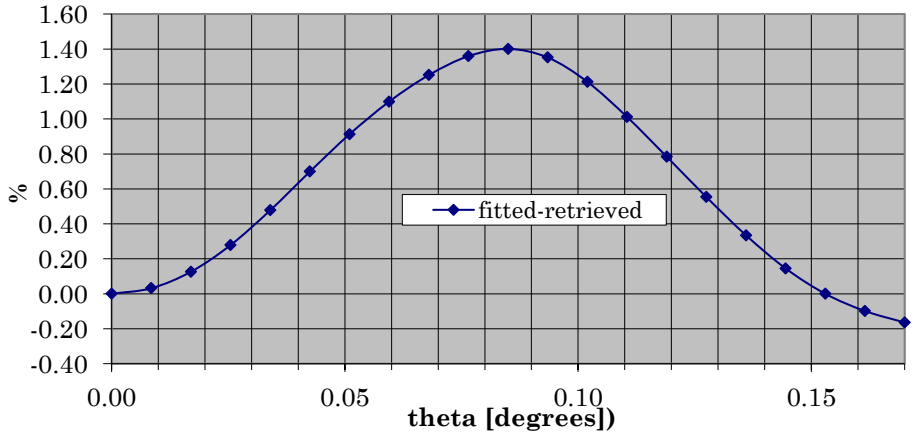

c) Difference

Figure 2-15 Kriging fitted measured and retrieved power pattern for 143 GHz detector, HFI-143-4a.

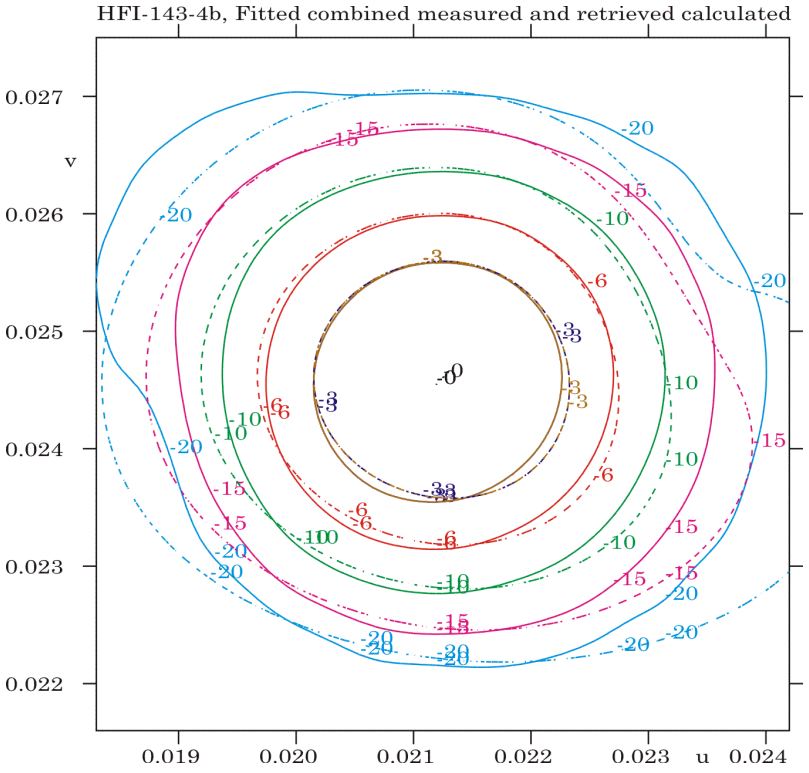

a) Measured (full line) and retrieved (dashed) power pattern

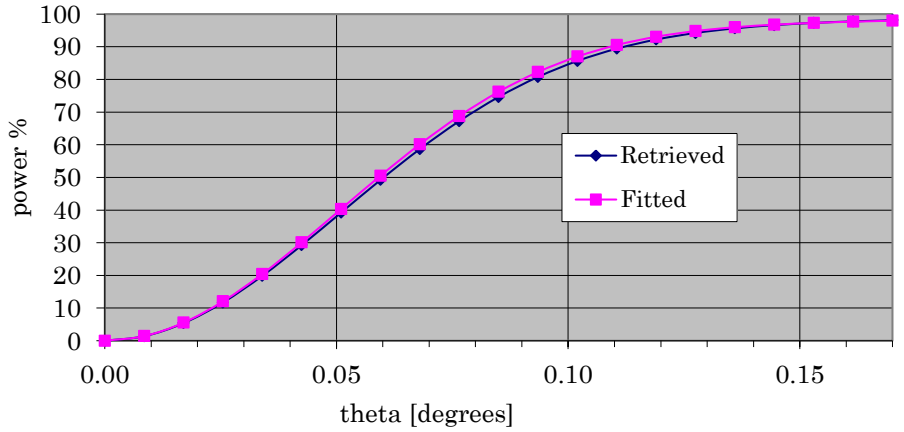

b) Azimuthally integrated power

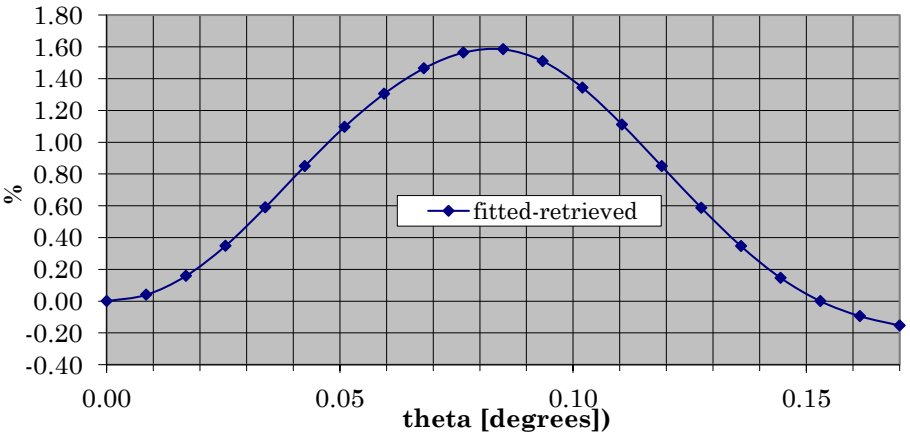

c) Difference

Figure 2-16 Kriging fitted measured and retrieved power pattern for 143 GHz detector, HFI-143-4b.

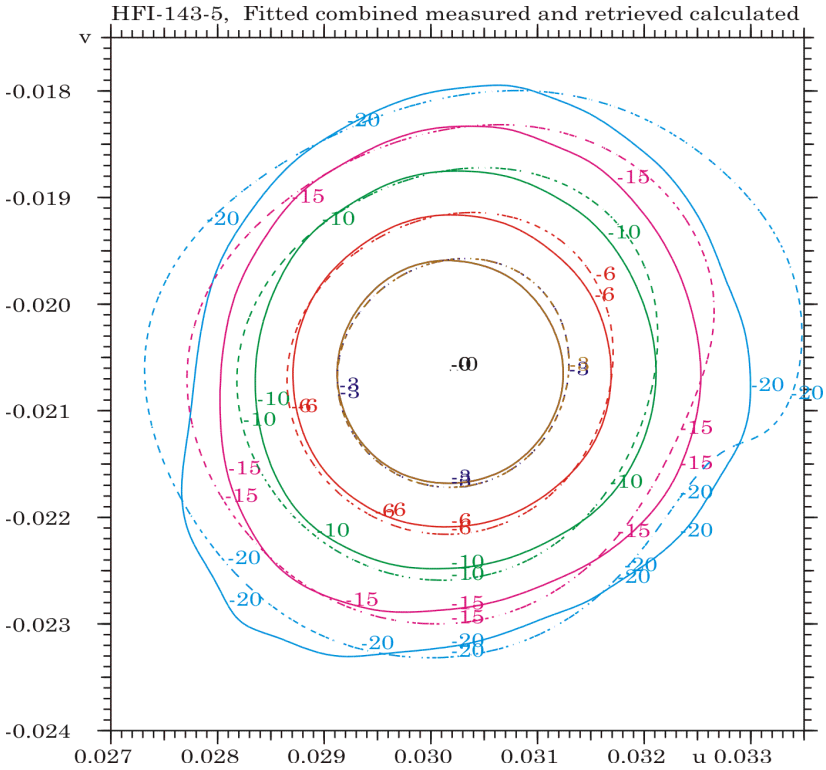

a) Measured (full line) and retrieved (dashed) power pattern

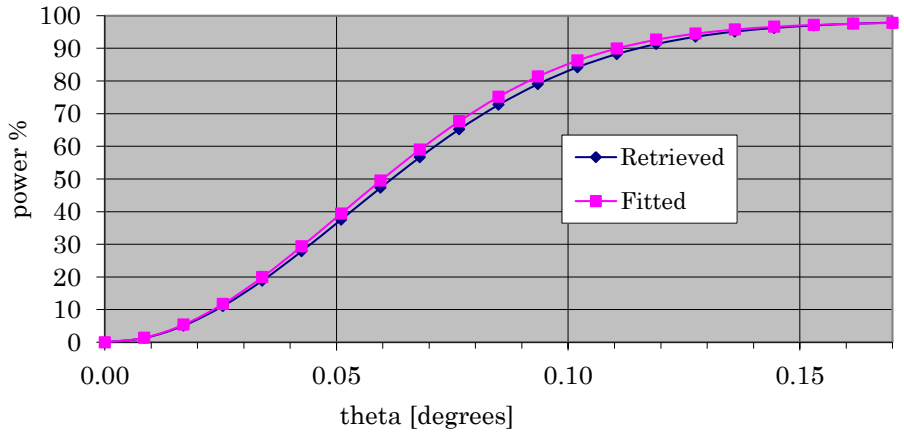

b) Azimuthally integrated power

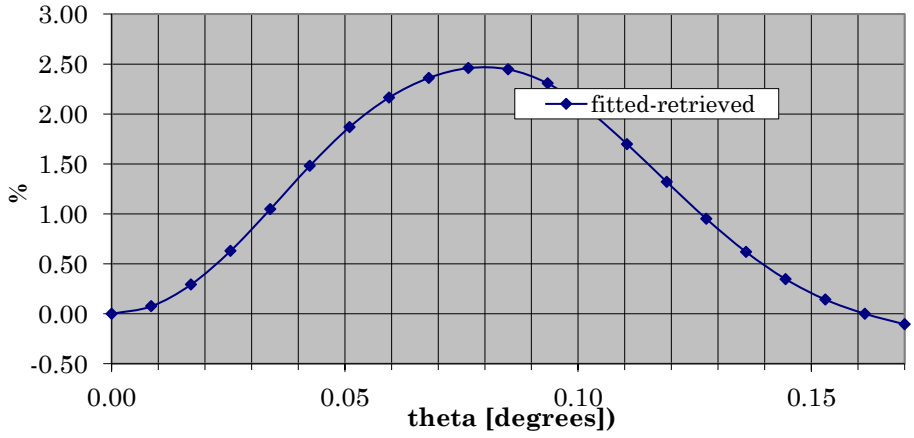

c) Difference

Figure 2-17 Kriging fitted measured and retrieved power pattern for 143 GHz detector, HFI-143-5.

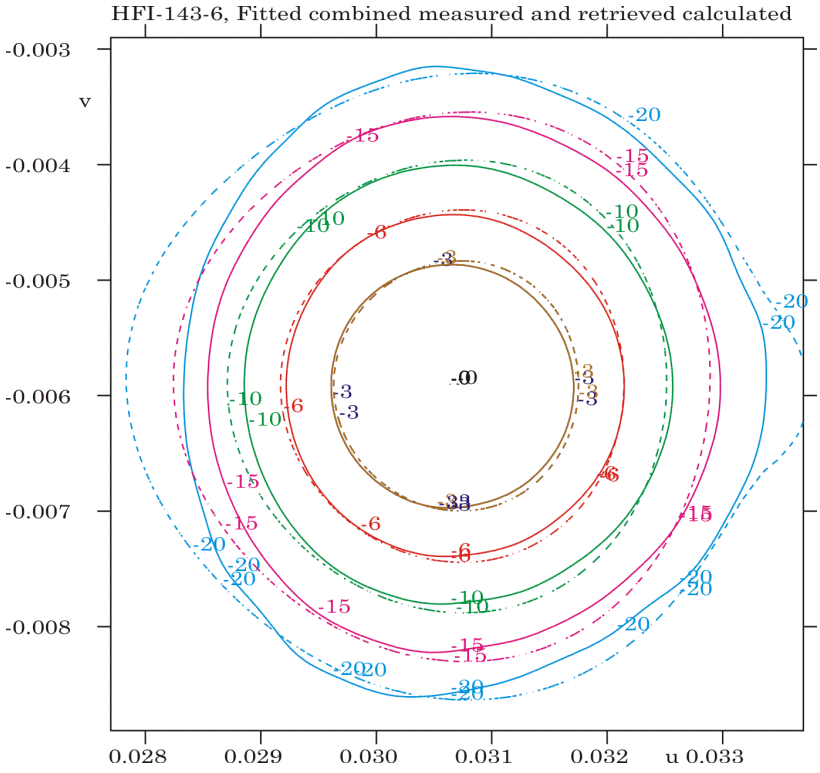

a) Measured (full line) and retrieved (dashed) power pattern

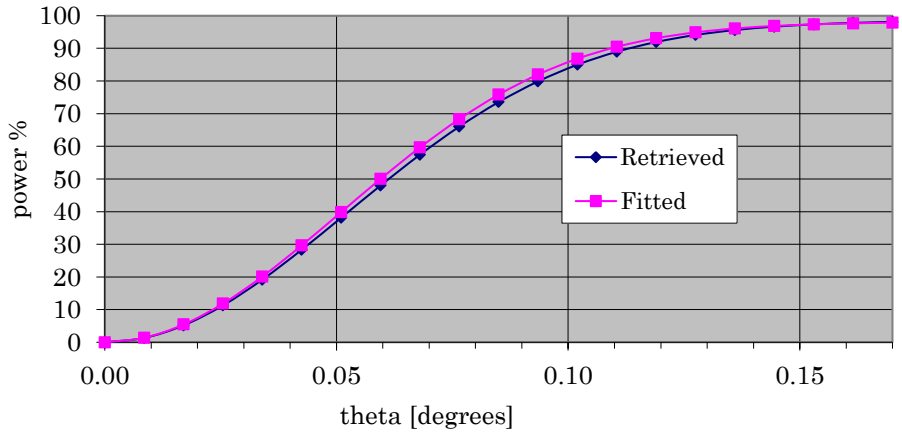

b) Azimuthally integrated power

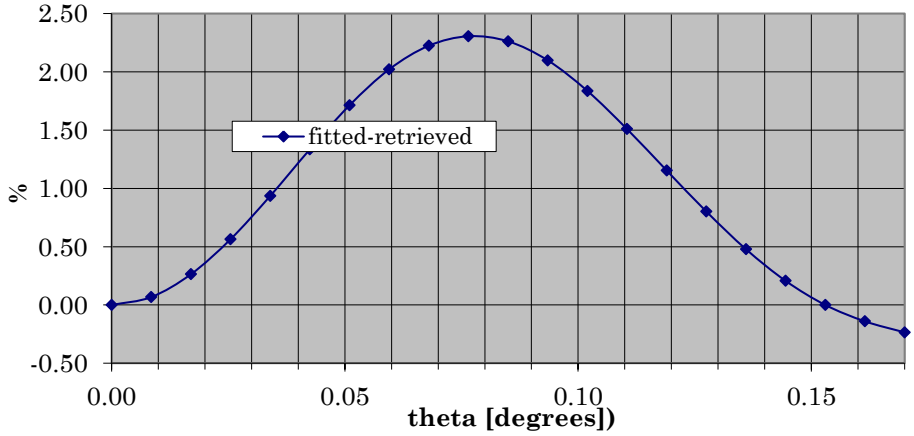

c) Difference

Figure 2-18 Kriging fitted measured and retrieved power pattern for 143 GHz detector, HFI-143-6.

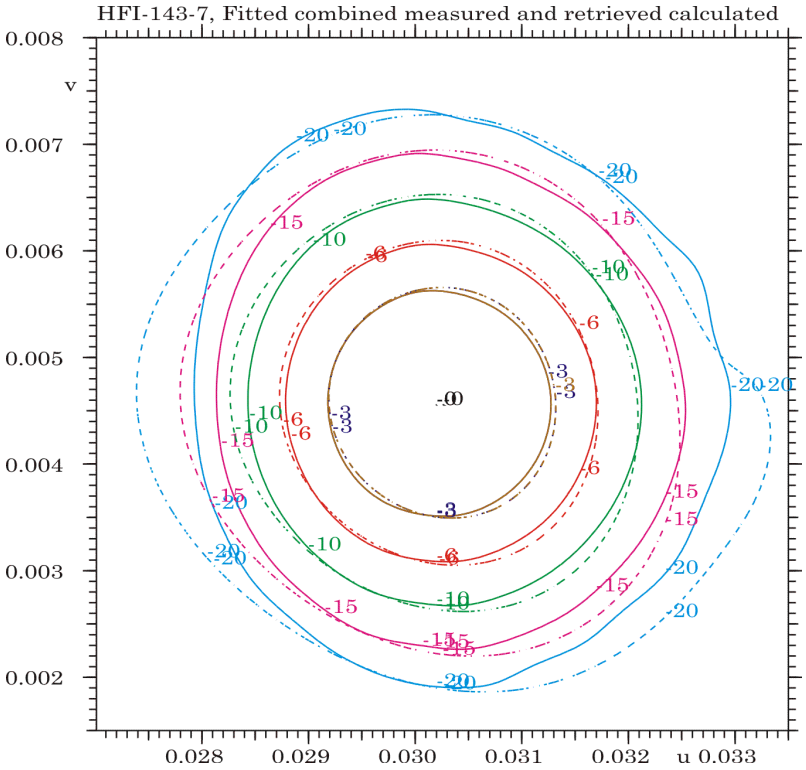

a) Measured (full line) and retrieved (dashed) power pattern

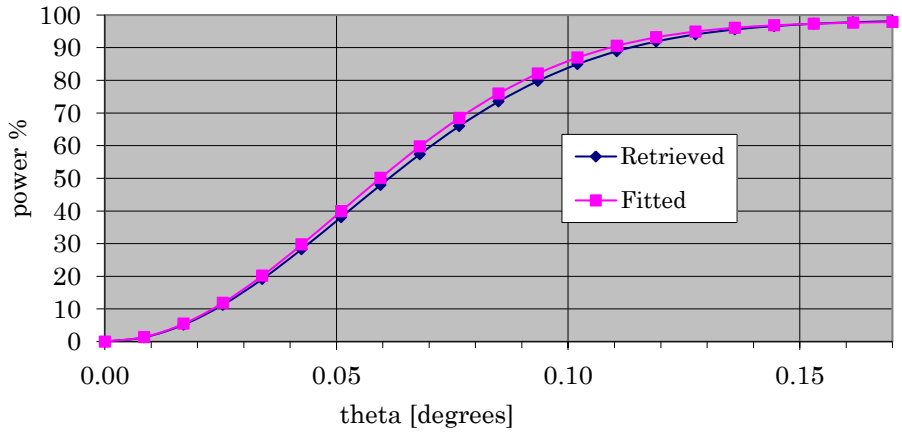

b) Azimuthally integrated power

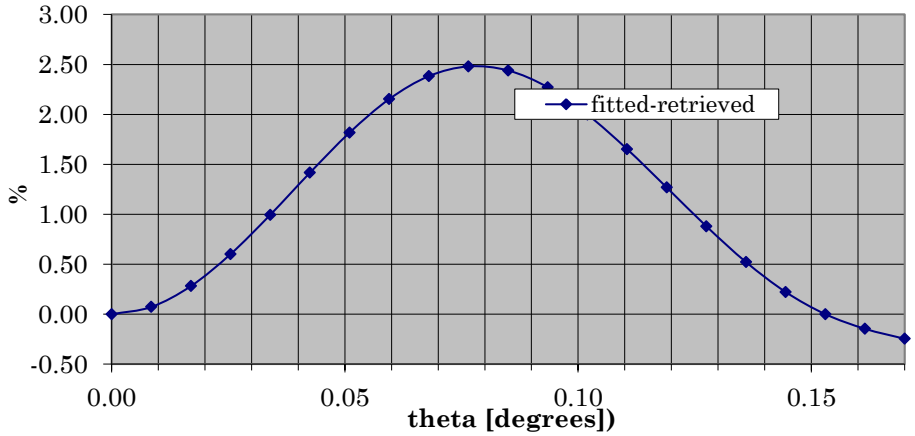

c) Difference

Figure 2-19 Kriging fitted measured and retrieved power pattern for 143 GHz detector, HFI-143-7.

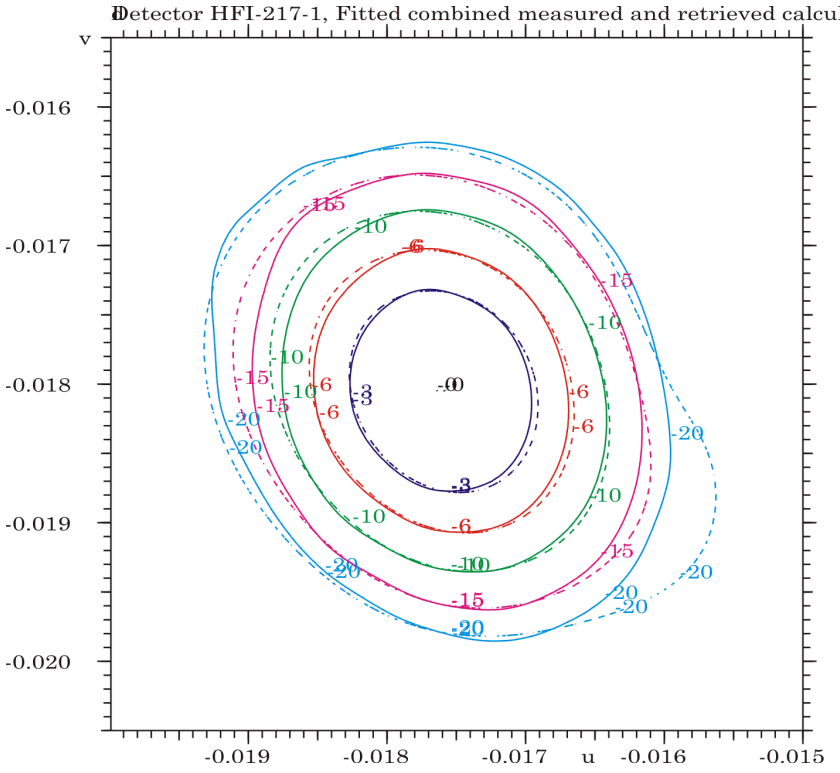

a) Measured (full line) and retrieved (dashed) power pattern

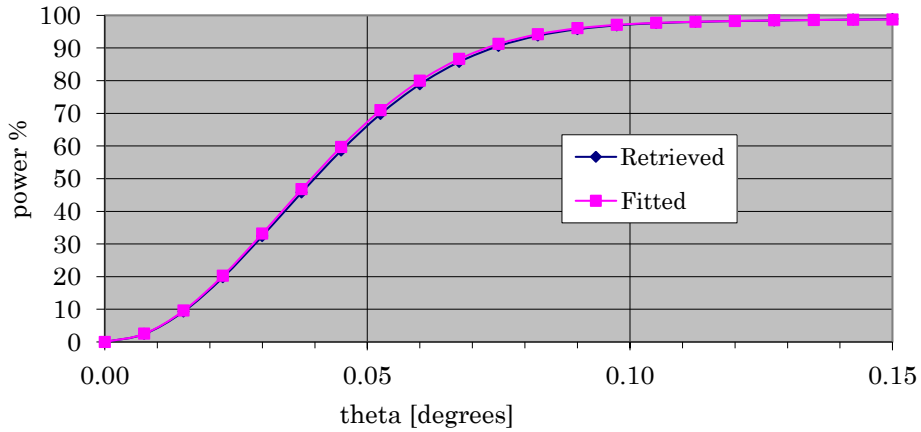

b) Azimuthally integrated power

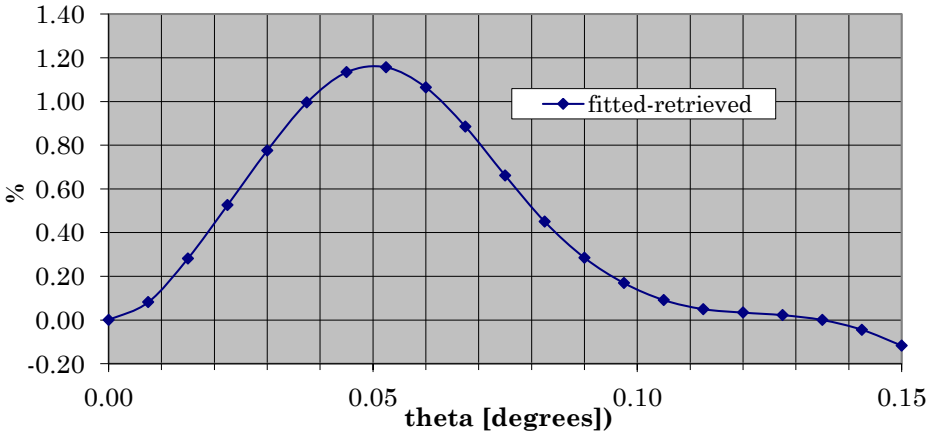

c) Difference

Figure 2-20 Kriging fitted measured and retrieved power pattern for 217 GHz detector, HFI-217-1.

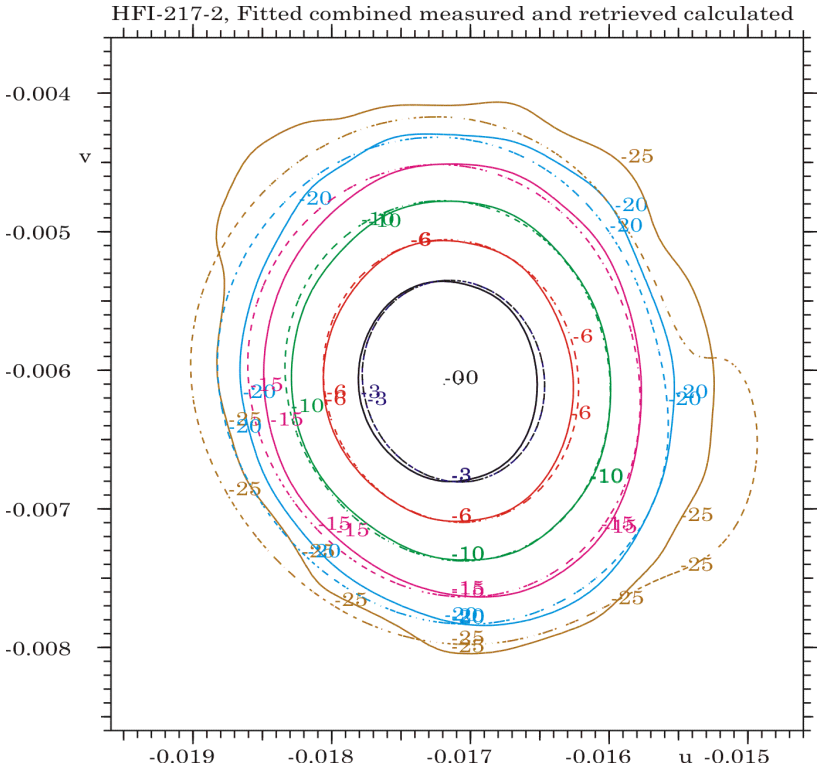

a) Measured (full line) and retrieved (dashed) power pattern

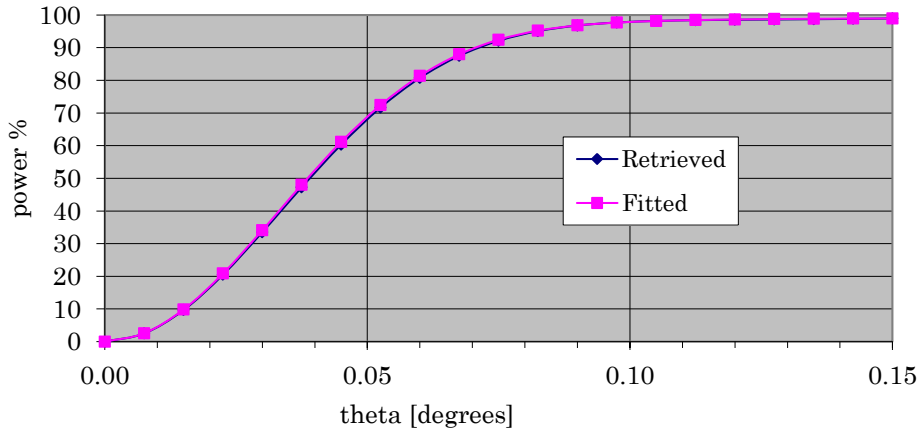

b) Azimuthally integrated power

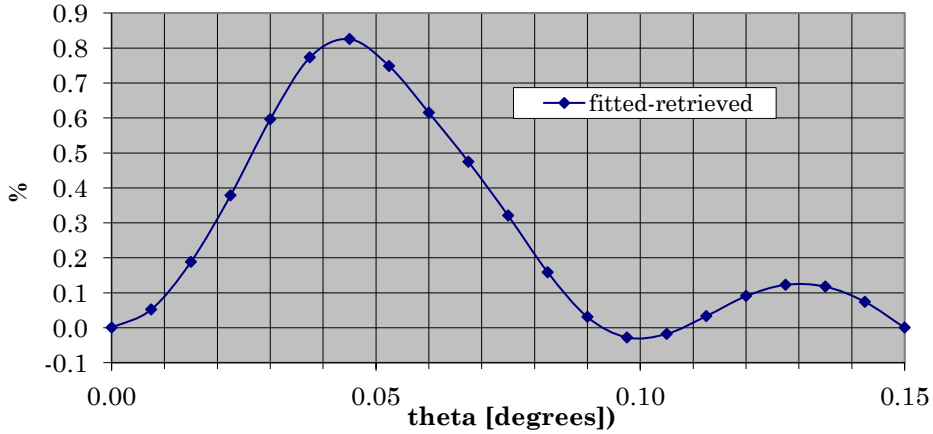

c) Difference

Figure 2-21 Kriging fitted measured and retrieved power pattern for 217 GHz detector, HFI-217-2.

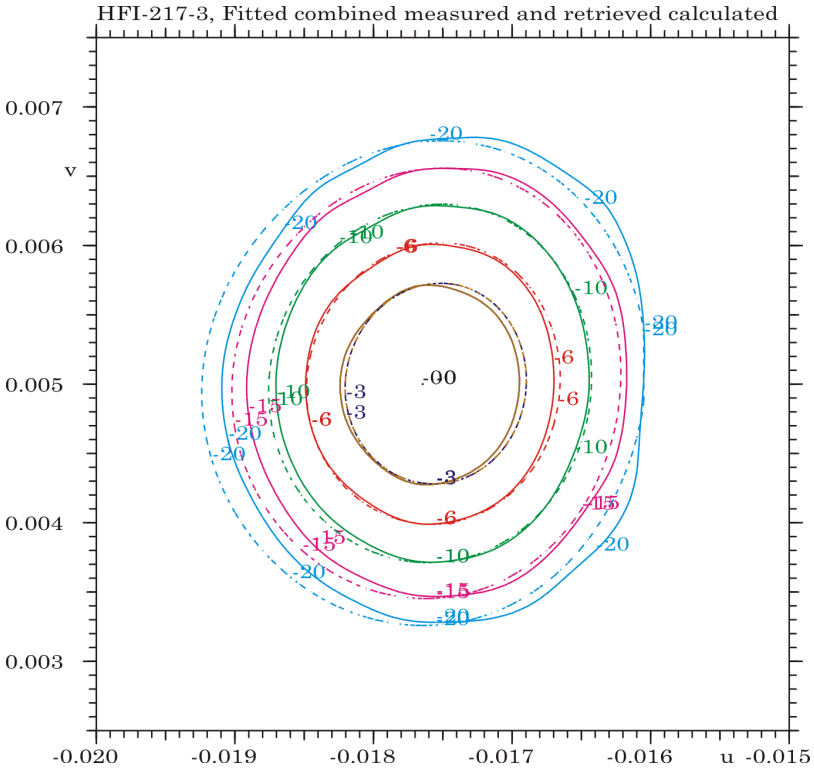

a) Measured (full line) and retrieved (dashed) power pattern

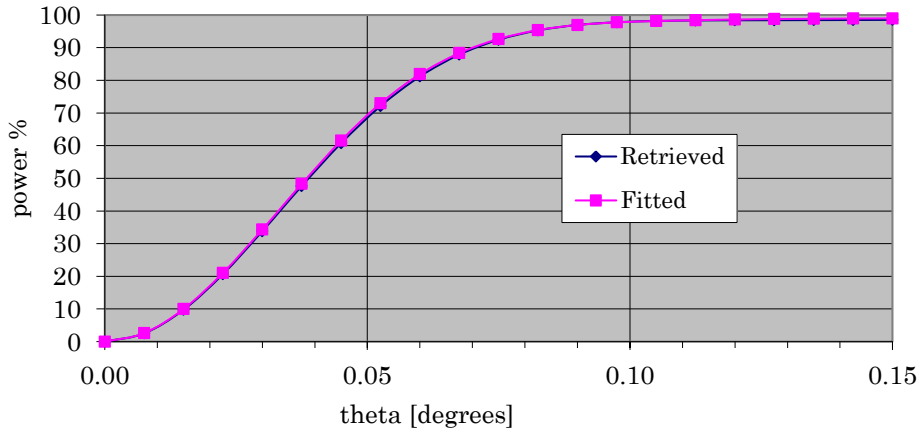

b) Azimuthally integrated power

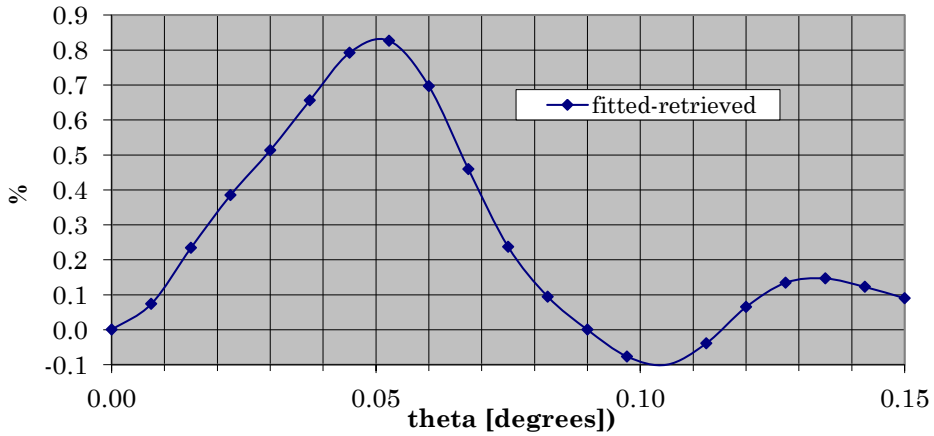

c) Difference

Figure 2-22 Kriging fitted measured and retrieved power pattern for 217 GHz detector, HFI-217-3.

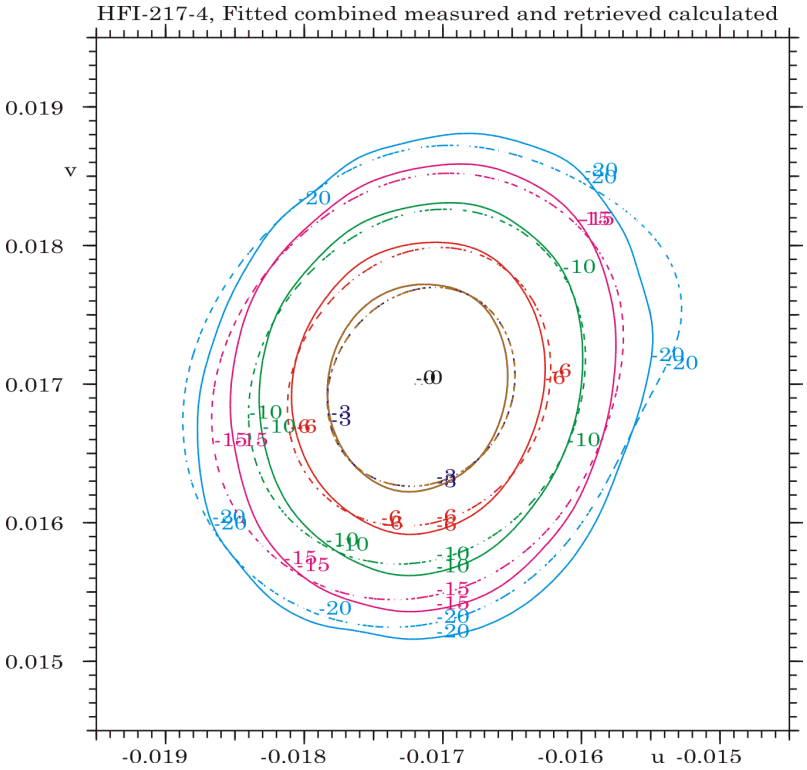

a) Measured (full line) and retrieved (dashed) power pattern

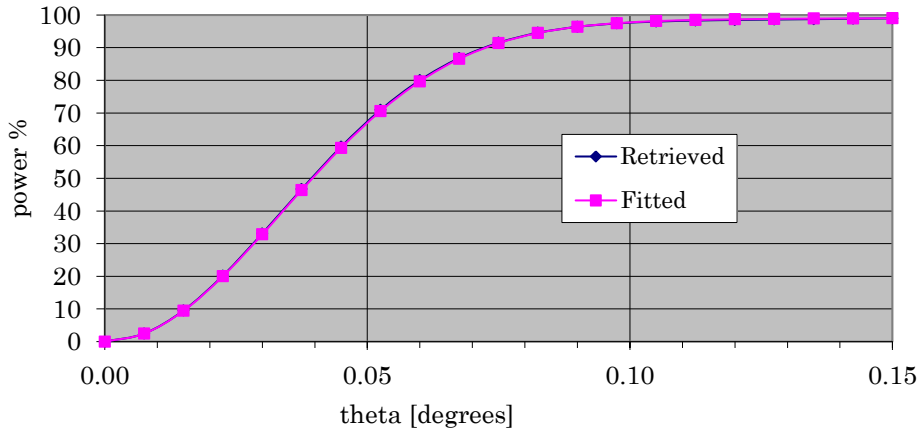

b) Azimuthally integrated power

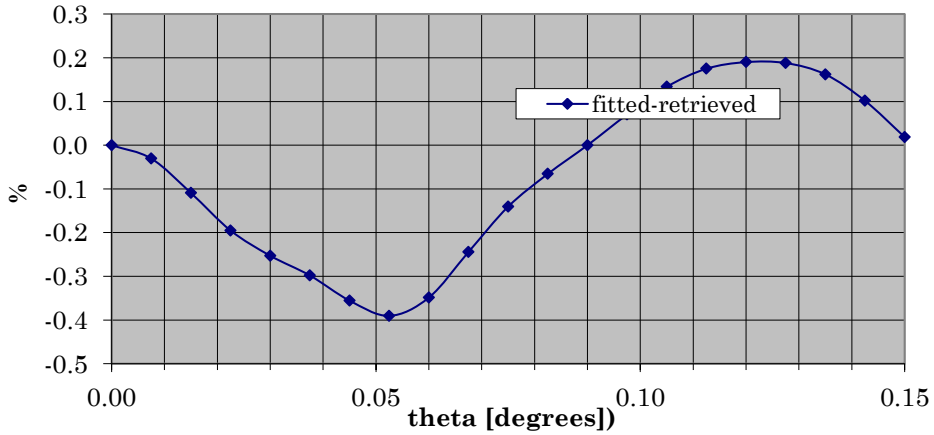

c) Difference

Figure 2-23 Kriging fitted measured and retrieved power pattern for 217 GHz detector, HFI-217-4.

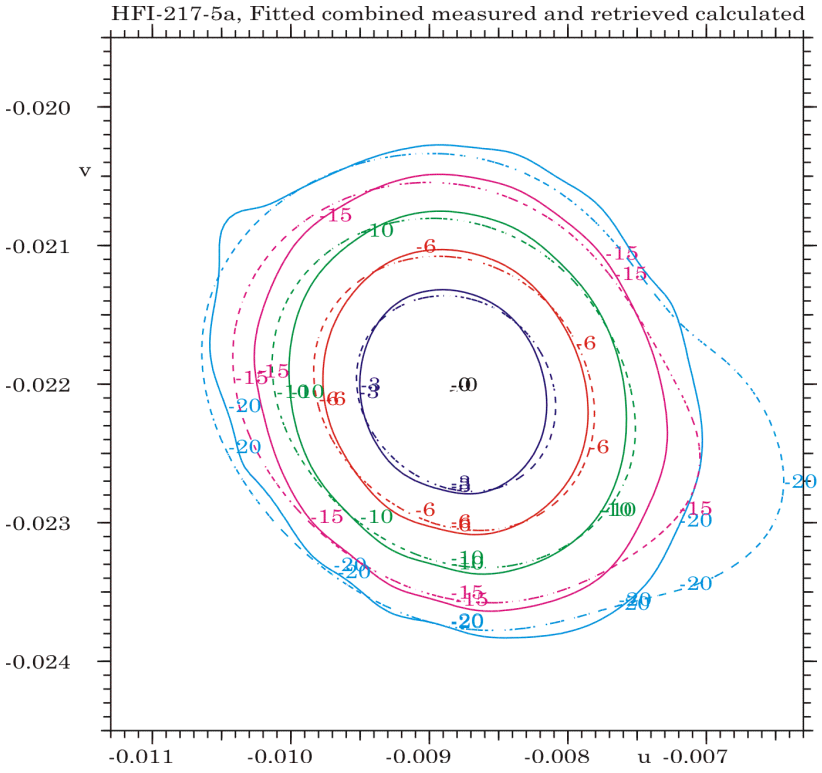

a) Measured (full line) and retrieved (dashed) power pattern

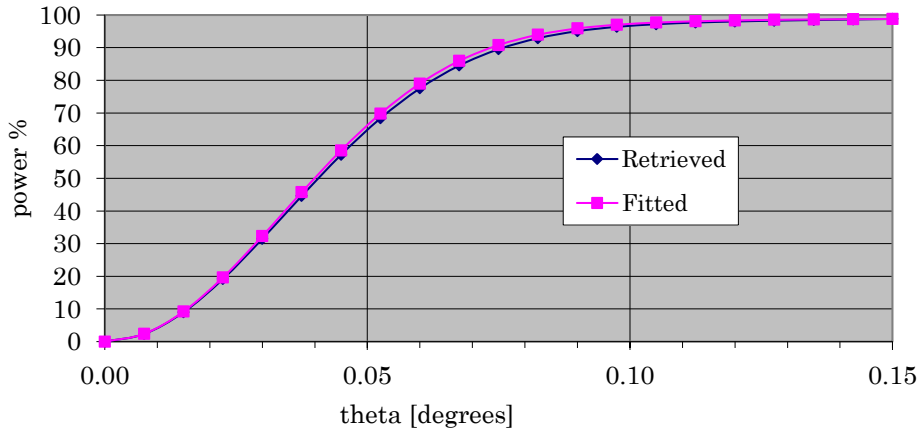

b) Azimuthally integrated power

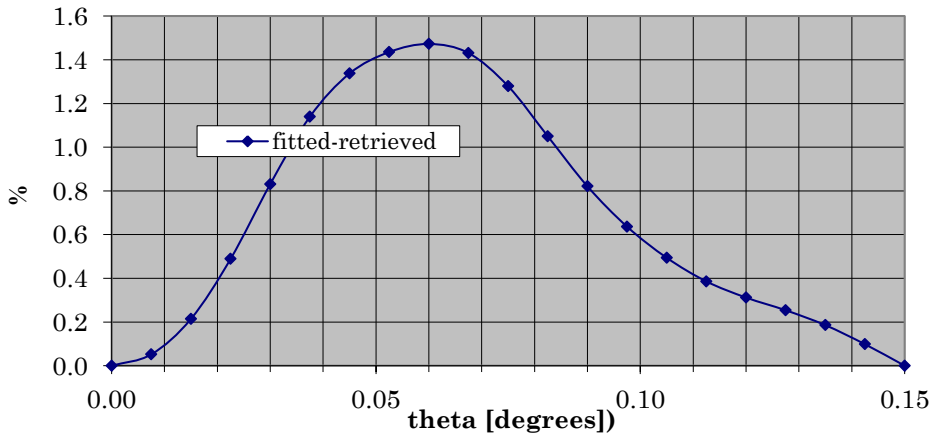

c) Difference

Figure 2-24 Kriging fitted measured and retrieved power pattern for 217 GHz detector, HFI-217-5a.

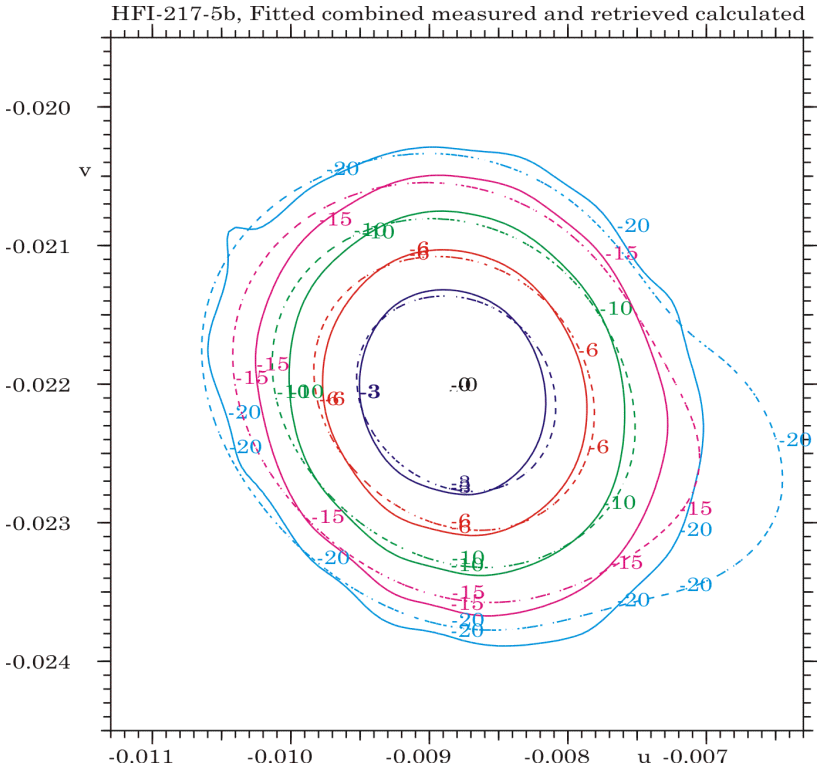

a) Measured (full line) and retrieved (dashed) power pattern

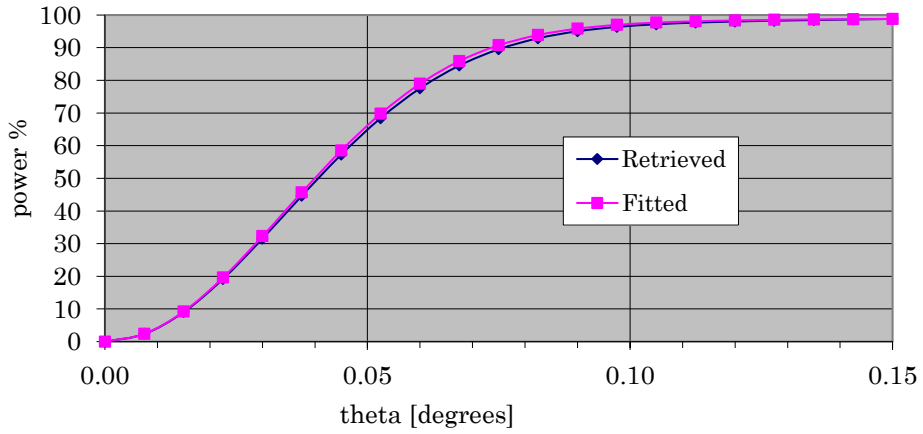

b) Azimuthally integrated power

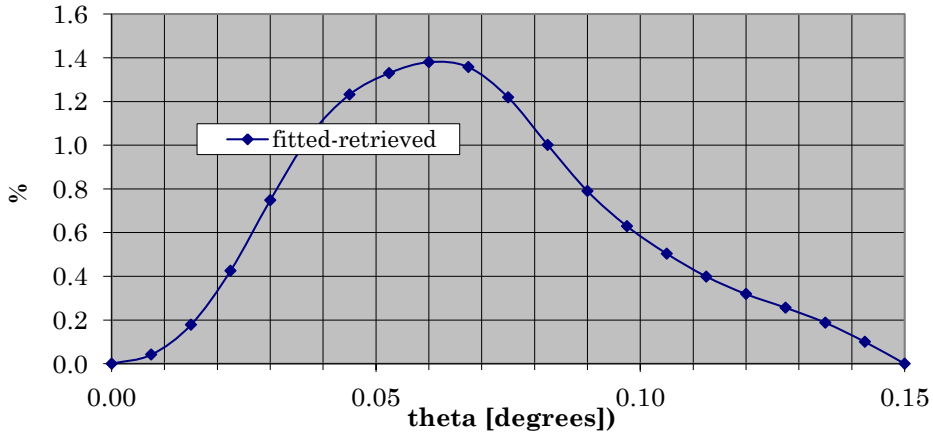

c) Difference

Figure 2-25 Kriging fitted measured and retrieved power pattern for 217 GHz detector, HFI-217-5b.

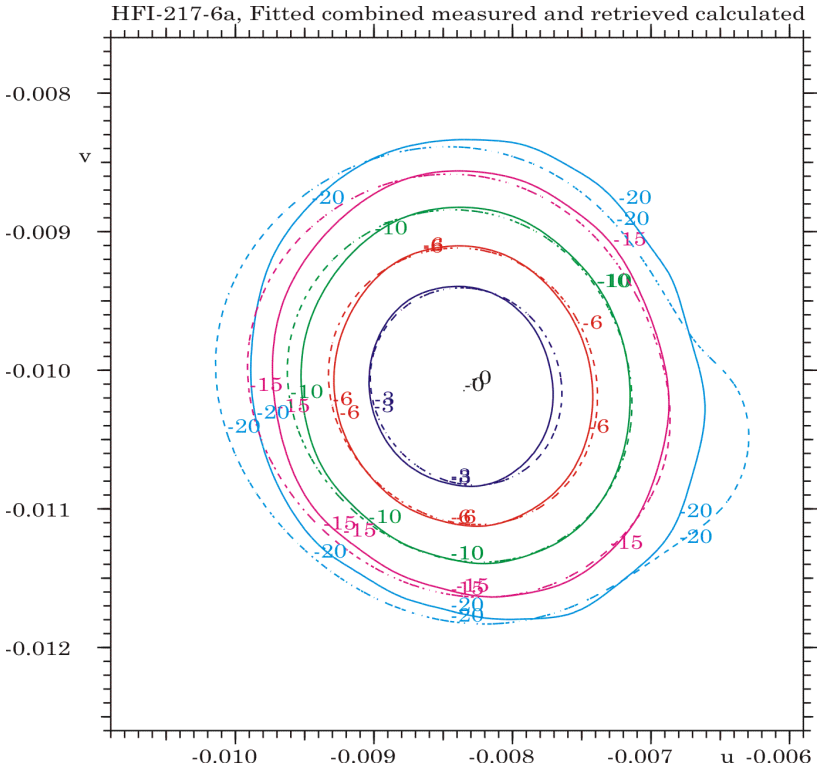

a) Measured (full line) and retrieved (dashed) power pattern

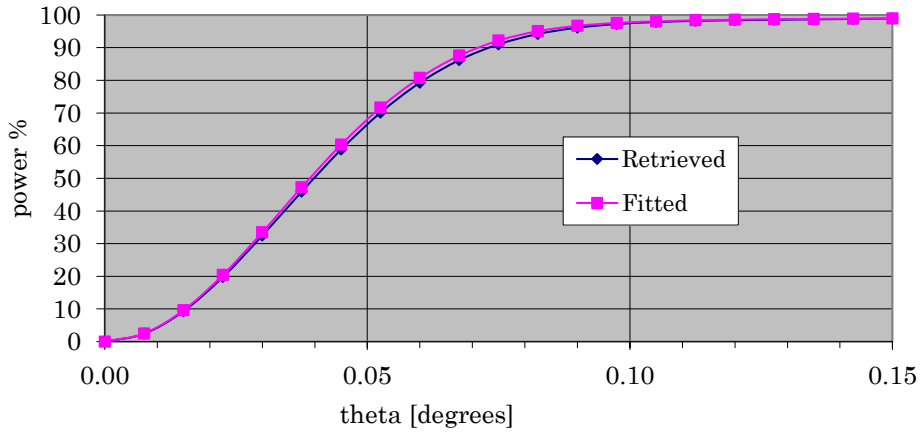

b) Azimuthally integrated power

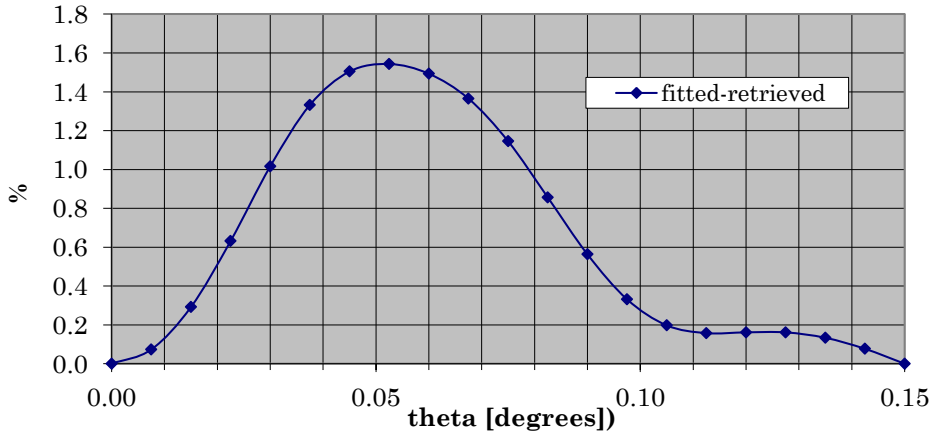

c) Difference

Figure 2-26 Kriging fitted measured and retrieved power pattern for 217 GHz detector, HFI-217-6a.

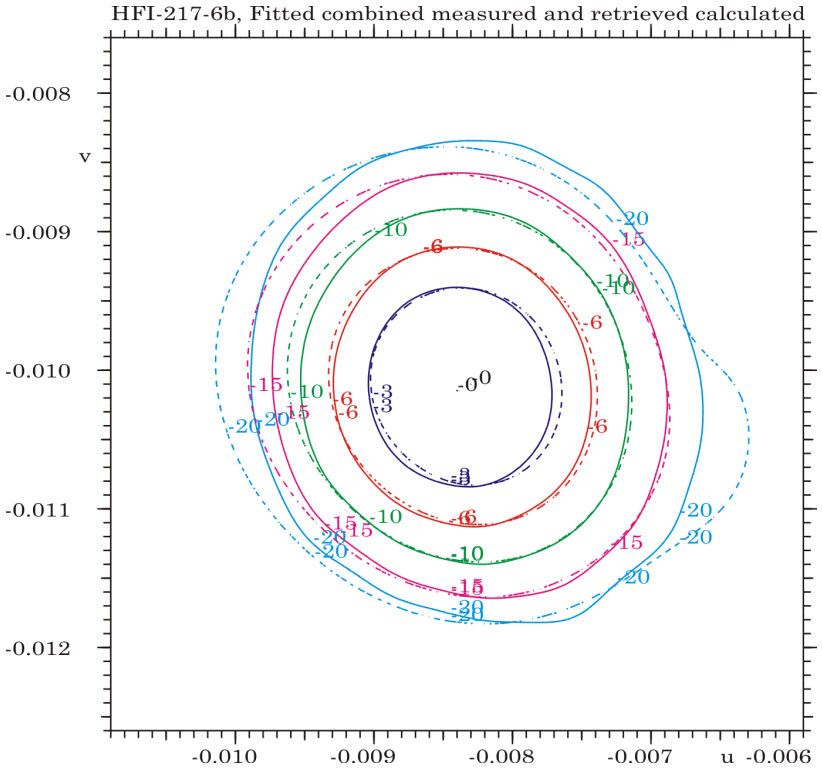

a) Measured (full line) and retrieved (dashed) power pattern

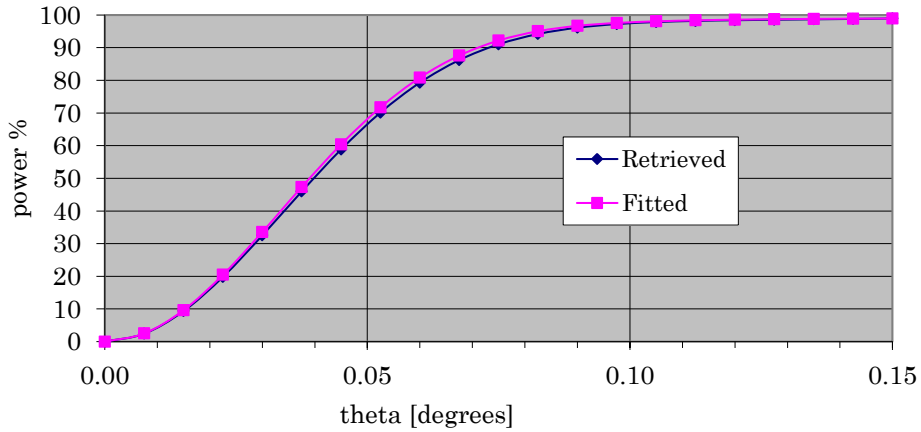

b) Azimuthally integrated power

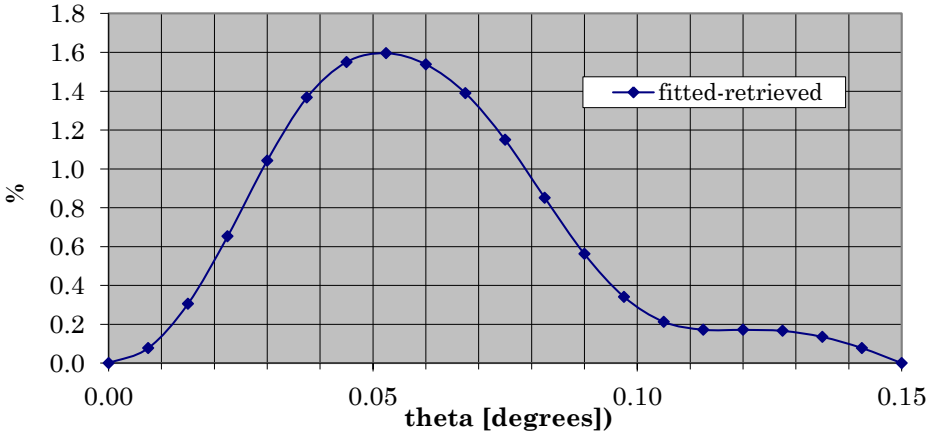

c) Difference

Figure 2-27 Kriging fitted measured and retrieved power pattern for 217 GHz detector, HFI-217-6b.

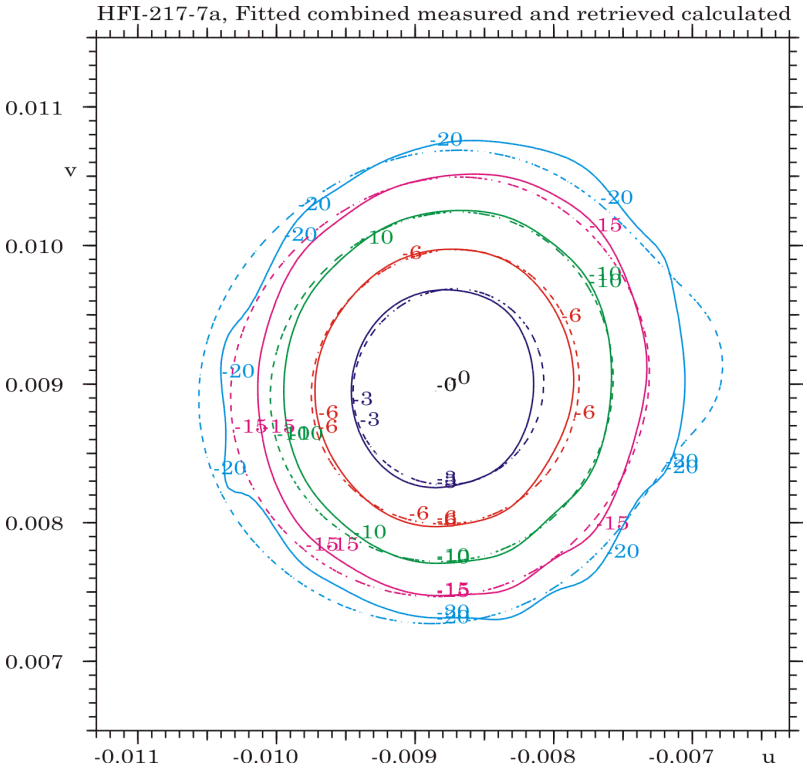

a) Measured (full line) and retrieved (dashed) power pattern

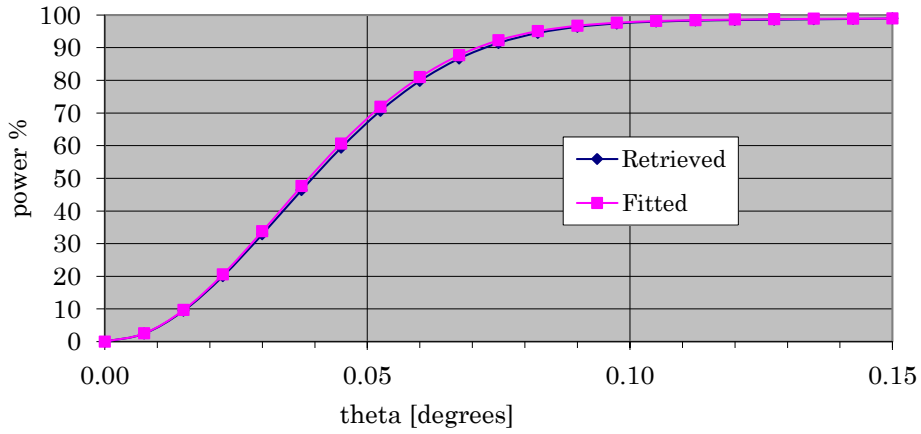

b) Azimuthally integrated power

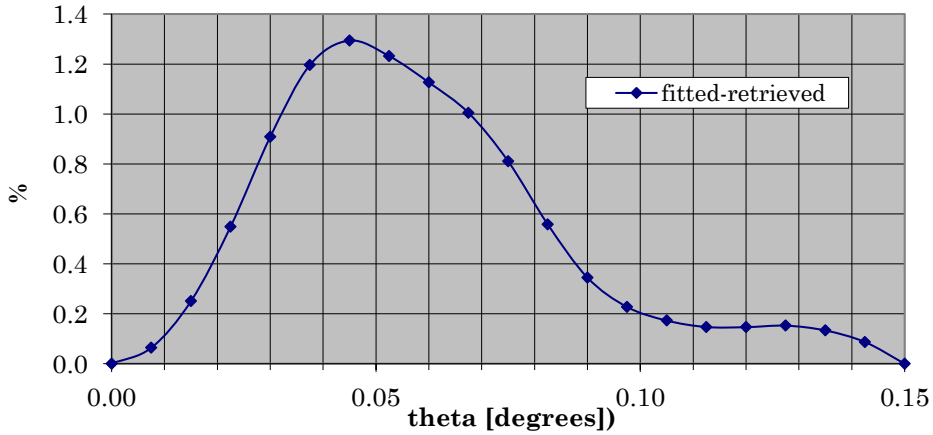

c) Difference

Figure 2-28 Kriging fitted measured and retrieved power pattern for 217 GHz detector, HFI-217-7a.

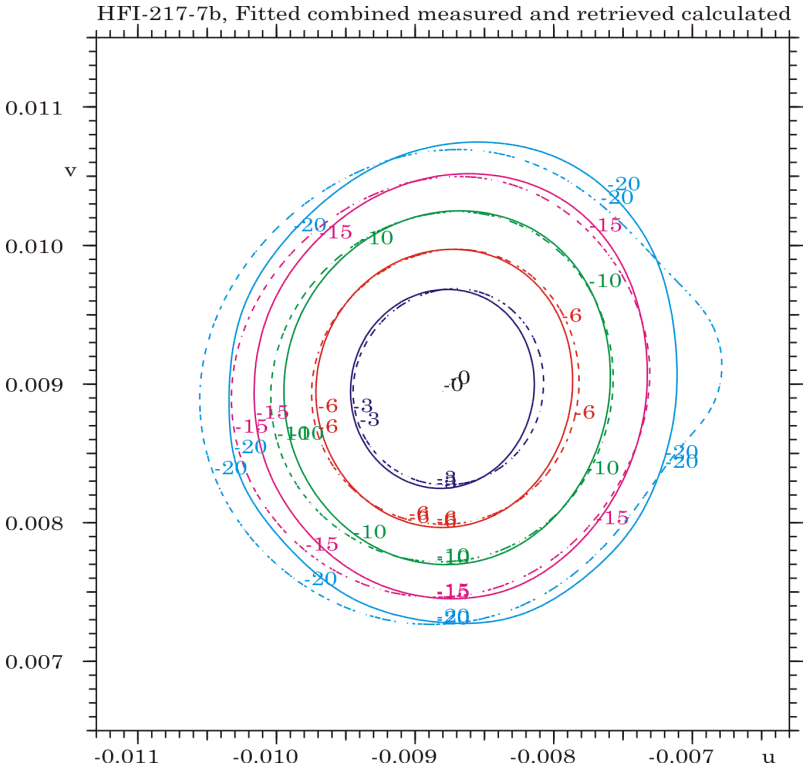

a) Measured (full line) and retrieved (dashed) power pattern

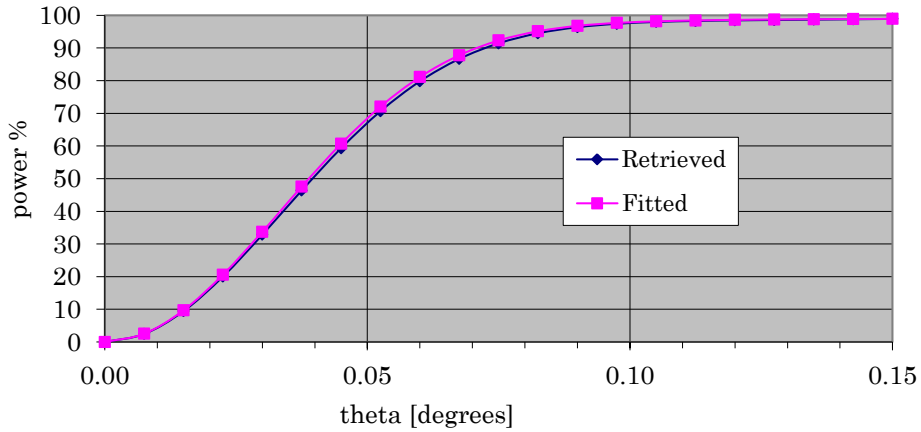

b) Azimuthally integrated power

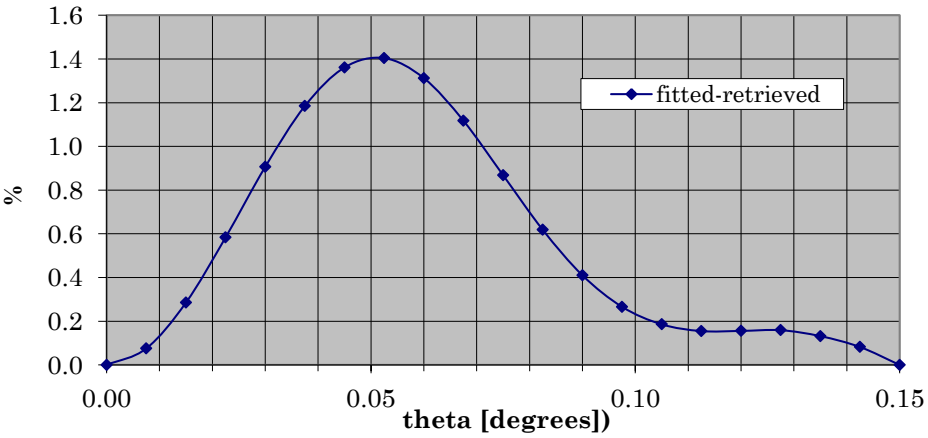

c) Difference

Figure 2-29 Kriging fitted measured and retrieved power pattern for 217 GHz detector, HFI-217-7b.

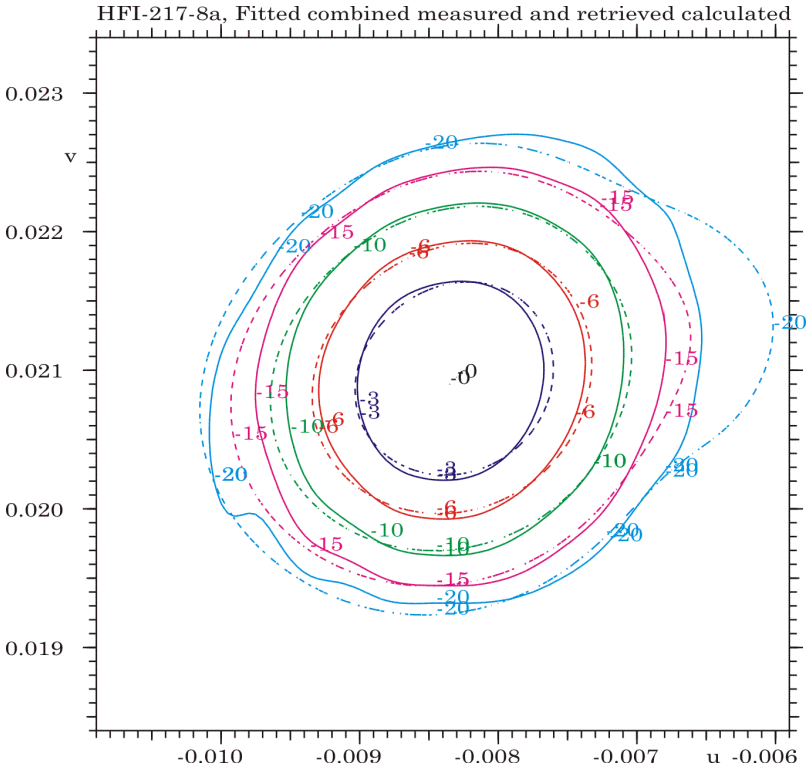

a) Measured (full line) and retrieved (dashed) power pattern

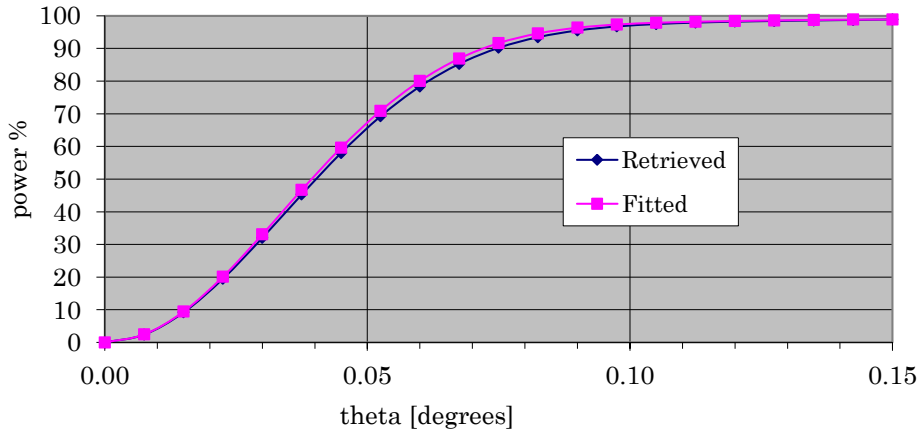

b) Azimuthally integrated power

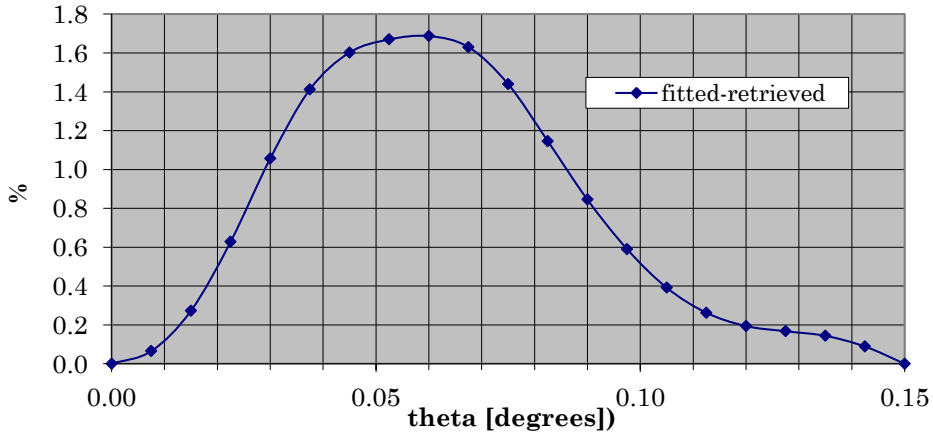

c) Difference

Figure 2-30 Kriging fitted measured and retrieved power pattern for 217 GHz detector, HFI-217-8a.

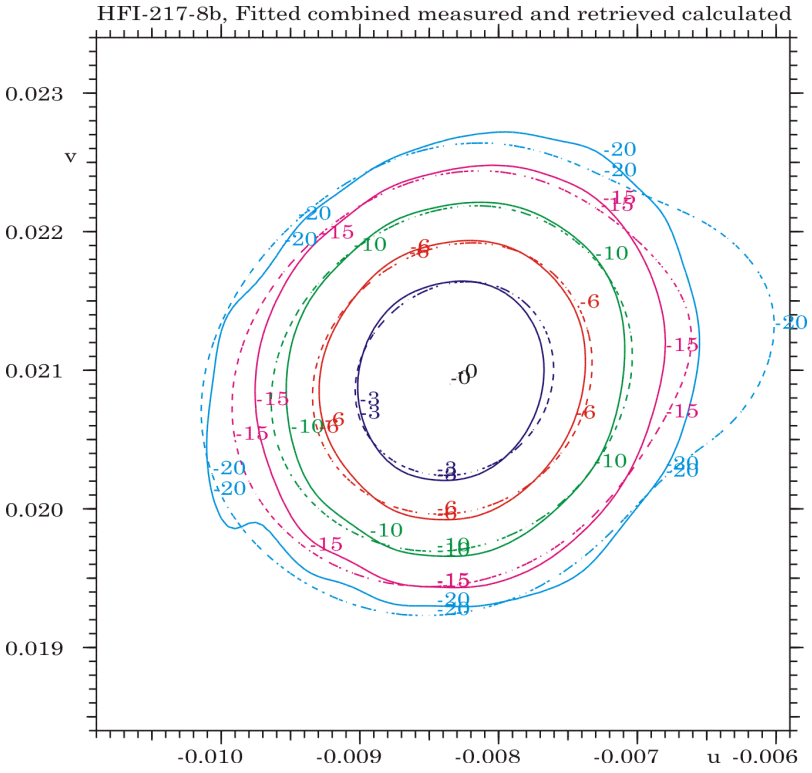

a) Measured (full line) and retrieved (dashed) power pattern

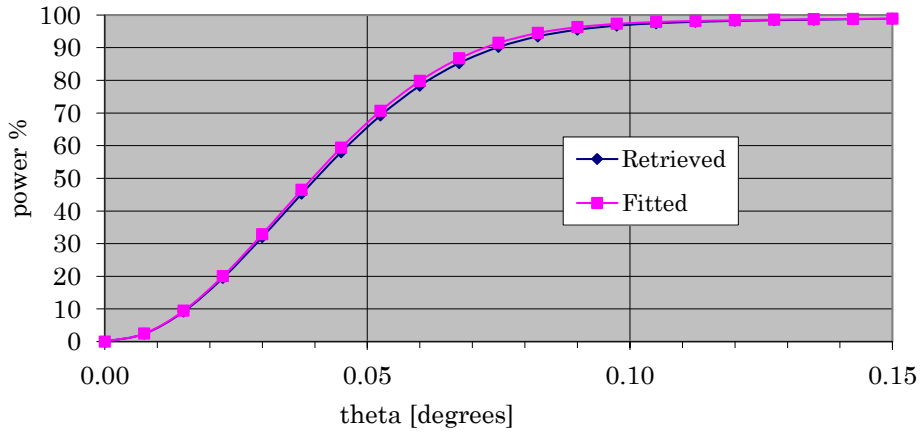

b) Azimuthally integrated power

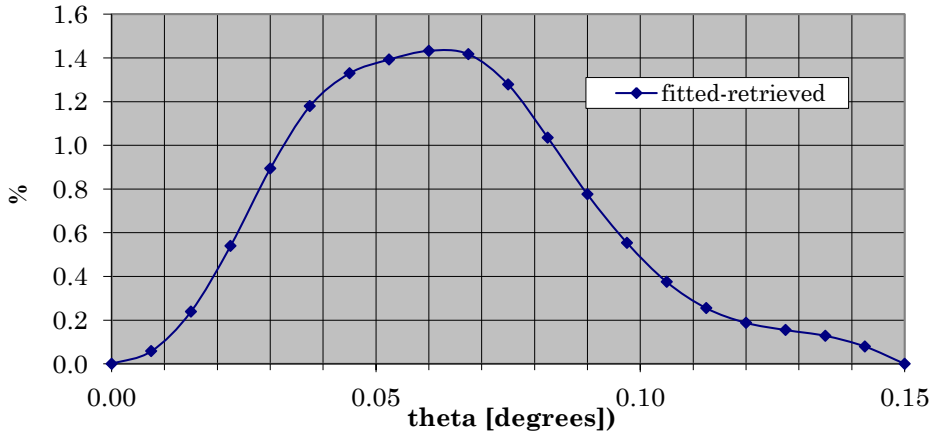

c) Difference

Figure 2-31 Kriging fitted measured and retrieved power pattern for 217 GHz detector, HFI-217-8b.

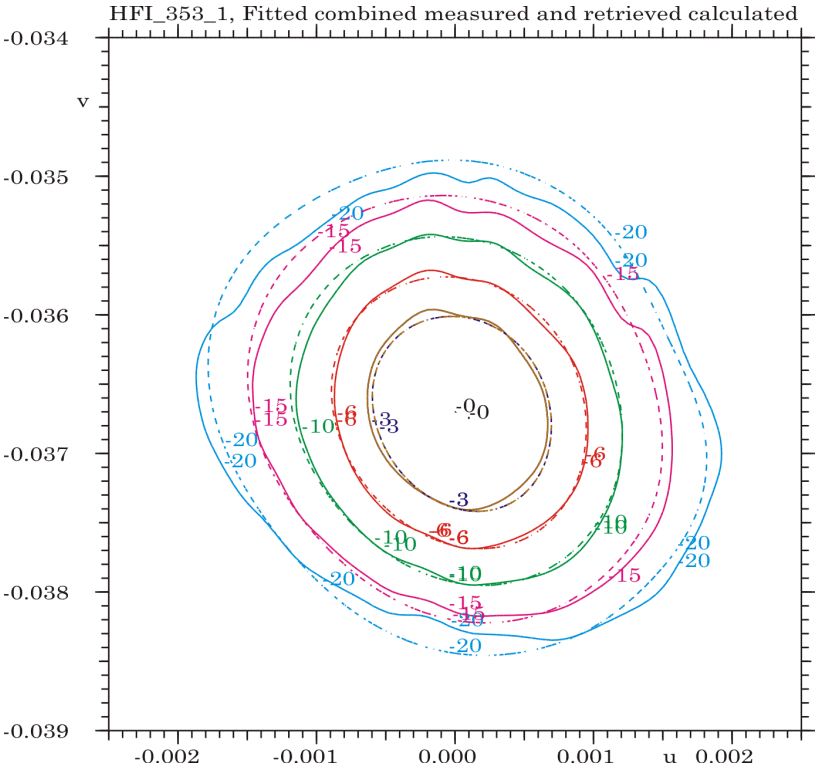

a) Measured (full line) and retrieved (dashed) power pattern

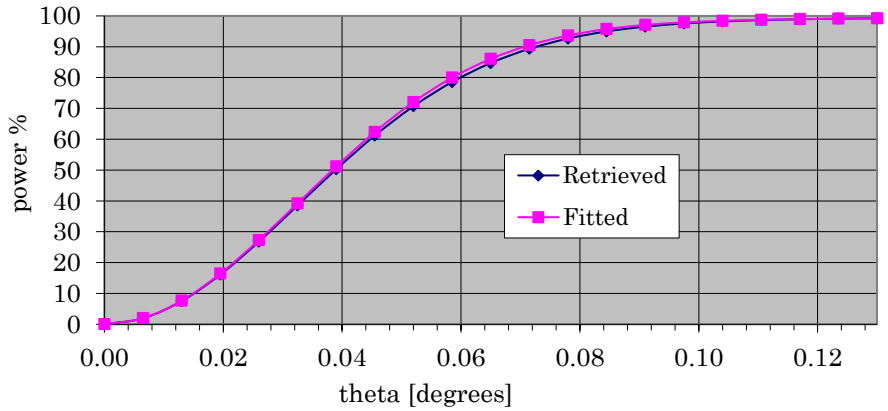

b) Azimuthally integrated power

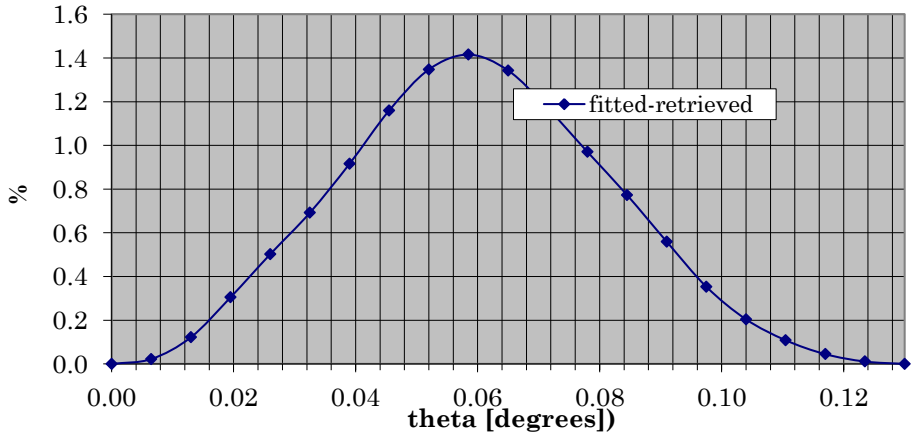

c) Difference

Figure 2-32 Kriging fitted measured and retrieved power pattern for 353 GHz detector, HFI-353-1.

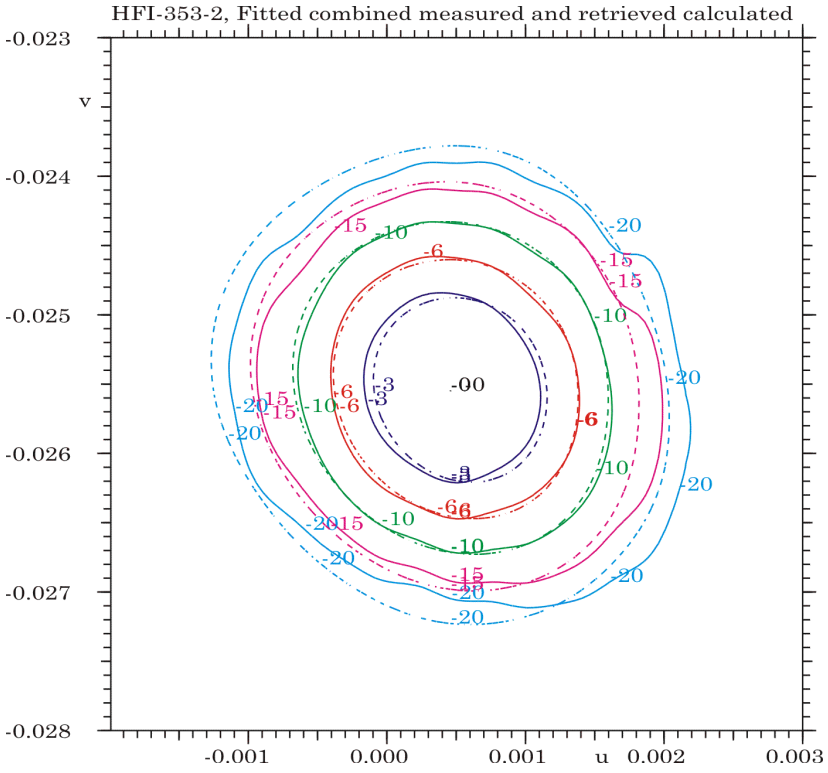

a) Measured (full line) and retrieved (dashed) power pattern

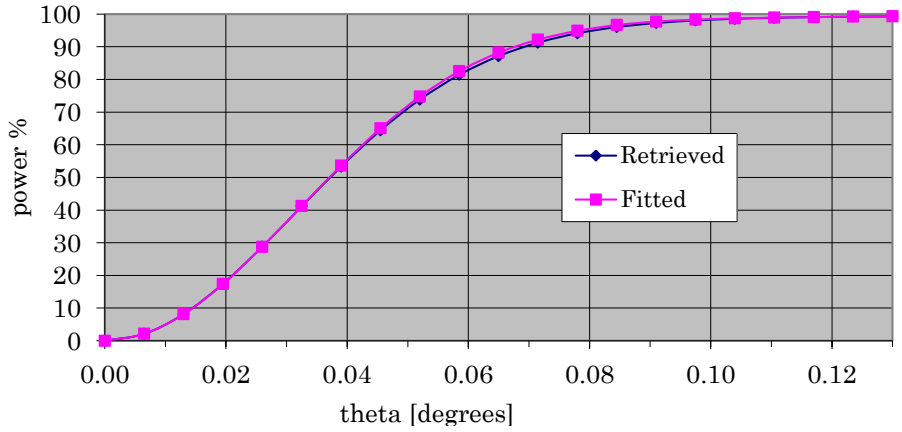

b) Azimuthally integrated power

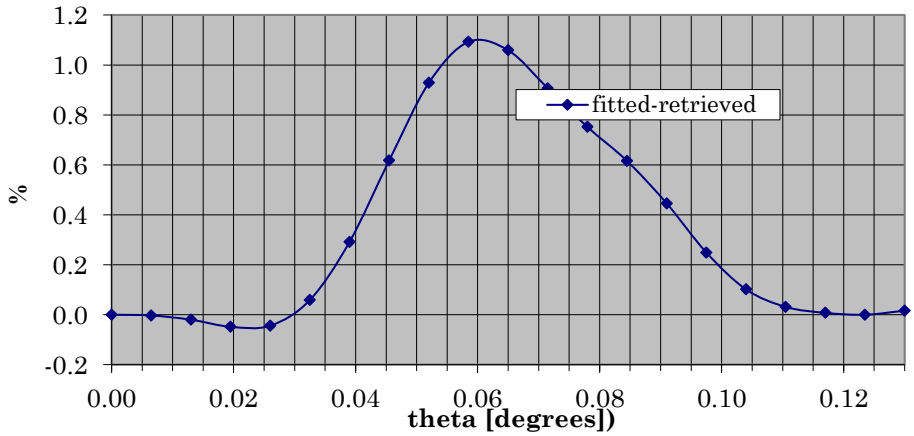

c) Difference

Figure 2-33 Kriging fitted measured and retrieved power pattern for 353 GHz detector, HFI-353-2.

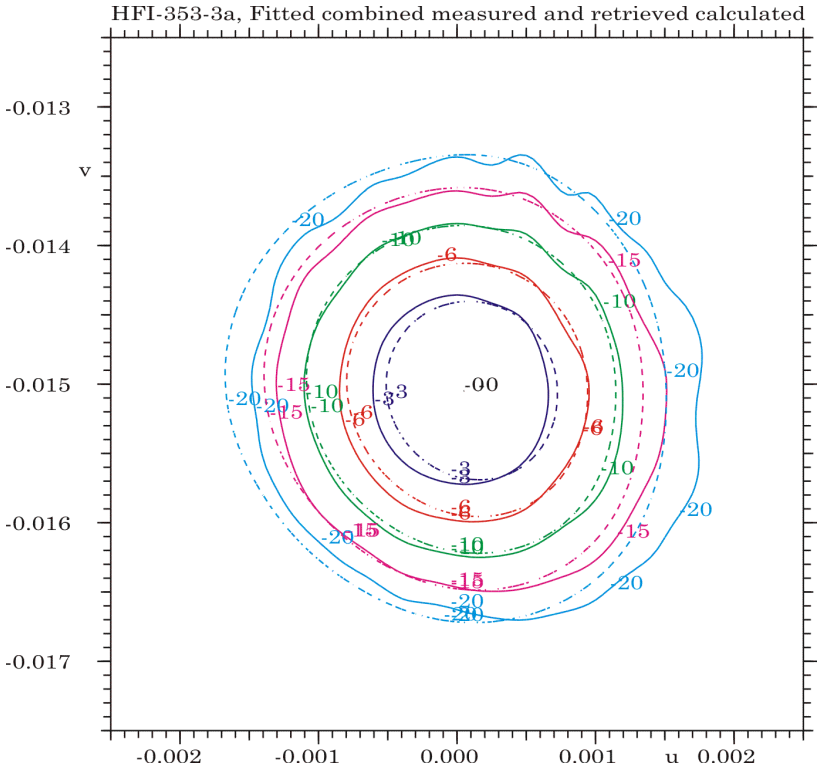

a) Measured (full line) and retrieved (dashed) power pattern

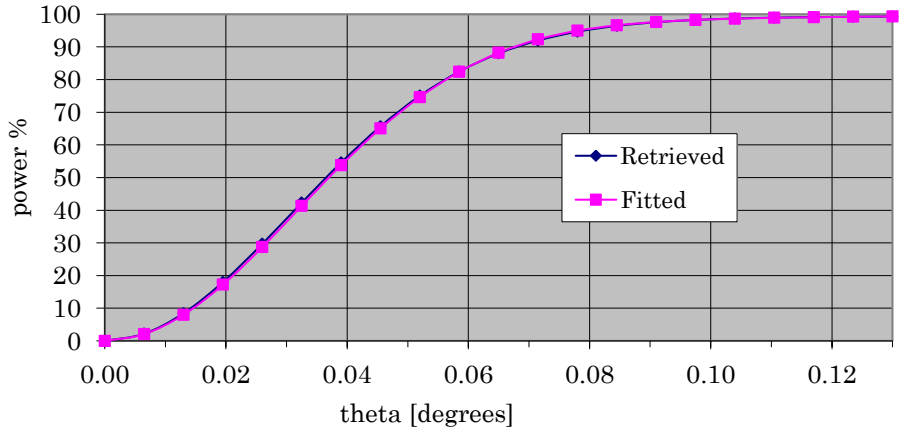

b) Azimuthally integrated power

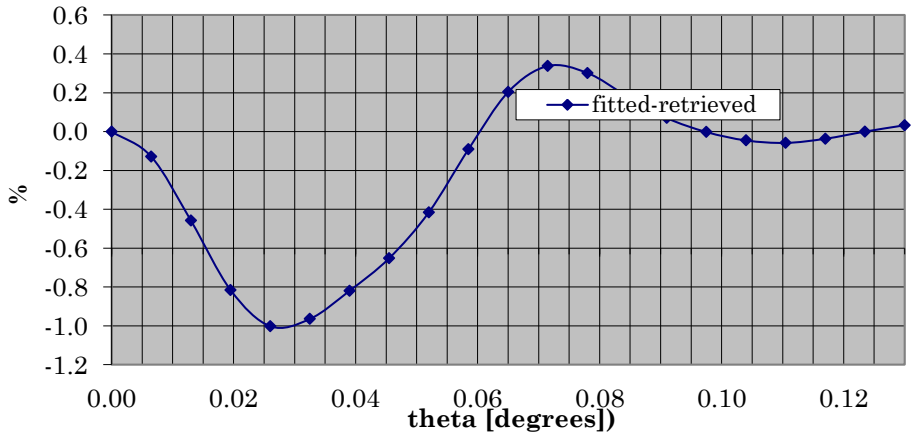

c) Difference

Figure 2-34 Kriging fitted measured and retrieved power pattern for 353 GHz detector, HFI-353-3a.

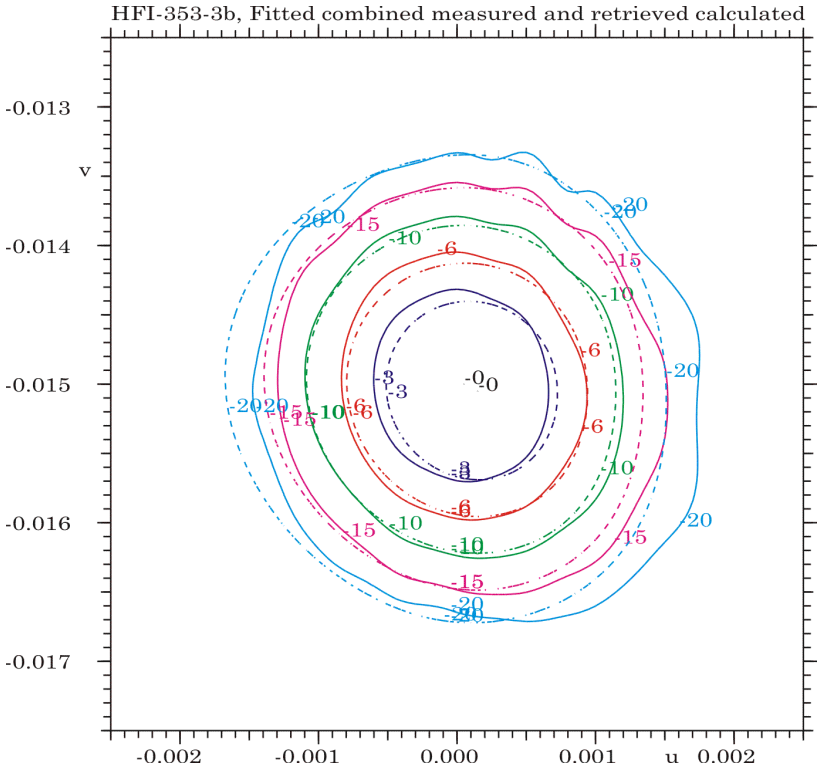

a) Measured (full line) and retrieved (dashed) power pattern

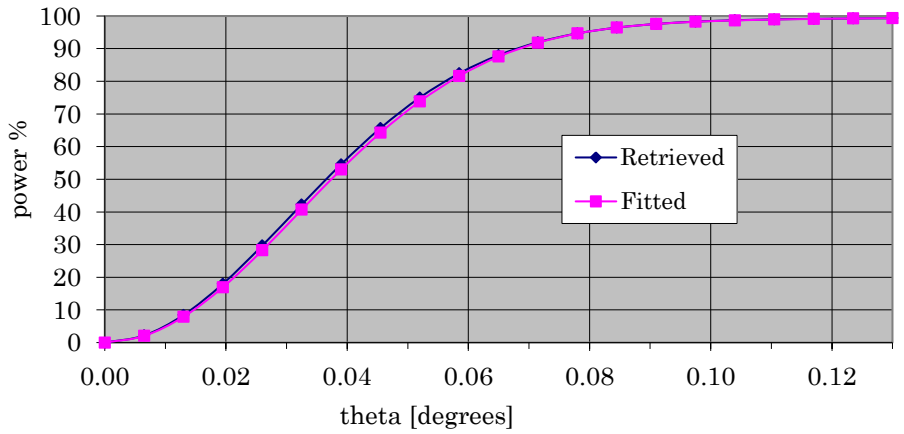

b) Azimuthally integrated power

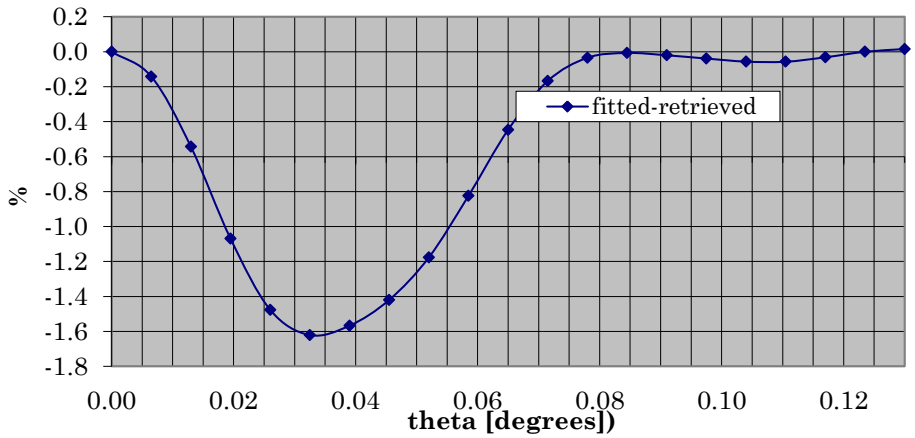

c) Difference

Figure 2-35 Kriging fitted measured and retrieved power pattern for 353 GHz detector, HFI-353-3b.

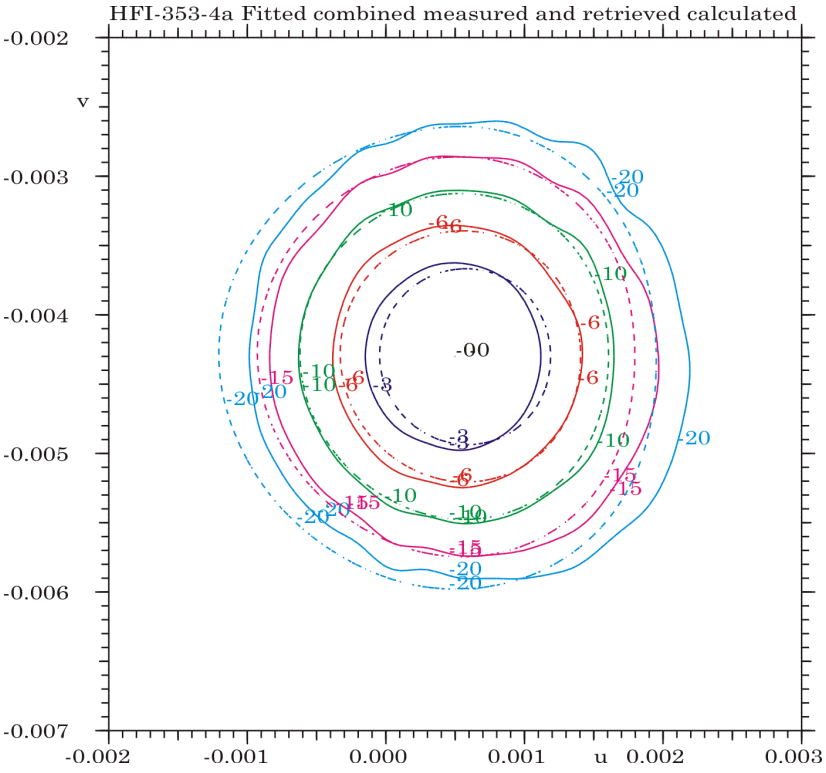

a) Measured (full line) and retrieved (dashed) power pattern

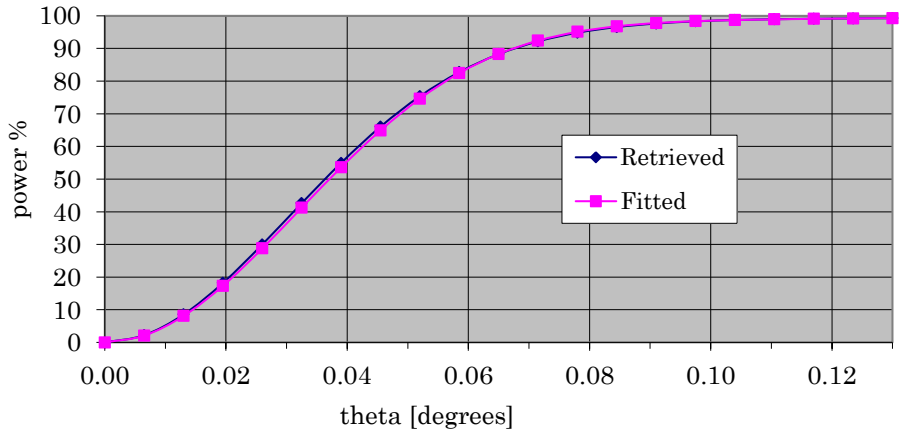

b) Azimuthally integrated power

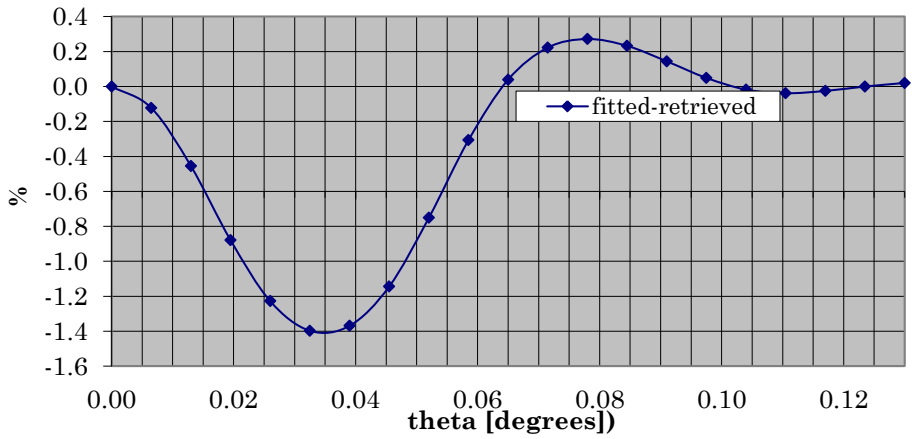

c) Difference

Figure 2-36 Kriging fitted measured and retrieved power pattern for 353 GHz detector, HFI-353-4a.

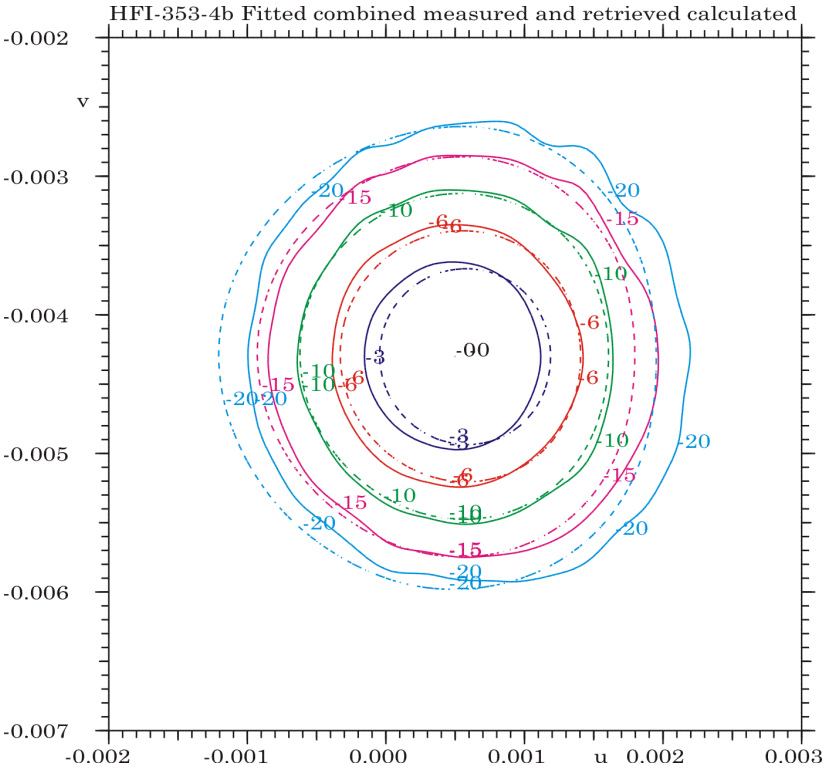

a) Measured (full line) and retrieved (dashed) power pattern

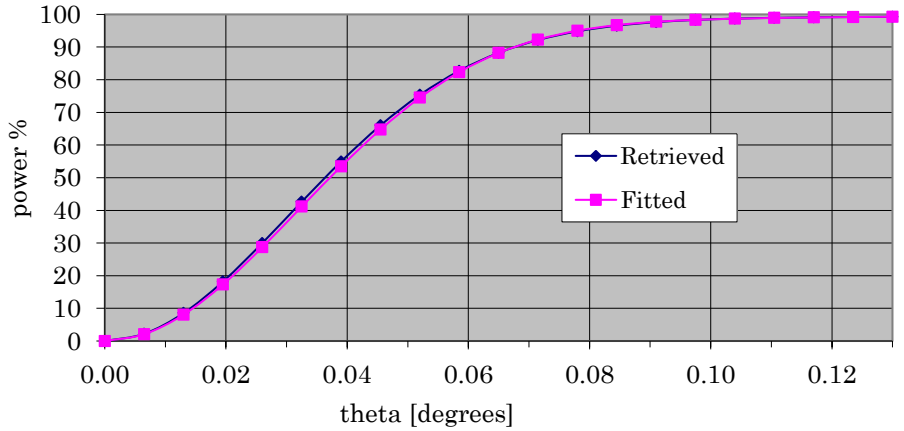

b) Azimuthally integrated power

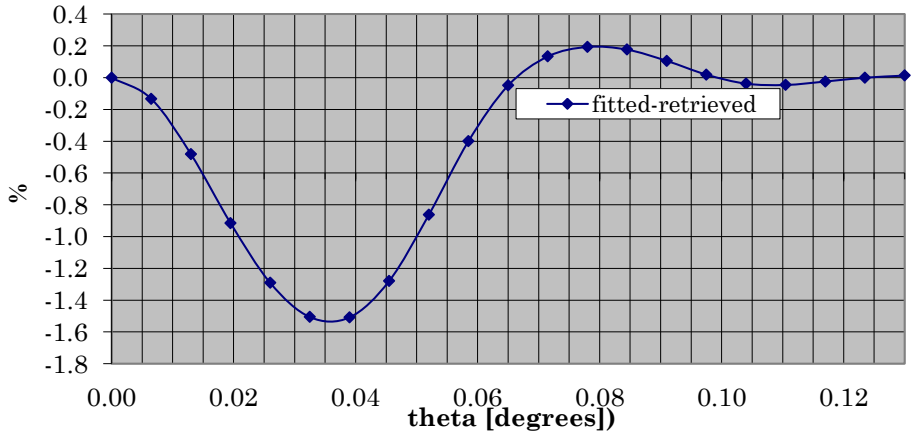

c) Difference

Figure 2-37 Kriging fitted measured and retrieved power pattern for 353 GHz detector, HFI-353-4b.

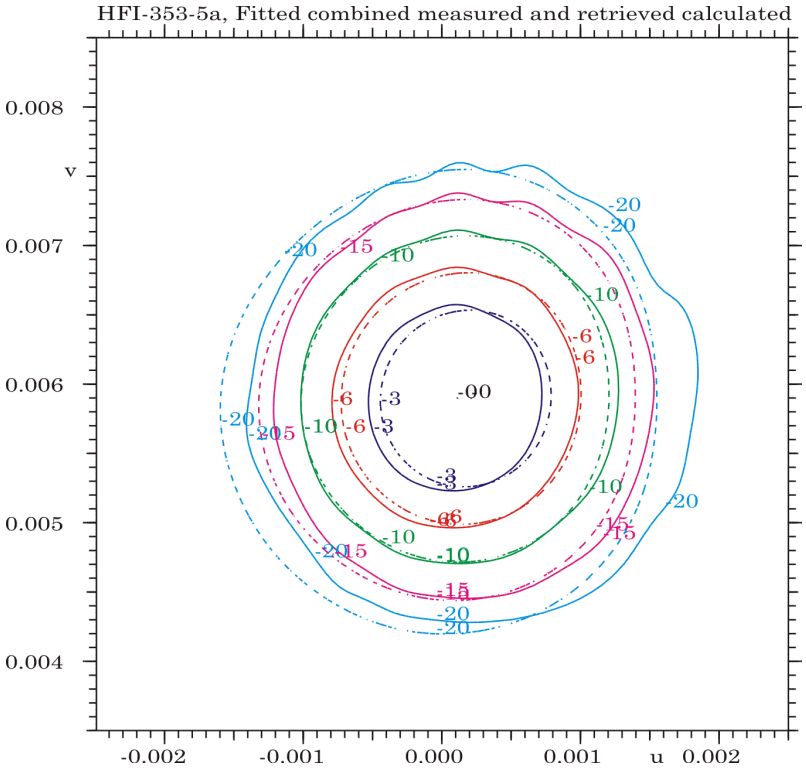

a) Measured (full line) and retrieved (dashed) power pattern

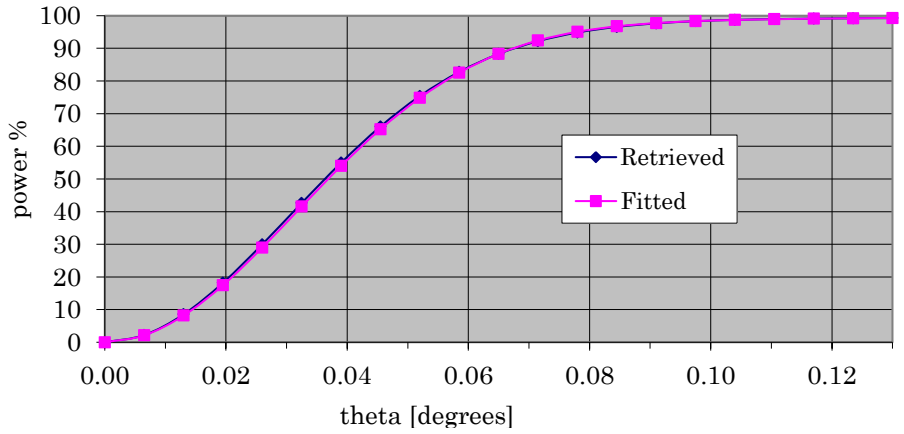

b) Azimuthally integrated power

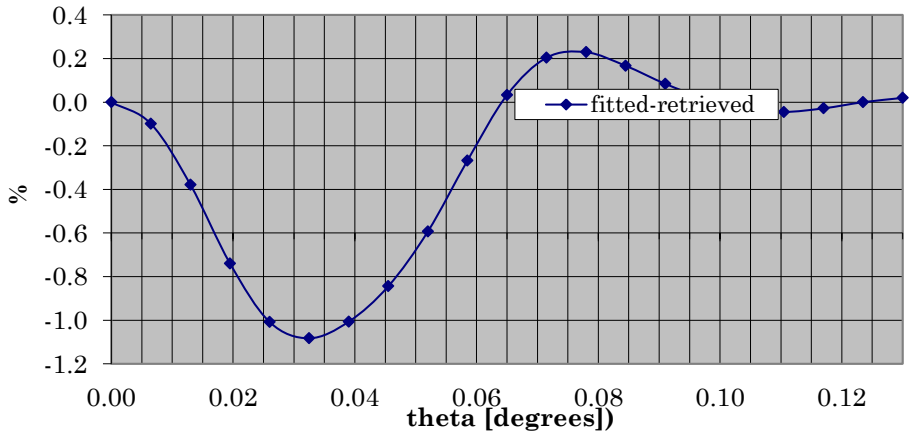

c) Difference

Figure 2-38 Kriging fitted measured and retrieved power pattern for 353 GHz detector, HFI-353-5a

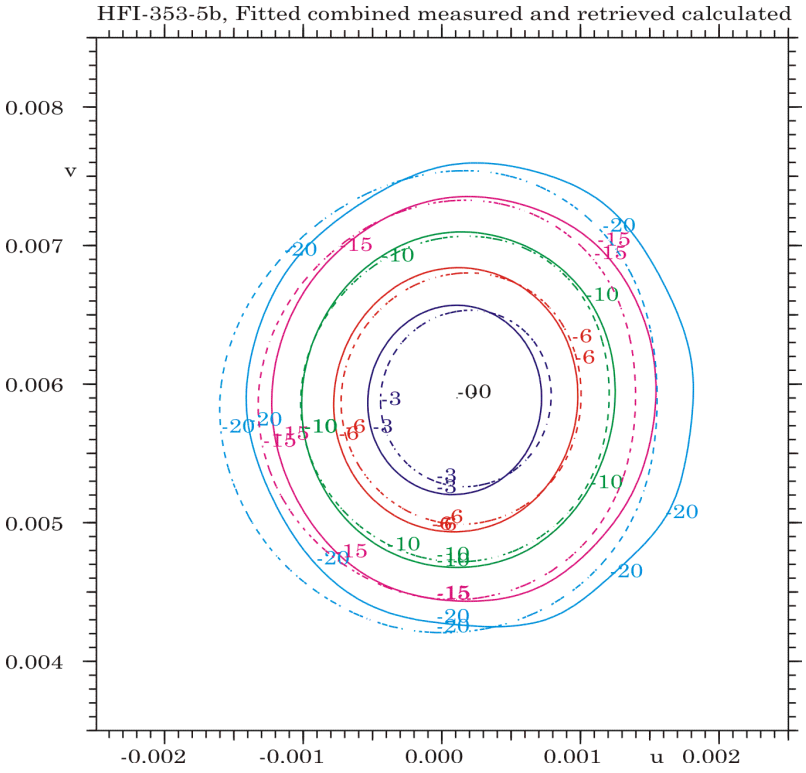

a) Measured (full line) and retrieved (dashed) power pattern

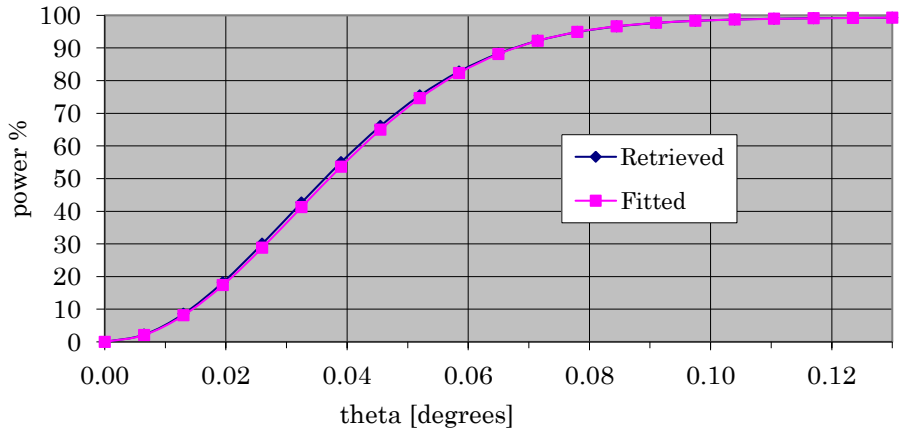

b) Azimuthally integrated power

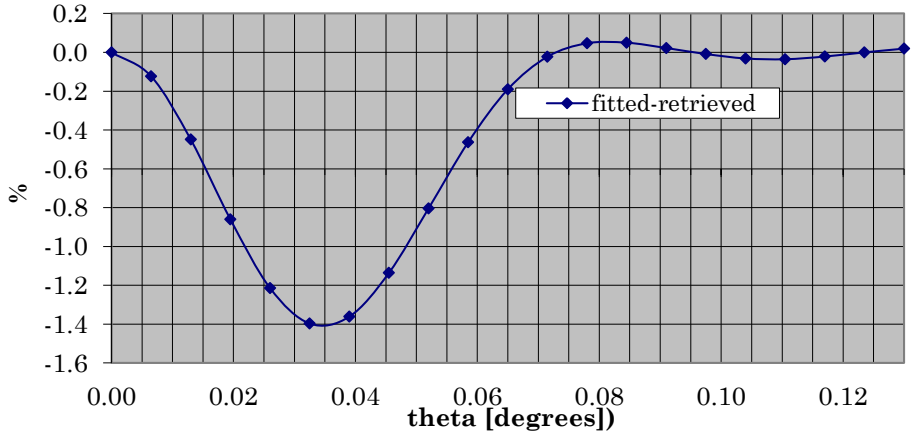

c) Difference

Figure 2-39 Kriging fitted measured and retrieved power pattern for 353 GHz detector, HFI-353-5b.

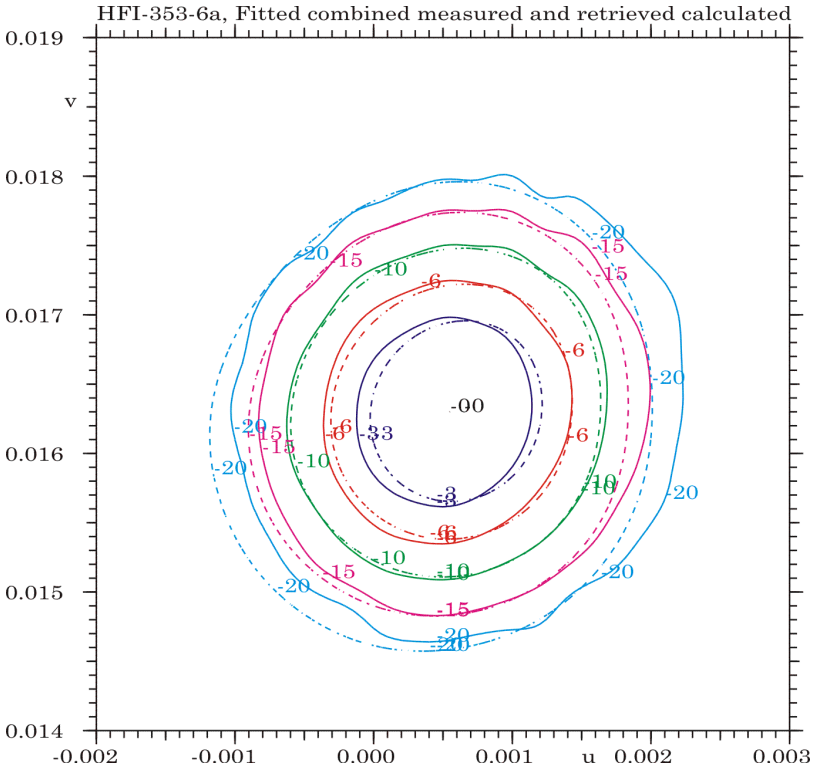

a) Measured (full line) and retrieved (dashed) power pattern

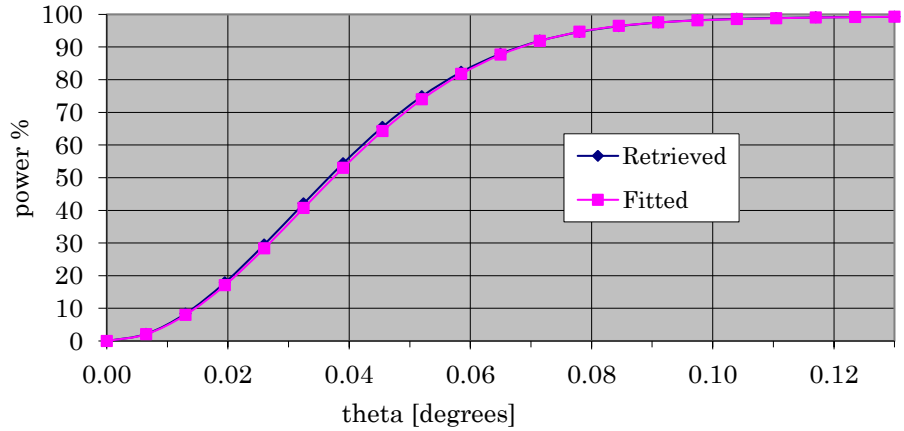

b) Azimuthally integrated power

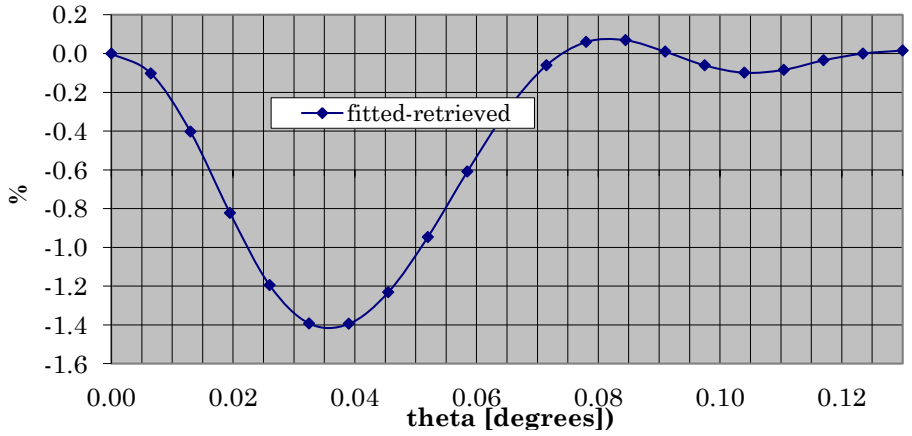

c) Difference

Figure 2-40 Kriging fitted measured and retrieved power pattern for 353 GHz detector, HFI-353-6a.

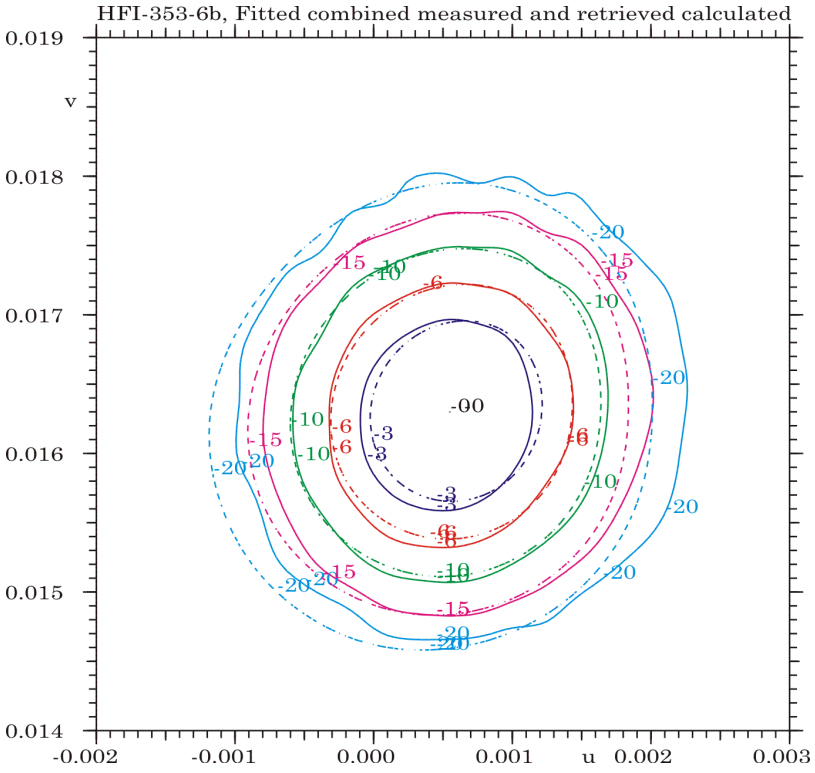

a) Measured (full line) and retrieved (dashed) power pattern

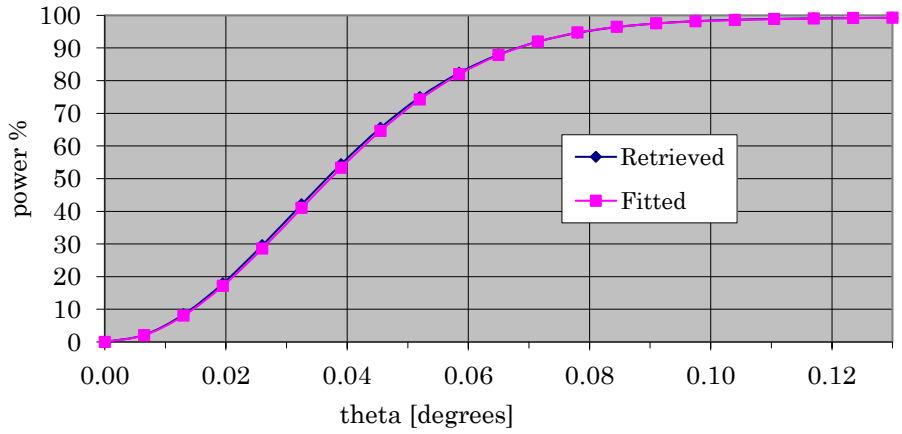

b) Azimuthally integrated power

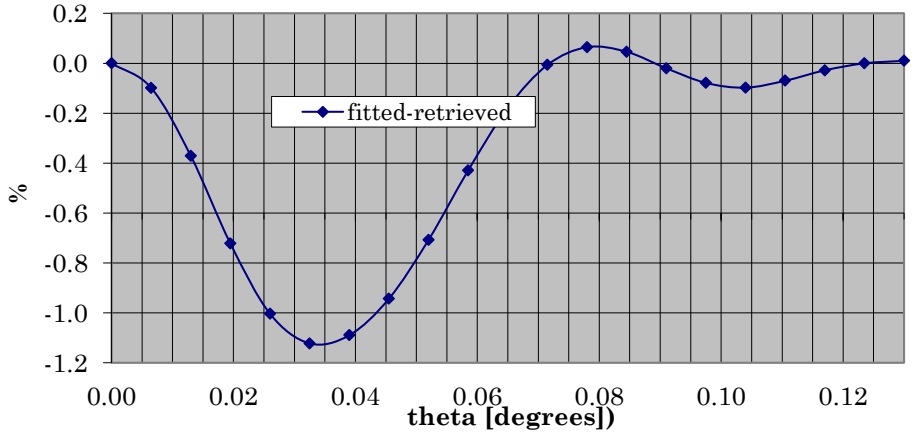

c) Difference

Figure 2-41 Kriging fitted measured and retrieved power pattern for 353 GHz detector, HFI-353-6b.

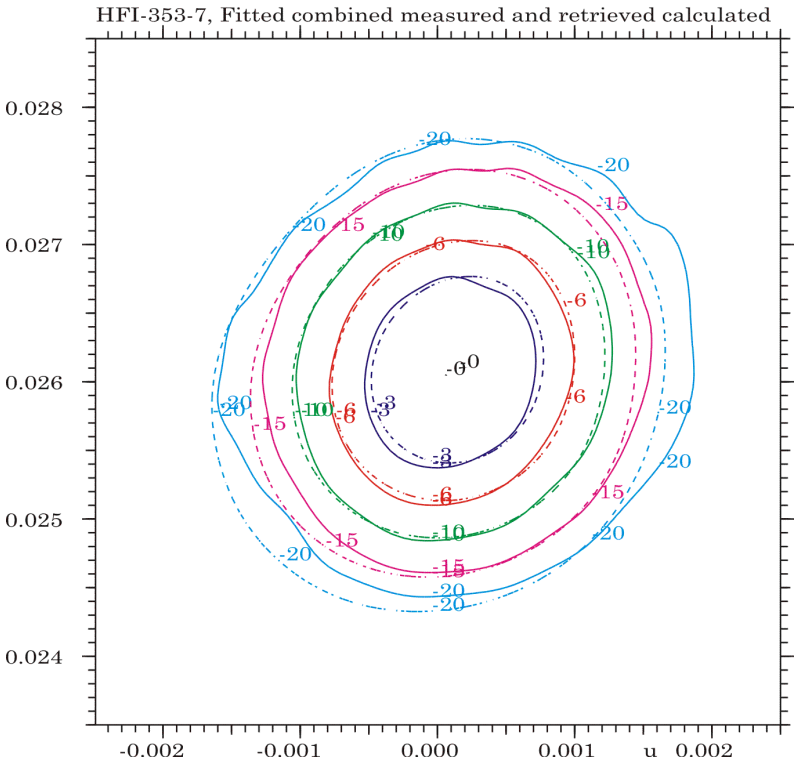

a) Measured (full line) and retrieved (dashed) power pattern

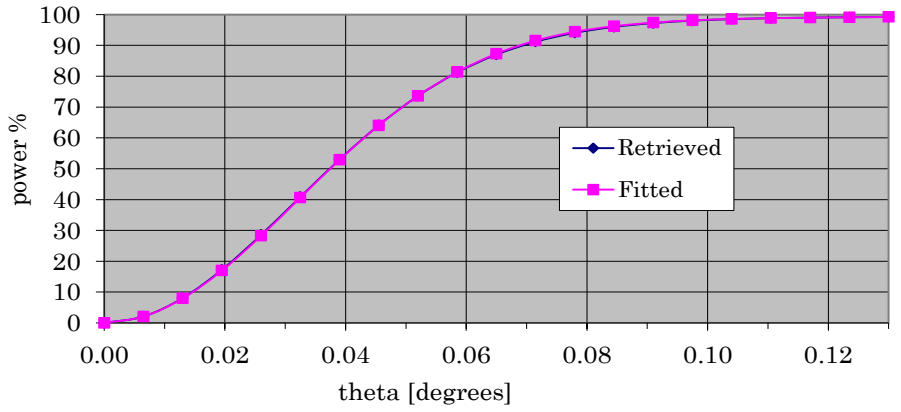

b) Azimuthally integrated power

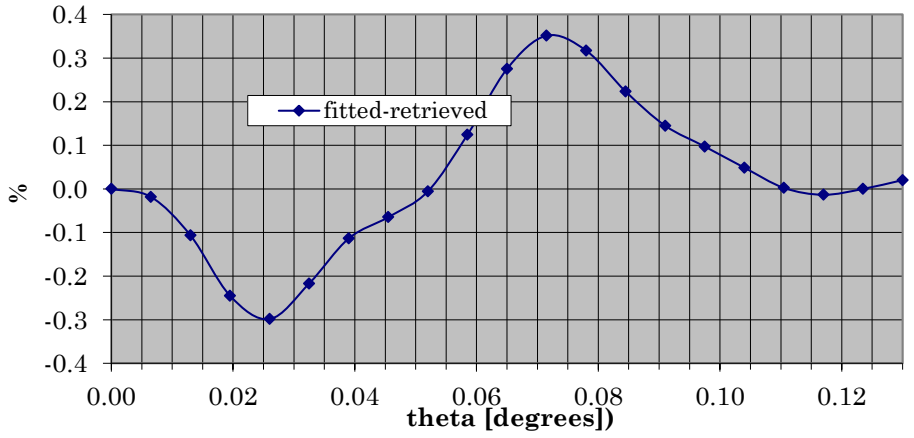

c) Difference

Figure 2-42 Kriging fitted measured and retrieved power pattern for 353 GHz detector, HFI-353-7.

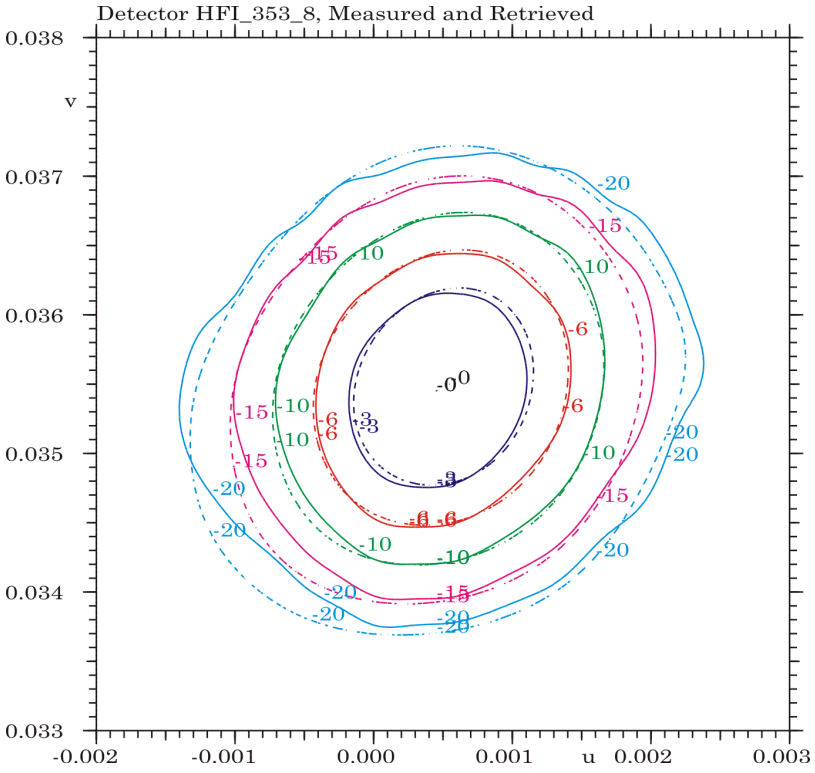

a) Measured (full line) and retrieved (dashed) power pattern

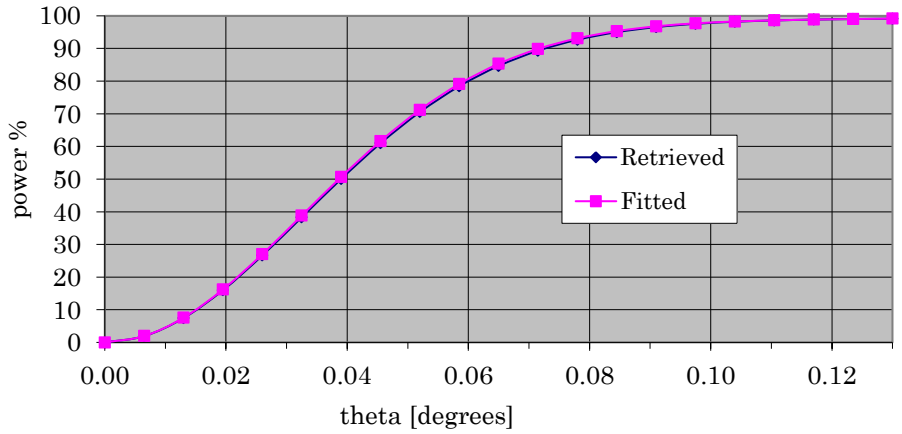

b) Azimuthally integrated power

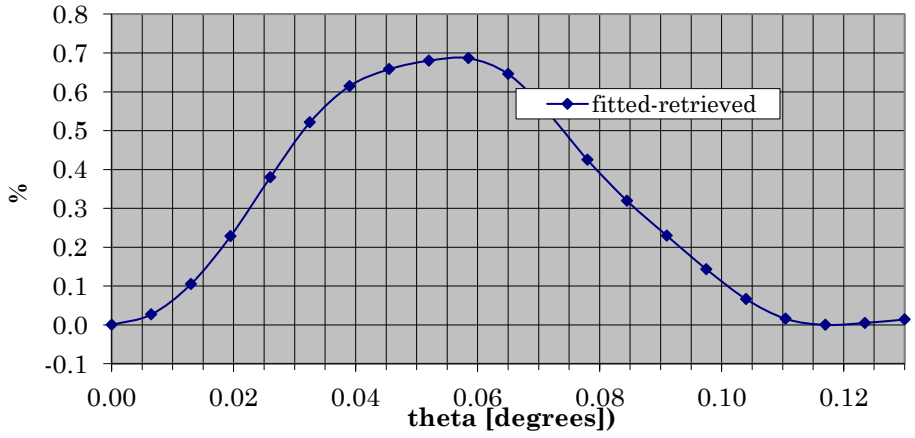

c) Difference

Figure 2-43 Kriging fitted measured and retrieved power pattern for 353 GHz detector, HFI-353-8.

3. Conclusion.

The RF performances from the final retrieved telescope geometry, RFM2, are shown to be significantly improved upon the RF calculations from the RFFM telescope geometry. The RFFM results are given in Report S-1563-05.

The remaining differences between the retrieved and the measured beams, see Table 3-1, may be due to measurement noise and inaccuracies in the beam directions. Moreover the delivered HFI beams were processed and combined from three different measurements of Saturn and Jupiter. The retrieval is also dependent on the calculated patterns from the detectors. The HFI detectors are advanced and shaped horns with filter sections and bolometers.

The integrated power differences are largest for the 143 GHz beams. Especially for detector 143_5, where the power difference is up to 2.5%. This large difference is also noticeable in Figure 2-17, where the measured and retrieved beams are plotted together. Notice, that the two calculated large shoulders are not present in the combined measured beam, but these shoulders are in fact present in the old Kriging fittet measured beam from the Mars scan in Report S-1531-14. The beam is plotted together with the new retrieved calculated beam in Figure 3-1. Even though the retrieval is performed with another set of beam measurements the agreement with the old Mars beam is remarkable. It is obvious that important beam characteristics have been eliminated by the stacking and fitting process of the new measured beams. This is clearly shown in Figure 3-2 where the two measured beams are compared.

Compared to the final variances and power differences in the retrieval of RFM1, see Report S-1563-07 Table 8-1, all beams are deteriorated due to the larger weight on the LFI beams in the retrieval.

All the measured and retrieved RFM2 beams are shown together in Figure 3-3 with contour levels down to 20 dB below peak.

HFI	Variance δ [dB]		Max power difference [%]	
Detector	a-pol	b-pol	a-pol	b-pol
HFI_100_1	0.21	0.23	0.8	1.0
HFI_100_2	0.27	0.25	1.6	1.5
HFI_100_3	0.26	0.25	1.4	1.4
HFI_100_4	0.19	0.19	1.0	1.0
HFI_143-1	0.51	0.53	1.6	1.3
HFI_143-2	0.38	0.39	1.5	1.2
HFI_143-3	0.46	0.43	1.2	1.6
HFI_143-4	0.64	0.63	1.4	1.6
HFI_143-5	0.52		**2.5**	
HFI_143-6	0.40		2.3	
HFI_143-7	0.43		**2.5**	
HFI_217-1	0.36		1.2	
HFI_217-2	0.37		0.8	
HFI_217-3	0.39		0.8	
HFI_217-4	0.51		0.4	
HFI-217-5	0.52	0.57	1.5	1.4
HFI-217-6	0.43	0.44	1.5	1.6
HFI-217-7	0.46	0.46	1.3	1.4
HFI-217-8	0.48	0.49	1.7	1.4
HFI_353-1	0.41		1.4	
HFI-353-2	0.56		1.3	
HFI-353-3	0.69	**0.71**	1.0	1.6
HFI-353-4	0.68	0.68	1.4	1.5
HFI-353-5	**0.71**	**0.71**	1.3	1.4
HFI-353-6	0.67	0.67	1.4	1.1
HFI-353-7	0.56		0.3	
HFI_353-8	0.40		0.7	
HFI Variance	0.49			

Table 3-1 Remaining variances of RFM1.

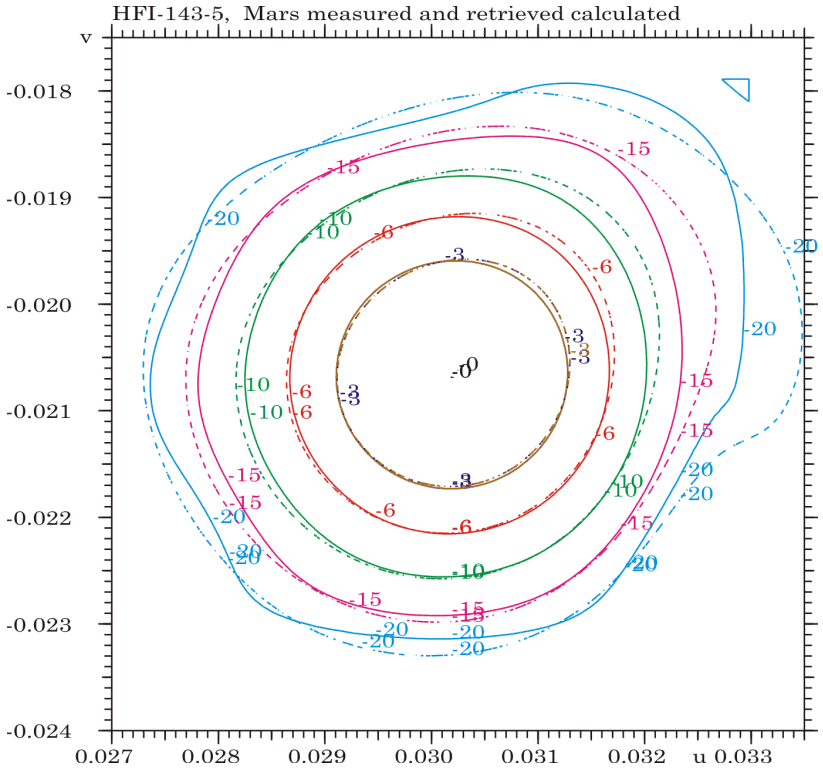

Figure 3-1 Old Mars measured (full line) and retrieved power (dashed) pattern for 143 GHz detector, HFI-143-5.

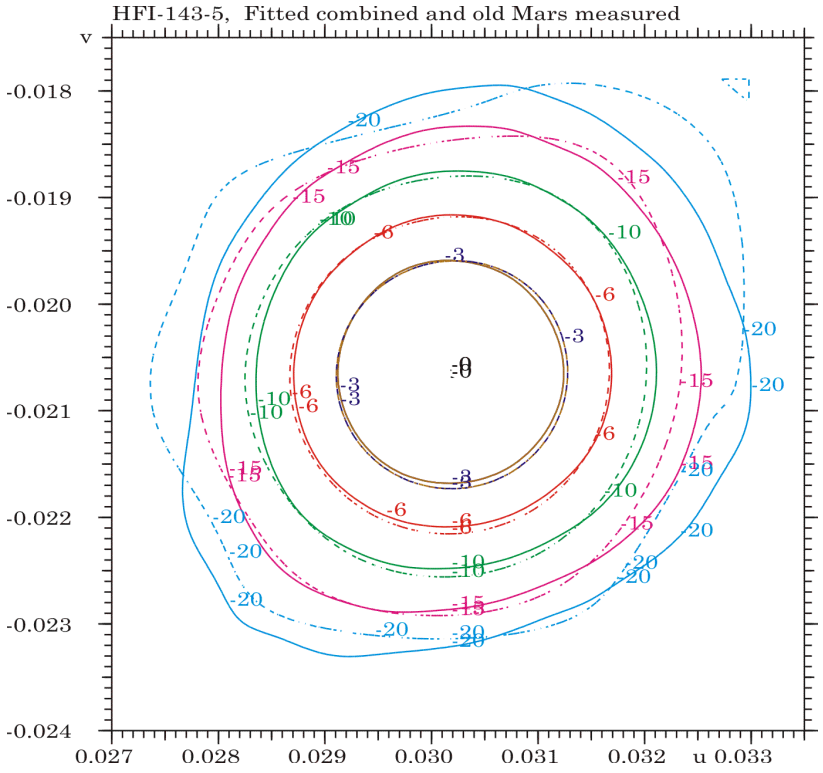

Figure 3-2 Fitted combined (full line) and Old Mars measured (dashed) pattern for 143 GHz detector, HFI-143-5.

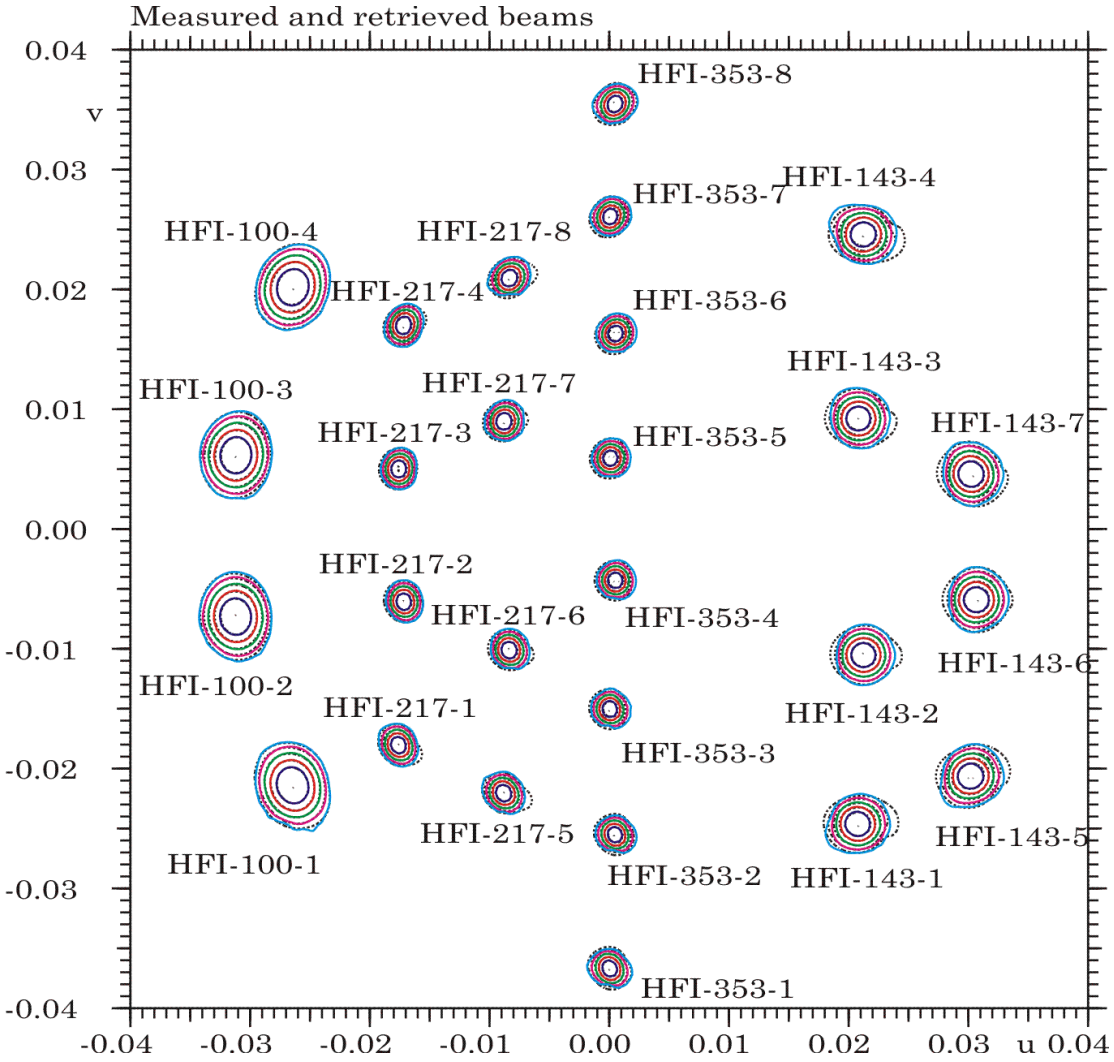

Figure 3-3 All measured (full line) and retrieved (dashed) HFI beams.

References

P. Nielsen, 2011
"In-flight Retrieval of Geometrical information on the Planck Telescope – Geometrical retrieval using HFI data from Mars scan 1", S-1531-14, dated October 2011.

P. Nielsen, 2013
"In-flight Retrieval of Geometrical information on the Planck Telescope – HFI optical beam data with IMO 1731634056801705766", S-1563-05, dated April 2013.

P. Nielsen, 2013
"In-flight Retrieval of Geometrical information on the Planck Telescope – Geometry retrieval using combined HFI data and LFI data from Jupiter scan 1", S-1563-07, dated November 2013.

P. Nielsen, 2015
"In-flight Retrieval of Geometrical information on the Planck Telescope – Geometry retrieval using combined HFI and LFI beam data", S-1563-13, dated December 2015.

A. Final RFM2 retrieved geometry

The final retrieved telescope geometry model, RFM2, is described by the following displacements and distortions defined in the telescope coordinate systems shown in Figure A-1.

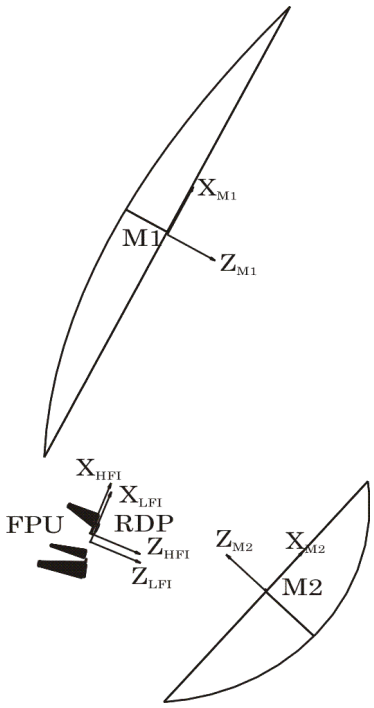

Figure A-1 Coordinate systems for RFM2.

The common LFI FPU coordinate system displacements are

- translation in X_{RDP}-direction of ÷0.06 mm
- translation in Y_{RDP}-direction of ÷0.01 mm
- translation in Z_{RDP}-direction of +0.05 mm
- rotation around the Z_{RDP}-axis of ÷4.1 arcmin

The common HFI FPU coordinate system displacements are

- translation in X_{RDP}-direction of +0.27 mm
- translation in Y_{RDP}-direction of ÷0.11 mm
- translation in Z_{RDP}-direction of +0.26 mm
- rotation around the Z_{RDP}-axis of +0.9 arcmin

All coordinate system displacements and rotations are relative to the respective NRFFM systems with the new detector positions described in Report S-1563-09.

The retrieved surface distortions on the reflectors are defined in the Z_{M1}- and Z_{M2}-directions and represented by the Zernike modes in Table A-1 and Table A-2.

Zernike mode		Amplitude	Rotation
m	n	[mm]	[degrees]
0	0	0.	0
0	2	-0.08	0
1	1	0.99	68
2	2	0.13	79
1	3	0.09	6
3	3	0.06	-58

Table A-1 Retrieved Zernike modes on main reflector.

Zernike mode		Amplitude	Rotation
m	n	[mm]	[degrees]
0	0	0.	0
0	2	0.00	0
1	1	1.37	-35
2	2	0.05	-69
1	3	0.29	-7
3	3	0.03	4

Table A-2 Retrieved Zernike modes on subreflector.

The LFI and HFI feed displacements in the individual retrieved FPU coordinate systems are given in Table A-3 and Table A-4, respectively.

Feed displacements	Deviation from retrieved RDP	
Detector	Δx [mm]	Δy [mm]
LFI18	0.03	0.11
LFI19	0.08	-0.13
LFI20	0.16	0.34
LFI21	-0.43	-0.36
LFI22	0.06	0.08
LFI23	0.15	0.00
LFI24	-0.20	-0.16
LFI25	-0.10	-0.05
LFI26	0.03	0.03
LFI27	-0.14	0.10
LFI28	-0.04	0.09

Table A-3 Retrieved LFI feed displacements.

Displacements	Deviation from RDP	
Detector	Δx [mm]	Δy [mm]
HFI-100-1	-0.05	0.00
HFI-100-2	-0.05	0.08
HFI-100-3	-0.02	0.09
HFI-100-4	**-0.12**	0.09
HFI-143-1	0.01	-0.01
HFI-143-2	0.02	-0.09
HFI-143-3	0.01	-0.08
HFI-143-4	0.01	-0.08
HFI-143-5	0.00	-0.05
HFI-143-6	-0.02	-0.11
HFI-143-7	-0.04	**-0.12**
HFI-217-1	0.04	0.04
HFI-217-2	0.05	0.09
HFI-217-3	0.05	0.14
HFI-217-4	-0.04	0.23
HFI-217-5	0.08	0.07
HFI-217-6	0.03	0.00
HFI-217-7	0.00	0.11
HFI-217-8	0.06	**0.11**
HFI-353-1	0.09	0.02
HFI-353-2	0.07	-0.07
HFI-353-3	0.09	0.03
HFI-353-4	0.10	0.01
HFI-353-5	**0.11**	0.06
HFI-353-6	0.09	0.05
HFI-353-7	0.06	0.01
HFI-353-8	-0.03	-0.01
Average	0.02	0.02

Table A-4 Retrieved HFI feed displacements.